



Research paper

2,6-Disubstituted 7-(naphthalen-2-ylmethyl)-7H-purines as a new class of potent antitubercular agents inhibiting DprE1

Vladimir Finger^{a,b}, Tomas Kucera^c, Radka Kafkova^d, Lubica Muckova^{b,c}, Rafael Dolezal^b, Jan Kubes^a, Martin Novak^{a,b}, Lukas Prchal^b, Levente Lakatos^{e,f}, Martin Andrs^b, Michaela Hympanova^{b,c}, Jan Marek^{b,c}, Martin Kufa^{a,b}, Vojtech Spiwok^g, Ondrej Soukup^b, Eva Mezeiova^b, Jiri Janousek^b, Lenka Nevosadova^a, Marketa Benkova^b, Russell R.A. Kitson^a, Martin Kratky^a, Szilvia Bösze^{e,f}, Katarina Mikusova^d, Ruben Hartkoorn^h, Jaroslav Roh^{a,**}, Jan Korabecny^{b,*}

^a Faculty of Pharmacy in Hradec Králové, Charles University, Akademika, Heyrovského 1203, 50005, Hradec Králové, Czech Republic

^b Biomedical Research Center, University Hospital Hradec Králové, Sokolska 581, 500 05, Hradec Králové, Czech Republic

^c Faculty of Military Health Sciences, University of Defence, Trebesska, 1575, 500 01, Hradec Králové, Czech Republic

^d Faculty of Natural Sciences, Department of Biochemistry, Comenius University in Bratislava, Mlynská Dolina, Ilkovičova 6, 842 15, Bratislava, Slovakia

^e ELKH-ELTE Research Group of Peptide Chemistry, Eötvös Loránd University, Pázmány Péter Sétány 1/A, H-1117, Budapest, Hungary

^f National Public Health Center, Albert Flórián út 2-6, Budapest, 1097, Hungary

^g Department of Biochemistry and Microbiology, University of Chemistry and Technology, Technická 5, 166 28, Prague, Czech Republic

^h Univ. Lille, CNRS, Inserm, CHU Lille, Institut Pasteur Lille, U1019-UMR 9017-CILIL-Center for Infection and Immunity of Lille, F-59000, Lille, France

ARTICLE INFO

Keywords:

Tuberculosis

Purine

Mycobacterium tuberculosis

DprE1

Structure-activity relationships

ABSTRACT

Phenotypic screening of an in-house library of small molecule purine derivatives against *Mycobacterium tuberculosis* (*Mtb*) led to the identification of 2-morpholino-7-(naphthalen-2-ylmethyl)-1,7-dihydro-6H-purin-6-one **10** as a potent antimycobacterial agent with MIC₉₉ of 4 μM. Thorough structure-activity relationship studies revealed the importance of 7-(naphthalen-2-ylmethyl) substitution for antimycobacterial activity, yet opened the possibility of structural modifications at positions 2 and 6 of the purine core. As the result, optimized analogues with 6-amino or ethylamino substitution **56** and **64**, respectively, were developed. These compounds showed strong *in vitro* antimycobacterial activity with MIC of 1 μM against *Mtb* H₃₇Rv and against several clinically isolated drug-resistant strains, had limited toxicity to mammalian cell lines, medium clearance with respect to phase I metabolic deactivation (27 and 16.8 μL/min/mg), sufficient aqueous solubility (>90 μM) and high plasma stability. Interestingly, investigated purines, including compounds **56** and **64**, lacked activity against a panel of Gram-negative and Gram-positive bacterial strains, indicating a specific mycobacterial molecular target. To investigate the mechanism of action, *Mtb* mutants resistant to hit compound **10** were isolated and their genomes were sequenced. Mutations were found in *dprE1* (Rv3790), which encodes decaprenylphosphoryl-β-D-ribose oxidase DprE1, enzyme essential for the biosynthesis of arabinose, a vital component of the mycobacterial cell wall. Inhibition of DprE1 by 2,6-disubstituted 7-(naphthalen-2-ylmethyl)-7H-purines was proved using radiolabelling experiments in *Mtb* H₃₇Rv *in vitro*. Finally, structure-binding relationships between selected purines and DprE1 using molecular modeling studies in tandem with molecular dynamic simulations revealed the key structural features for effective drug-target interaction.

1. Introduction

Tuberculosis (TB) is a widespread infectious disease caused by the

pathogenic *Mycobacterium tuberculosis* (*Mtb*) that is among the ten leading causes of death in low- and middle-income countries. TB represents an immense social and economic burden as well, with an estimated 10.6 million new cases diagnosed each year. According to the

* Corresponding author.

** Corresponding author.

E-mail addresses: jaroslav.roh@faf.cuni.cz (J. Roh), jan.korabecny@fnhk.cz (J. Korabecny).

<https://doi.org/10.1016/j.ejmech.2023.115611>

Received 4 May 2023; Received in revised form 27 June 2023; Accepted 27 June 2023

Available online 3 July 2023

0223-5234/© 2023 The Authors. Published by Elsevier Masson SAS. This is an open access article under the CC BY license (<http://creativecommons.org/licenses/by/4.0/>).

World Health Organization's (WHO) global TB report 2022, one-quarter of the world's population is infected by the latent form of TB. Further-

non-covalent [13]. The presence of a nitro group is essential for covalent DprE1 inhibitors, which undergo metabolic reduction to the nitroso

Abbreviations

DMSO	dimethyl sulfoxide;
CNCTC	Czech National Collection of Type Cultures
CL _s	cardiolipin
Cl _{int}	intrinsic clearance
EtOAc	ethyl acetate
DprE1	decaprenylphosphoryl-β-D-ribose 2'-oxidase
ESBL	extended-spectrum beta-lactamase
HLM	human liver microsomes
INH	isoniazid
MDR	multidrug-resistant

MIC	minimum inhibitory concentration
PE	phosphatidylethanolamine;
RIF	rifampicin
SAR	structure-activity relationships
TB	tuberculosis
TMM	trehalose monomycolates
TDM	trehalose dimycolates
THF	tetrahydrofuran
TLC	thin layer chromatography
WHO	World Health Organization
XDR	extensively drug-resistant

more, in 2021 1.4 million people died from TB among HIV-negative and a further 187,000 deaths were among HIV-positive people [1,2].

Standard TB treatment caused by drug-susceptible strains of *Mtb* starts with a two-month administration of four *anti*-TB drugs (isoniazid/INH/, rifampicin/RIF/, pyrazinamide, and ethambutol/EMB/), also known as first-line drugs. This period is followed by INH and RIF only for another four months. However, the emergence of TB strains resistant to first-line drugs has become a major concern. Specifically, multidrug-resistant TB strains (MDR-TB) are characterized by non-response to at least INH and RIF. This problem is exacerbated by the existence of extensively drug-resistant TB (XDR-TB) strains that fulfil the definition of MDR-TB and which are also resistant to any fluoroquinolone and at least one additional Group A drug [3]. Treatment of MDR-TB and XDR-TB is even more complicated, involving the administration of a cocktail of second-line drugs selected according to the susceptibility of the mycobacterial strain [4,5]. Among the second-line drugs, bedaquiline, delamanid, and pretomanid are the latest to have received approval from the FDA for treating TB. However, shortly after their entrance to the clinic, resistance to them was reported [6].

To make TB treatment more effective, safer and shorter, new *anti*-TB agents are being developed, with 17 drug candidates currently undergoing various stages of clinical trials. Out of these, phase II drugs like BTZ-043, PBTZ169, OPC-167832, and TBA-7371 (Fig. 1) target decaprenylphosphoryl-β-D-ribose oxidase (DprE1; EC:1.1.98.3) [7–10]. DprE1 catalyses the oxidation of decaprenylphosphoryl-D-ribose to decaprenylphosphoryl-D-2'-keto-erythro-pentofuranose (DPX) which is reduced by DprE2 into decaprenyl-D-arabinose (DPA) [11], an arabinosyl donor crucial for the biosynthesis of mycobacterial cell wall polysaccharides lipoarabinomannan and arabinogalactan [12]. Recent research revealed two classes of DprE1 inhibitors; covalent and

group by DprE1 itself, forming a stable semimercaptal adduct between the drug and the sulfanyl group of Cys387 in the active site of DprE1 [14]. Two covalent inhibitors, BTZ-043 and PBTZ169, exhibit even higher *anti*-TB activity than all currently used *anti*-TB drugs (MIC of 1 ng/mL and ≤0.19 ng/mL for BTZ043 and PBTZ169, respectively) [7,8]. Non-covalent inhibitors also act in the active site of the enzyme; however, the presence of Cys387 is not essential for their activity. Indeed, BTZ-043-resistant strains carrying the mutation in Cys387 are susceptible to OPC-167832 and TBA-7371. *Anti*-TB activity of OPC-167832 is defined by MIC = 0.5 ng/mL, whilst TBA-7371 shows less pronounced *anti*-TB activity (MIC = 0.64 μg/mL) [9,10].

Several other structural chemotypes have been identified acting as non-covalent inhibitors of DprE1 (Fig. 2). Given their structural diversity, it is evident that they also exert distinct interactions with the DprE1 active site [15]. For example, *Mtb* strains resistant to TCA1, to inhibitors 1 and 2 or to the TBA-7371-derived compound AZ exhibit the Y314H mutation in DprE1 [9,16–18]. This mutation also caused resistance to above-mentioned compounds OPC-167832 and TBA-7371 [9,10]. In contrast, E221Q mutation has been observed in strains resistant to compounds AZ, TCA1, inhibitor 1 and GSK 710 [17,19], while *Mtb* strains resistant to compound Ty38c have G17C and L368P mutations [20].

In this work, we identified the 2,6-disubstituted 7-(naphthalen-2-ylmethyl)-7H-purine family of compounds as a new class of potent antitubercular agents. The 2-morpholino-purin-6-one hit compound 10 (Fig. 3) was identified upon our small molecule library screening (Fig. 3, Table 1), exhibiting low micromolar MIC₉₉ value against the virulent H₃₇Rv *Mtb* strain (MIC₉₉ = 4 μM). Additional experiments revealed acceptable aqueous solubility, selectivity towards *Mtb* over other *Mycobacterium* strains and other bacteria, and low cytotoxic effect

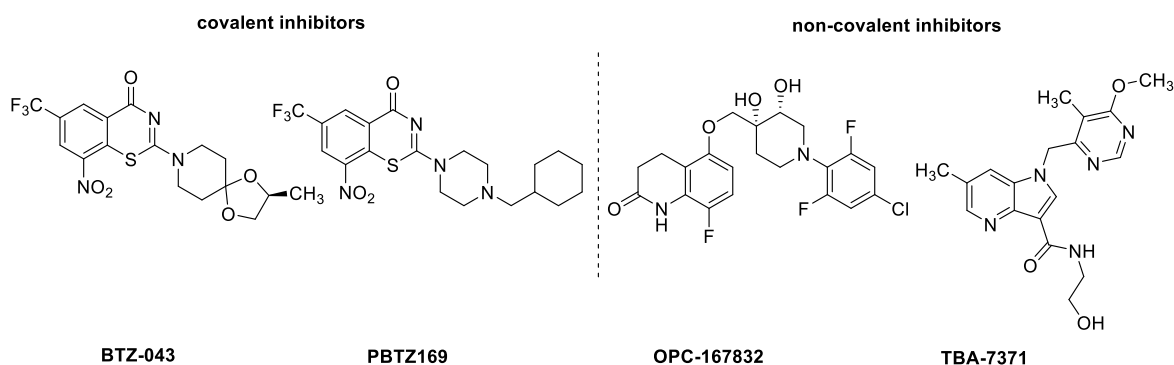


Fig. 1. Inhibitors of DprE1 in phase II clinical trials.

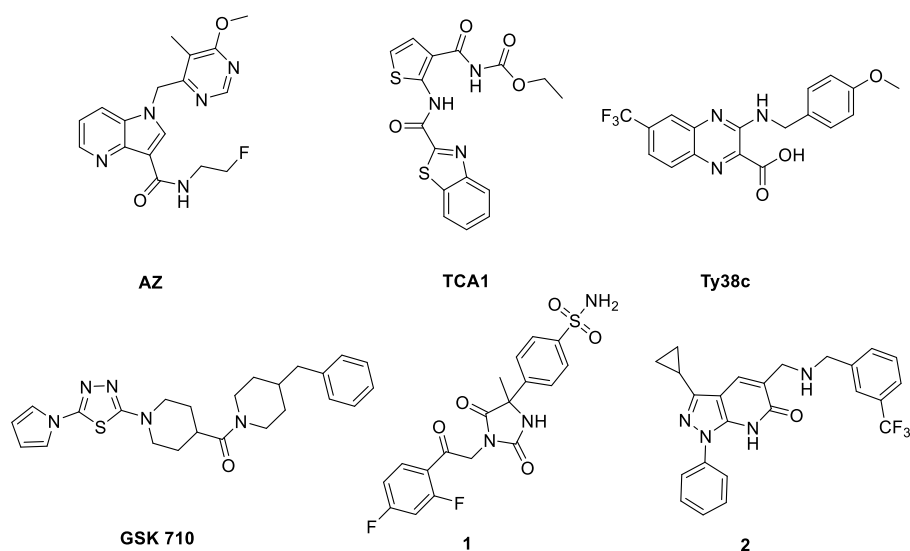


Fig. 2. Early-stage drug candidates classified as non-covalent inhibitors of DprE1.

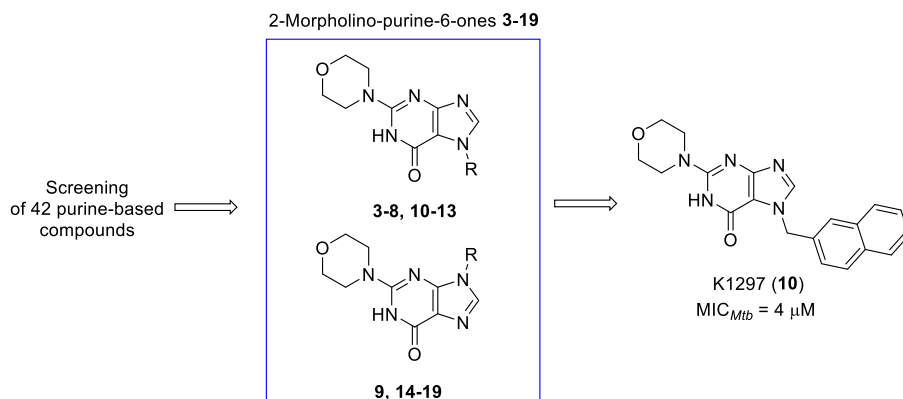


Fig. 3. Screening leading to the identification of derivative 10 with promising anti-TB activity.

against HepG2 cells resulting in a good selectivity index (determined as the ratio between cytotoxicity IC₅₀ and antitubercular MIC values).

Herein we describe the structure-activity relationship (SAR) with respect to antimycobacterial activity, cytotoxicity, microsomal and plasma stability, and the determination of the molecular target of compound 10 and structurally related 2,6-disubstituted 7-(naphthalene-2-ylmethyl)-7H-purine derivatives.

2. Results and discussion

Chemistry. The synthesis of 2-morpholino-purin-6-one derivatives **3–9** and **11–19** (Table 1) that have been screened for their antitubercular activity is described in the literature [21]. All derivatives designed and developed within this study are listed in Tables 2 and 3 with their general synthetic pathways for their preparation displayed in Schemes 1–4. 7-Substituted 2,6-dichloro-7H-purines **23a–c** were prepared by the reaction of commercially available 2,6-dichloro-9H-purine (**20**) with alkylating agents 2-(bromomethyl)naphthalene (**21a**), 2-(bromomethyl)-6-fluoronaphthalene (**21b**) or 2-(bromomethyl)quinoline (**21c**), respectively, in the presence of potassium carbonate in DMF (Scheme 1). 7-Substituted (**23a–c**) and 9-substituted (**22a–c**) regioisomers were separated *via* column chromatography. The *N*-7 substituted derivatives (**23a–c**) were minor products possessing higher retention on silica (lower R_f) than the *N*-9 products [21]. Derivatives **23a–c** were isolated in 16–23% yields, respectively, representing key intermediates for the

subsequent synthetic steps.

Purin-6-one **24** was prepared by hydrolysis of compound **23a** in a solution of 1 M NaOH in excellent yield (Scheme 1). Alkylation of compound **24** at *N*-1 by iodomethane in DMF using NaH as base afforded compound **39** (Scheme 1) in 62% yield [22]. Derivatives **10**, **25–38** and **40** were prepared from **24** and **39**, respectively, in 39–62% yields by nucleophilic aromatic substitution under microwave irradiation using an excess of the appropriate amine in *tert*-butanol [21].

2,6-Diamino purine derivatives **54–66** (Scheme 2) were prepared by nucleophilic aromatic substitutions replacing both chlorine atoms successively. Initially, the chlorine substitution with the appropriate amine at position 6 of compounds **23a–c** proceeded under mild conditions (45 °C), generating compounds **41–53** in good yields (45–98%). Only two intermediates resulted in lower yields, namely 6-(pyridine-4-ylmethyl)amino derivative **49** (27%) and 6-amino derivative **51** (36%). The second nucleophilic aromatic substitution at position 2 required more forcing microwave-assisted conditions, with derivatives **54–66** obtained in 34–81% yield.

Derivative **23a** served as a starting material in the synthesis of compounds **67–70**. Compounds containing 6-methoxy (**67**) and 6-ethoxy (**68**) groups with a chlorine at position 2 were prepared by the reaction of **23a** with sodium methoxide and sodium ethoxide in yields of 74% and 64%, respectively. Derivative **69**, having two morpholine rings at positions 2 and 6, was prepared *via* microwave-assisted one-pot synthesis (76% yield). Compound **70** bearing two sulfanyl groups at

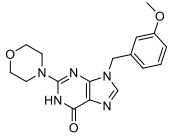
Table 1

Compounds 3–19 from the in-house library of small molecules screened for their antitubercular activity against *M. tuberculosis*, *M. avium*, and *M. kansasii*. Activity is expressed as MIC₉₉ (μM) assessed after (7), 14 or 21 days of incubation.

Compound	Structure	<i>Mtb</i> H ₃₇ Rv	<i>M. avium</i>	<i>M. kansasii</i>
		MIC ₉₉ (μM)	MIC ₉₉ (μM)	MIC ₉₉ (μM)
		14/21 days	14/21 days	7/14/21 days
3		>500/>500	>500/>500	>500/>500/>500
4		16/32	>500/>500	>500/>500/>500
5		16/32	>500/>500	>500/>500/>500
6		>500/>500	>500/>500	125/250/>500
7		32/64	>500/>500	500/>500/>500
8		500/>500	500/>500	>500/>500/>500
9		>250/>250	>250/>250	>250/>250/>250
10		4/4	>500/>500	32/64/125
11		>500/>500	>500/>500	>500/>500/>500
12		>500/>500	>500/>500	>500/>500
13		>250/>250	>250/>250	>250/>250/>250
14		>500/>500	>500/>500	>500/>500/>500
15		>250/>250	>250/>250	>250/>250/>250
16		125/>250	>250/>250	>250/>250/>250
17		>500/>500	>500/>500	>500/>500/>500
18		>500/>500	>500/>500	>500/>500/>500

(continued on next page)

Table 1 (continued)

Compound	Structure	<i>Mtb</i> H ₃₇ Rv	<i>M. avium</i>	<i>M. kansasii</i>
		MIC ₉₉ (μM)	MIC ₉₉ (μM)	MIC ₉₉ (μM)
		14/21 days	14/21 days	7/14/21 days
19		>500/>500	>500/>500	>500/>500/>500

positions 2 and 6 was obtained in 87% yield by the reaction of **23a** with an excess of thiourea under reflux in EtOH (Scheme 3) [23].

The attempts to prepare 6-alkoxy derivatives **72** and **73** from **67** and **68**, respectively, were fruitless due to the fact that not only chlorine at position 2 but also the alkoxy group was substituted with a morpholine ring. For this reason, an alternative synthetic approach was utilized. Firstly, 6-oxo compound **10** was converted into 6-chloro derivative **71** with POCl₃ and heating (48% yield) [24]. This intermediate was reacted with sodium alkoxides/thiolates to provide compounds **72–75** in 61–93% yield (Scheme 3).

Derivative **78** was prepared following the same procedure as in the case of compounds **23a-c** (Scheme 4). 6-Chloro-9H-purine (**76**) was selected as starting material, employing **21a** as an alkylating agent. Derivative **78** was isolated in 16% yield. Hydrolysis of compound **78** enabled the formation of purin-6-one **79** in 96% yield, with the hydrolysis carried out according to the same procedure as in the case of compound **24**. Compound **80** was prepared from derivative **78** in 89% yield using the same procedure as for the preparation of dithione **70** (Scheme 4) [23].

To clarify the role of nitrogen at position 9 of the purine core in the antimycobacterial activity, we prepared 9-deazapurine derivative **84** (Scheme 4). Alkylation of 2,6-dichloro-9-deazapurine proceeded smoothly and regioselectively, providing compound **82** in 86% yield. Following hydrolysis [25] and introduction of morpholine at position 2, deaza analogue **84** was obtained as an analogue to hit compound **10** (Scheme 4).

Antimycobacterial activity – structure-activity relationship determination. Initial screening of 42 purine-based compounds pinpointed hit compound **10** with good antimycobacterial activity against *Mtb* H₃₇Rv strain (MIC₉₉ = 4 μM). The results of its structurally related analogues further showed that only 7-substituted 2-morpholino-purin-6-one derivatives **4**, **5** and **7** retained *anti*-TB activity, but were 4–8 fold less potent compared to compound **10**. Strikingly, 9-substituted counterparts were completely inactive, including the 9-(naphthalen-2-ylmethyl)- regioisomer **9** of hit compound **10**. Moreover, 7-(naphthalen-1-yl)methyl analogue **11** that differs from hit compound **10** just in the way of naphthalene group attachment, showed no antimycobacterial activity. Thus, we hypothesized that the (naphthalen-2-yl)methyl substituent (as a part of hit compound **10**) at position 7 of purine core is essential to maintain high *anti*-TB activity (Table 1).

Firstly, structural modifications of compound **10** were focused on position 2 of the purine scaffold. To follow these changes rationally, we were inspired by the study of Gundersen et al. [26,27] reporting highly active purine derivatives containing various benzyl moieties at position 9. In this work, small hydrophobic substituents, e.g. chlorine attached to position 2 of the purine moiety exerted the highest antitubercular activity [26,27]. Considering this fact, derivatives containing a halogen at position 2 (i.e., **23a**, **24**, **39**, **41–53**, **67–68**, **82–83**) that usually served as the intermediates in the synthesis of final compounds were also tested for their potential antitubercular activity (Table S1). However, only a few exhibited weak antimycobacterial activity, while the majority were completely inactive.

Next, we inspected the effect of the 2-morpholino substitution on *anti*-TB activity. Various secondary and primary amines were introduced

at position 2, while the rest of the structural features related to hit compound **10** were preserved (compounds **25–38**, Table 2). The introduction of the morpholine analogues, i.e., six-membered secondary amines like piperidine (**30**) and thiomorpholine (**33**), slightly enhanced the *anti*-TB activity (MIC₉₉ = 2 μM). Derivative **27**, having a pyrrolidine heterocycle, exerted a two-to four-fold drop in the activity compared to compound **10**, whilst analogue **38**, bearing a spirocyclic morpholine analogue, completely lost *anti*-TB activity. The incorporation of other amines also led to completely inactive compounds. Derivative **35**, bearing a non-cyclic secondary cyclopropyl (methyl)amino group at position 2, delivered moderate *anti*-TB activity (MIC₉₉ = 16 μM). N¹-Methylation yielded compound **40** with significantly decreased *anti*-TB activity (MIC₉₉ = 32 μM). Intriguingly, the nitrogen at position 9 proved to be a decisive factor responsible for the *anti*-TB activity, as the 9-deazapurine analogue **84** was completely inactive.

6-Oxo group replacement by various alkylamino, alkoxy or alkylthio groups showed promising results in terms of antimycobacterial activity. Accordingly, compounds containing amino (**64**), ethylamino (**56**), and ethoxy (**73**) groups at position 6 were the most active (Table 2), surpassing the *anti*-TB activity of hit compound **10**, both with MIC₉₉ values of 1 μM. Methylamino (**54**), methoxy (**72**), and methylthio (**74**) analogues showed slightly lower MIC₉₉ values compared to their ethyl analogues **56**, **73**, and **75**, respectively. Elongation of the alkylamino groups at position 6 of the purine core led to a slight drop in antitubercular activity compared to ethylamino derivative **56**. Derivatives containing the propylamino (**57**) and butylamino (**58**) moieties at position 6 of the purine scaffold demonstrated *anti*-TB activity identical to hit compound **10** (MIC₉₉ = 4 μM), whilst cyclobutylamine (**59**) and benzylamine-containing derivative **63** showed slightly better activity (MIC₉₉ = 2 μM). The presence of secondary amines at position 6 was not favorable and N,N-dimethylamino derivative **55** also revealed lower activity (MIC₉₉ = 8 μM). The incorporation of bulkier secondary amines such as morpholine in 2,6-dimorpholino analogue **69** led to complete activity loss (MIC₉₉ = 125 μM) and the replacement of the oxo group by chlorine led to a drop in activity (compound **71**, MIC₉₉ = 16 μM).

Next, we inspected the efficiency of non-substituted derivatives at position 2 as such purine-based compounds were reported to possess an *anti*-TB profile [27–32]. Note that many of those highly active derivatives were also endowed with sulfanyl and oxo groups at position 6. In line with these prerequisites, 6-chloro (**78**), 6-oxo (**79**), and 6-sulfanyl derivatives (**80**) were prepared. In addition, compound **70** bearing two sulfanyl groups at positions 2 and 6 was developed. Unfortunately, all of them turned out to be inactive (Table 2).

By setting the cut-off at an MIC value of 2 μM for *Mtb* H₃₇Rv, we highlighted derivatives **10**, **30**, **33**, **56**, **59**, **63**, **64**, **72**, and **73** and tested them against clinically isolated MDR-TB and XDR-TB strains (Table 3). Pleasingly, the most active compounds **56**, **64**, and **73** against *Mtb* H₃₇Rv strain also demonstrated high potency (MIC₉₉ = 2–4 μM). Furthermore, we explored the ability of compound **56** to kill intracellularly localized *Mtb* H₃₇Rv using infected MonoMac6 cell model [33,34]. In the pilot experiment, we first determined that IC₅₀ value of compounds **56** against MonoMac6 cells was 57 ± 11 μM after 48 h of incubation. Based on IC₅₀ value we chose the concentration of 25 μM (~half IC₅₀) for the following pilot experiment and found that compound **56** at this

Table 2

In vitro antimycobacterial activities of final compounds 25–38, 40, 54–66, 69–75, 78–80 and 84. Activity is expressed as MIC₉₉ (μM) assessed after (7), 14 or 21 days of incubation.

Compound	Structure	<i>Mtb</i> H ₃₇ Rv MIC ₉₉ (μM)	<i>M. avium</i> MIC ₉₉ (μM)	<i>M. kansasii</i> MIC ₉₉ (μM)
		14/21 days	14/21 days	7/14/21 days
25		250/500	>500/>500	250/500/500
26		>500/>500	>500/>500	>500/>500/>500
27		8/16	>500/>500	>500/>500/>500
29		>500/>500	>500/>500	>500/>500/>500
30		2/4	>500/>500	>500/>500/>500
31		>500/>500	>500/>500	>500/>500/>500
32		>500/>500	>500/>500	>500/>500/>500
33		2/4	>500/>500	32/64/125
34		>500/>500	>500/>500	>500/>500/>500
35		16/16	>500/>500	125/250/500
36		>500/>500	>500/>500	>500/>500/>500
37		>500/>500	>500/>500	>500/>500/>500
38		>500/>500	>500/>500	>500/>500/>500
40		32/64	>500/>500	500/>500/>500
54		4/4	>500/>500	8/8/8
55		8/16	500/500	32/64/125
56		1/1	250/250	4/8/8
57		4/4	125/125	8/8/16
58		4/4	64/125	8/8/8

(continued on next page)

Table 2 (continued)

Compound	Structure	<i>Mtb</i> H ₃₇ Rv MIC ₉₉ (μM)	<i>M. avium</i> MIC ₉₉ (μM)	<i>M. kansasii</i> MIC ₉₉ (μM)
		14/21 days	14/21 days	7/14/21 days
59		2/4	250/500	8/8/8
60		32/64	>500/>500	64/125/250
61		32/64	500/500	64/125/125
62		8/8	250/500	64/64/64
63		2/4	64/64	4/4/8
64		1/2	>500/>500	4/8/16
65		4/8	>500/>500	16/16/16
66		4/8	>250/>250	64/64/64
69		125/125	250/500	125/125/250
70		>500/>500	>500/>500	>500/>500/>500
71		16/16	>500/>500	16/32/64
72		2/4	250/500	16/32/64
73		1/2	>500/>500	8/16/16
74		8/8	>500/>500	32/64/64
75		4/4	>500/>500	32/64/125
78		125/125	>1000/>1000	1000/>1000/>1000

(continued on next page)

Table 2 (continued)

Compound	Structure	<i>Mtb</i> H ₃₇ Rv MIC ₉₉ (μM)	<i>M. avium</i> MIC ₉₉ (μM)	<i>M. kansasii</i> MIC ₉₉ (μM)
		14/21 days	14/21 days	7/14/21 days
79		>500/>500	>500/>500	125/>500/>500
80		>500/>500	>500/>500	>500/>500/>500
84		>500/>500	>500/>500	>500/>500/>500

Table 3

In vitro antimycobacterial activities of the most potent purine compounds **10**, **30**, **33**, **56**, **59**, **63**, **64**, **72** and **73** and common *anti*-TB drugs against clinically isolated MDR/XDR strains of *Mtb*.^{a,b}

	<i>Mtb</i> (MDR/XDR strains)						
	PRAHA 1	PRAHA 4	PRAHA 131	9449/2007	234/2005	7357/1998	8666/2010
10	32/64	16/32	32/32	32/64	16/32	32/64	32/64
30	16/16	8/16	8/16	8/16	16/16	16/16	8/8
33	16/16	8/16	8/16	8/16	16/16	16/16	8/8
56	ND	ND	2/4	2/4	ND	ND	2/2
59	4/4	4/8	4/8	4/8	4/8	4/8	4/8
63	4/4	4/4	4/4	4/4	2/4	2/4	4/4
64	ND	ND	2/4	2/4	ND	ND	2/4
72	16/16	8/16	8/16	8/16	16/16	16/16	8/8
73	ND	ND	2/4	2/4	ND	ND	2/2
INH	16 (R)	16 (R)	16 (R)	64 (R)	16 (R)	16 (R)	32 (R)
EMB ^b	32 (R)	16 (R)	32 (R)	8 (S)	16 (R)	16 (R)	16 (R)
RIF	>8 (R)	>8 (R)	>8 (R)	>8 (R)	>8 (R)	>8 (R)	>8 (R)
STR ^b	16 (R)	>32 (R)	>32 (R)	>32 (R)	32 (R)	>32 (R)	>32 (R)
AMI ^b	0.5 (S)	1 (S)	>32 (R)	0.5 (S)	0.5 (S)	1 (S)	2 (S)
GEN ^b	1 (S)	0.5 (S)	>8 (R)	1 (S)	0.25 (S)	1 (S)	2 (S)
CFZ ^b	0.5 (R)	0.5 (R)	0.25 (S)	0.125 (S)	0.125 (S)	0.125 (S)	2 (R)
OFX ^b	1 (S)	>16 (R)	16 (R)	2 (S)	0.5 (S)	8 (R)	8 (R)

^a The result are expressed as MIC₉₉ (μM) after 14 and 21 days of incubation and 14 days of incubation of *anti*-TB drugs.

^b AMI, amikacin; CFZ, clofazimine; GEN, gentamicin; OFX, ofloxacin; STR, streptomycin; R, resistant; S, susceptible.

concentration reduced the CFU count of intracellular *Mtb* H₃₇Rv in MonoMac6 cells by ≥ 80% compared to untreated control.

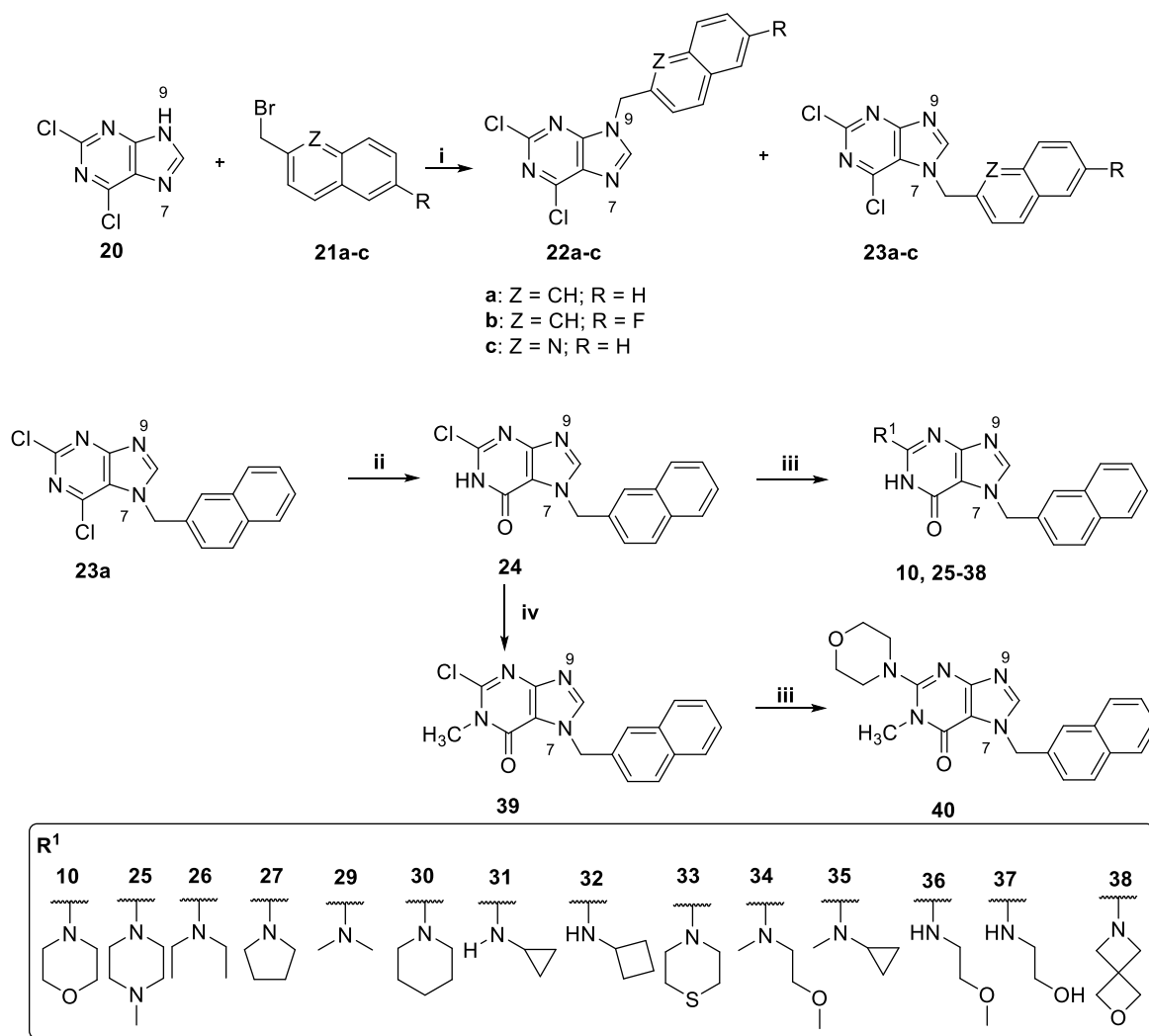
To summarize the observation from *anti*-TB activities against *Mtb* H₃₇Rv and MDR/XDR-TB, the essential features to preserve high anti-tubercular activity in the purine-based class of *anti*-TB agents developed herein are associated with i) the presence of 6-oxo, 6-alkoxy or 6-alkylamine substitution, ii) retaining a six-membered cyclic amine in position 2, iii) fixing the nitrogen atom at N9, and iv) the presence of a 7-(naphthalen-2-yl)methyl moiety at N7 of the purine (Fig. 4).

6-Ethylamino derivative **56** was selected as a new lead candidate for final structure optimization. Initially, we introduced the fluorine at the naphthyl 6-position to prevent possible metabolization/oxidation of the naphthalene core [35]. This structural change was expected to yield a derivative with improved microsomal stability and higher *anti*-TB potency than derivative **56**. The second structural modification was the replacement of naphthalene by quinoline, mainly to improve water solubility. Both structural changes resulted in a minor drop in activity (from MIC₉₉ = 1 μM to MIC₉₉ = 4 μM) for both 6-fluoronaphthalene (**65**) and quinoline derivatives (**66**).

Antibacterial activity. To shed light on the interspecies selectivity, we evaluated the antibacterial activity in top-ranked *anti*-TB purine-based compounds, namely **4**, **5**, **10**, **26**, **30**, **33**, **35**, **54**, **55**, **56**, **57**, **58**, **59**, **60**, **63**, **64**, **65**, **66**, **71**, **72**, **73**, **74**, and **75**. The compounds underwent testing against eight bacterial strains (*Staphylococcus aureus* subsp. *aureus*, methicillin-resistant *S. aureus* subsp. *aureus*, *S. epidermidis*, vancomycin-resistant *Enterococcus faecium*, *Escherichia coli*, *Klebsiella pneumoniae* ESBL negative, *Klebsiella pneumoniae* ESBL positive, multidrug-resistant *Pseudomonas aeruginosa*). None of the compounds

exhibited any antibacterial effect (see Table S5, Supporting Information), suggesting the high mycobacterial specificity of this class of compounds. Only derivative **59**, containing cyclobutylamine at the 6-position, showed mild antibacterial activity against all four strains of gram-positive bacteria (*S. aureus* subsp. *aureus*, methicillin-resistant *S. aureus* subsp. *aureus*, *S. epidermidis* and vancomycin-resistant *Enterococcus faecium*). Notably, the most active *anti*-TB compounds (i.e., **56**, **64** and **73**) were inactive against all bacterial strains even at the highest tested concentration (125 μM).

In Vitro Effects of the Investigated Compounds on Cell Proliferation. The cytotoxicity of final compounds exerting high anti-mycobacterial activity (**4**, **5**, **10**, **30**, **33**, **35**, **54–60**, **63–66**, and **71–75**) was evaluated using the well-established cell-line model in TB drug discovery, human hepatocellular carcinoma cells (HepG2) [36]. Initially, we determined IC₅₀ values for HepG2 cell line after 24 h incubation with studied compounds (Table 4). Data revealed that *Mtb* MIC values were substantially lower than HepG2 IC₅₀ values that ranged between 18.9 μM and >125 μM, suggesting an excellent selectivity profile (SI; calculated as the ratio between HepG2 IC₅₀ and *Mtb* H₃₇Rv MIC₉₉). The only exception was derivative **60** with SI value < 1; the other molecules displayed SI ranging between 4.09 (**71**) – >125 (**64**). Thus, derivatives **56** and **64** were promoted not only for their high antitubercular efficacy (both *Mtb* H₃₇Rv MIC₉₉ = 1 μM), but also for their low cytotoxicity profile (**56**: HepG2 IC₅₀ = 63.88 μM, SI = 63.88; **64**: HepG2 IC₅₀ > 125 μM; SI > 125), suggesting a large therapeutic window of these compounds. These positive outcomes were confirmed by additional experiments in which selected derivatives **10**, **30**, **33**, **56**, **64**, **72**, and **73** were incubated with HepG2 and with noncancerous rat



Scheme 1. Synthesis of purine-based compounds **10**, **25–38** and **40**^a. ^a Reagents and conditions: (i) K₂CO₃, DMF, 24 h, RT, 16–23%; (ii) 1 M NaOH, 100 °C, 24 h, 94%; (iii) MW, amine, *t*-BuOH, 110 °C, 150 W, 3 h, 39–62%; (iv) NaH, iodomethane, DMF, 4 h, RT, 62%.

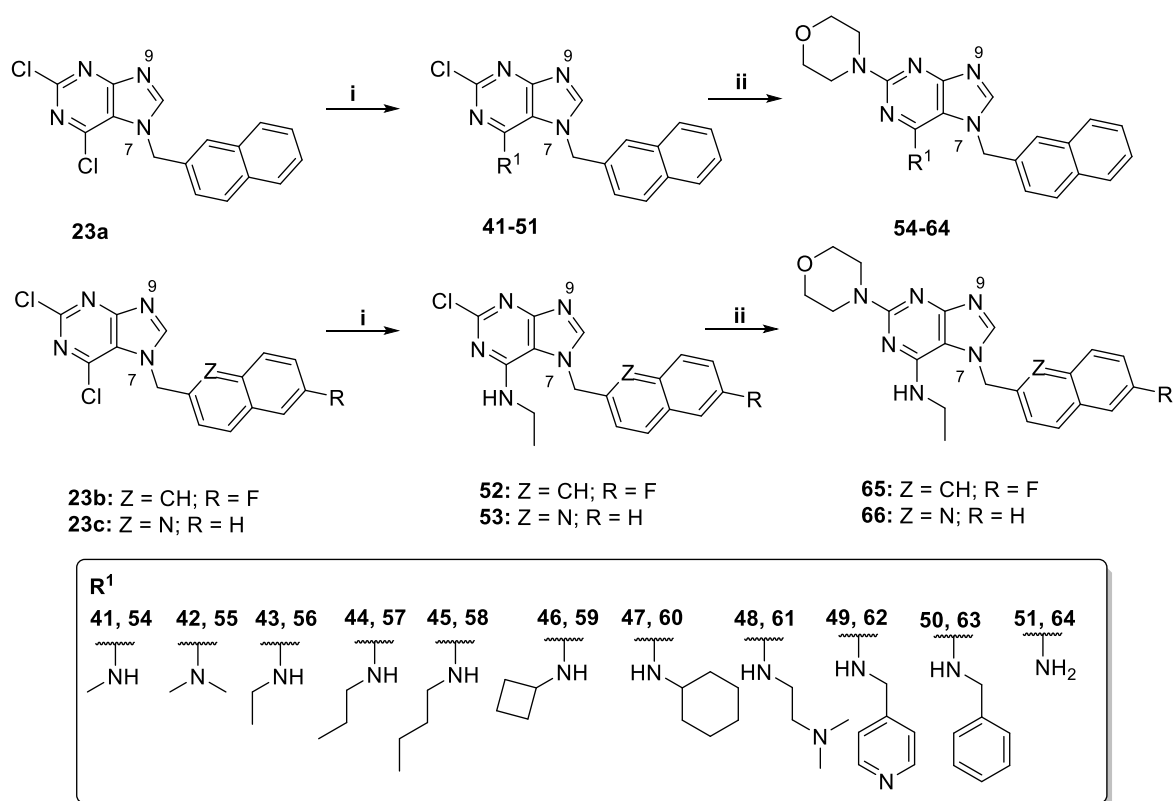
heart myoblast H9c2 cell lines for 72 h. However, longer incubation times led to the precipitation of some of the studied compounds in the cell culture medium. Therefore, when IC₅₀ was not reached, the data were presented as the percent of cell viability at a concentration of 50 μM (cell viability of control vehicle-treated samples was set as 100%). Importantly, these experiments with prolonged incubation times confirmed the limited cytotoxicity of the studied compounds (Table 5).

Aqueous solubility, microsomal and plasma stability evaluation. Aqueous solubility is a fundamental prerequisite for delineating the drug's ADME properties. In this study, we determined this feature for the initial hit **10** and other compounds exerting *Mtb* H₃₇Rv MIC₉₉ below 4 μM (**30**, **33**, **56**, **59**, **63**, **64**, and **73**). The results show that the introduction of alkylamino and ethoxy-groups at position 6 is beneficial in enhancing aqueous solubility. Indeed, the derivatives with cyclobutylamino **59** (159 μM), ethylamino **56** (150 μM), amino **64** (98 μM), ethoxy **73** (81 μM) and benzylamino **63** (59 μM) groups at position 6 showed better solubility profile than oxo derivatives **10** (47 μM), **33** (9 μM) and **30** (8 μM). In the series of oxo derivatives **10**, **30** and **33**, replacement of morpholine at position 2 of compound **10** by piperidine in compound **30** and by thiomorpholine in compound **33** led to a decrease in solubility (Table 6).

To investigate the drug-likeness of the studied purines, human liver microsomal (HLM) and plasma stabilities were also addressed. Herein, we used reference drugs diazepam and verapamil with low and high

metabolic clearance, respectively, and compared their HLM stability after 45 min of incubation with selected lead candidates from newly developed purine-based family of antitubercular agents (Table 6). In line with the literature, microsomal stability of verapamil displayed high intrinsic clearance (CL_{int} = 146 μL/min/mg) and short half-life (T_{1/2} = 9.53 min), whereas diazepam exerted low metabolic clearance (CL_{int} = 3.2 μL/min/mg) and long half-life (T_{1/2} = 433 min) [37,38]. Hit compound **10** revealed the highest metabolic stability from the newly tested compounds as expressed by HLM T_{1/2} and CL_{int}, showing ten times higher microsomal stability than verapamil, but four times lower compared to diazepam. All other compounds displayed microsomal stability spanning between the values of the reference drugs. As expected, the lowest stability was found in derivative **33** due to the presence of thiomorpholine group which is prone to sulfur oxidation. The most potent compounds **56**, **64** and **73** can be classified as compounds with medium clearance with respect to phase I metabolic deactivation [39]. Presuming that these compounds follow first-order kinetics, it can be expected that they will not accumulate in the body when properly dosed, and simultaneously are stable enough to exert their pharmacodynamic effect.

Finally, plasma stability of the studied compounds has been observed after 2 h incubation, indeed all the compounds including **56**, **64** and **73** demonstrated high plasma stability. Overall, compounds tested for hepatic clearance and plasma stability did not reveal any structural



Scheme 2. Synthesis of purine-based compounds **54–66**^a. ^a Reagents and conditions: (i) appropriate amine, CH₃CN, 24 h, 45 °C, 45–98%; (ii) morpholine, MW, dioxane/water, 180 °C, 150 W, 3 h, 34–81%.

liabilities. From this perspective, the compounds can be recommended for *in vivo* pharmacokinetic study.

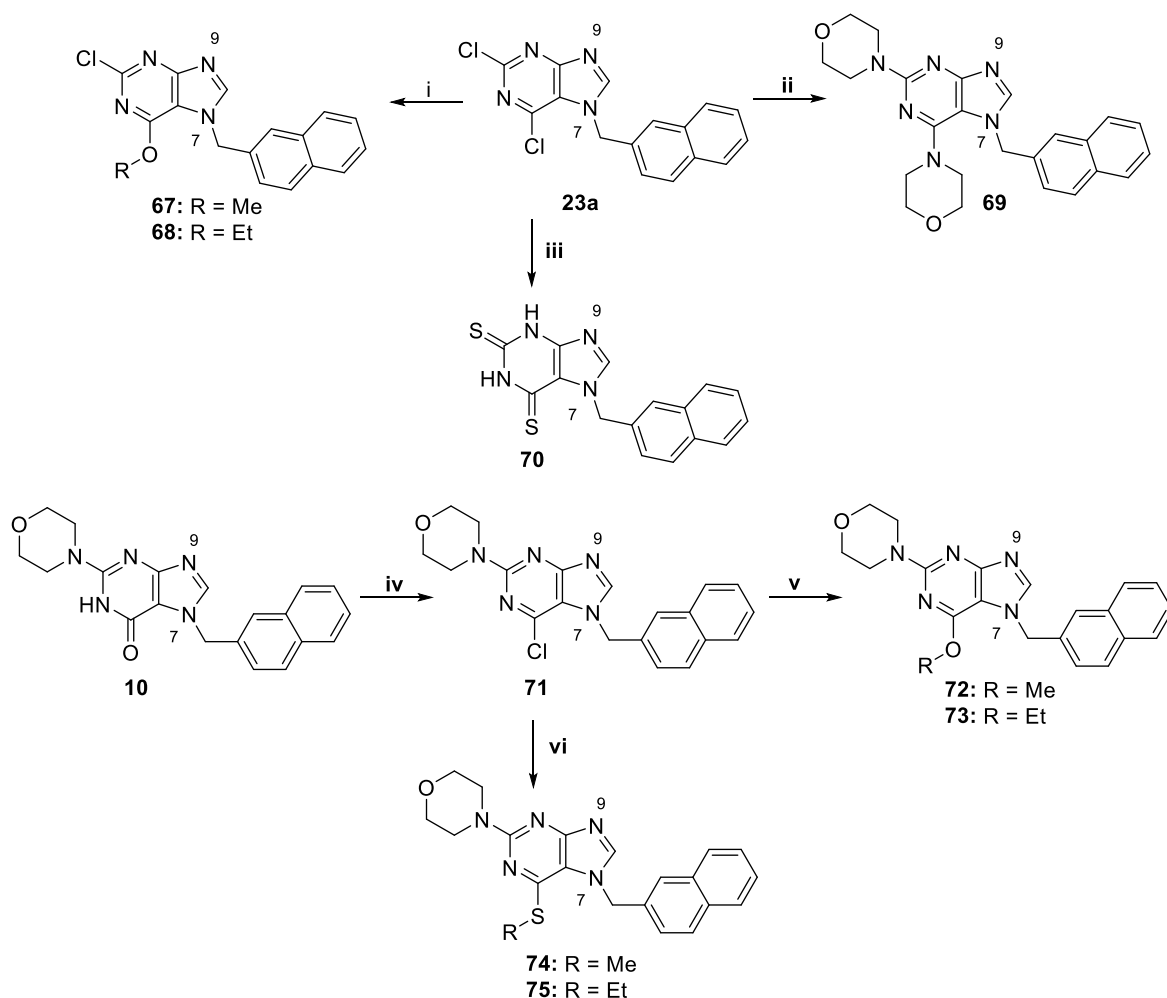
Identification of On-Target Mode of Action. To gain insight into the mechanism of anti-tuberculosis action of 2,6-disubstituted 7-(naphthalen-2-ylmethyl)-7H-purines, spontaneous H₃₇Rv mutants resistant to compound **10** were selected and characterized. Selection on solid media containing 128 μM, 64 μM and 32 μM of compound **10** led to the selection of resistant colonies at a similar frequency of resistance of around 1×10^{-8} (five to eight colonies following the plating of 50 μL of OD₆₀₀ = 50). Three resistant colonies from the selection on 128 μM of compound **10** were confirmed to be fully resistant to **10** (MIC > 128 μM) and subjected to whole genome sequencing together with the parental H₃₇Rv strain. Variant analysis identified two isolates to share an identical genome, with non-synonymous mutations in *dprE1* (Rv3790: t1103c - > L368P) as well as a mutation in *Rv1356c* (t103 g - > W35G). The third resistant strain carried another mutation in *dprE1* (Rv3790: g661c - > E221Q), while sharing the mutation in *Rv1356c* and a synonymous mutation in *nuoL* Rv3156. With DprE1 being an essential protein in *Mtb*, and as the identified loci of resistance were previously described in resistance to other DprE1 targeting agents [17,19,20], DprE1 was considered the most likely target from this analysis. As *Rv1356c* encodes for a non-essential conserved hypothetical protein, it was considered unlikely to be a primary target of **10**, though its potential role in resistance was not further investigated.

Previously we showed that inhibition of DprE1 in mycobacteria leads to accumulation of specific extractable cell wall lipids, trehalose dimycolates and trehalose monomycolates [40,41]. This effect is caused by a defect in the synthesis of the cell wall arabinan chains, which serve as primary attachment sites for mycolic acids. To investigate this phenomenon for the developed purine derivatives, we performed [¹⁴C]-acetate labeling of *Mtb* H₃₇Rv grown in the presence of hit compound **10** and its potent alkylamino and alkoxy analogues **56** and **73**, respectively. As shown in Fig. 5, lipid profiles of bacteria treated with

the tested compounds and the control drug BTZ-043 were comparable, which supports DprE1 being the target of purine-based compounds described in this work.

Proposed Binding Mode of Selected Purine-Based Compounds in the Active Site of DprE1. To identify the plausible binding mode of compound **10** and the most active representative **56** from the series, we carried out a molecular modeling study in tandem with molecular dynamic simulations. Moreover, we also modeled compound **11** as a regioisomer of **10**, and deazapurine derivative **84**, both demonstrating no antimycobacterial activity, to justify the results obtained from *in vitro* testing. The selection of DprE1 crystal structure (PDB ID: 4P8N) used for the *in silico* experiments was justified by the i) high resolution of DprE1 crystal structure (1.79 Å) and ii) non-covalent nature of inhibitors, namely 2-carboxyquinoxaline QN118, soaked into DprE1 enzyme [20]. The docking protocol reproduced the crystallographic pose of QN118 (data not shown). Across all the experimental results, no significant change in the conformation and shape of the active site and the cofactor FAD was observed.

Initially, the hit compound **10** revealed that the purine core is accommodated in the FAD vicinity (Fig. 6A and B), similarly to other non-covalent DprE1 inhibitors [15]. Oxygen from the morpholine ring is engaged in a hydrogen bond with the backbone amide of Asn385. Most importantly, N3 and N9 of compound **10** form hydrogen bonds with the protonated terminal amino group of Lys418. The naphthalen-2-yl-methyl moiety occupies the pocket of the enzyme formed by Leu317, Asp318 and Phe320, forming a coplanar conformation; the latter two interactions seem to be pivotal in delivering DprE1 affinity. Similarly, the top-ranked candidate from the family of purine-based derivatives, compound **56**, displayed very close spatial orientation in the DprE1 active site as ligand **10** (Fig. 6G and H). These interactions account for i) the hydrogen bond between morpholine oxygen and Asn385, ii) the hydrogen bond between N9 and the protonated terminal amino group of Lys418, and iii) purine lodging in the proximity



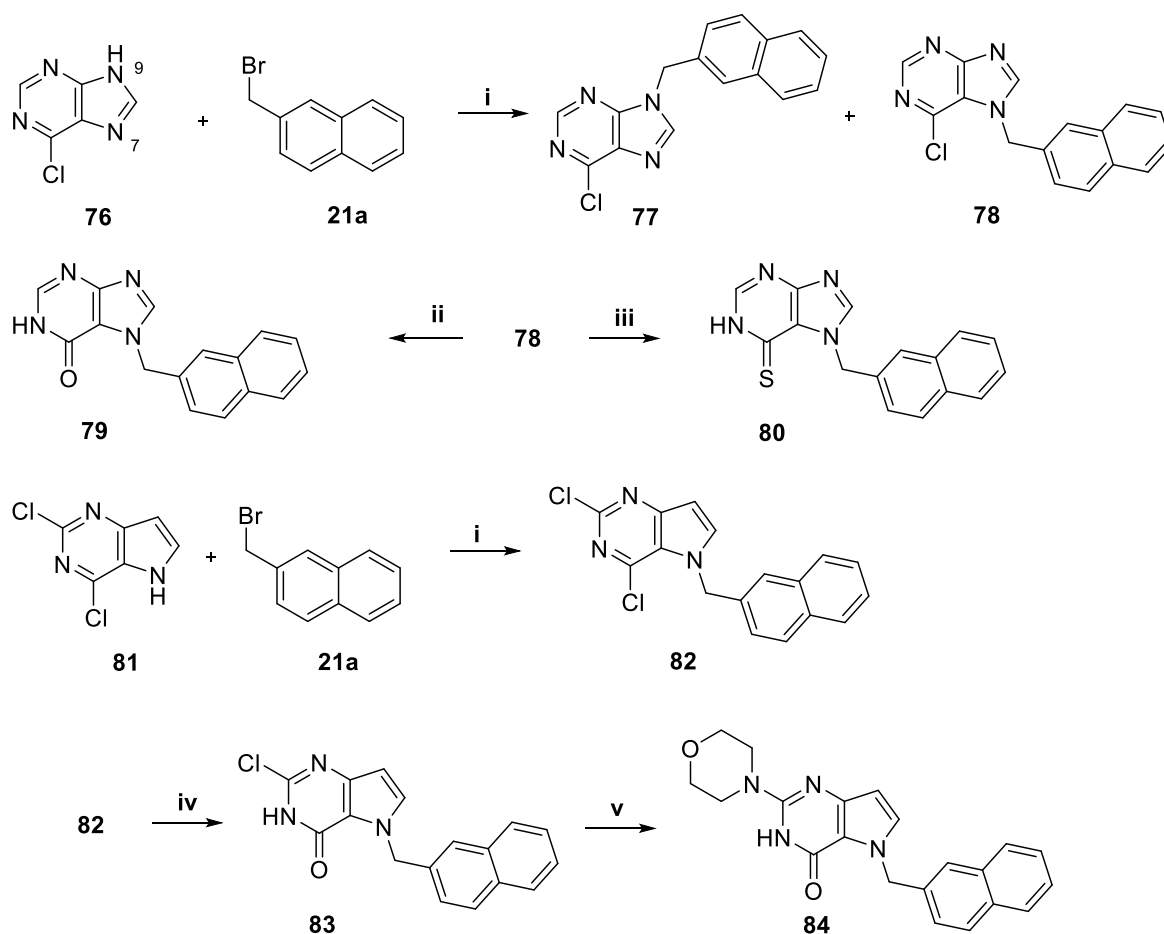
Scheme 3. Synthesis of purine-based compounds **67–75**. ^a Reagents and conditions: (i) sodium alkoxide, alcohol, reflux, 2 h, 64–74%; (ii) morpholine, MW, dioxane/water, 180 °C, 150 W, 3 h, 76%; (iii) thiourea, EtOH, reflux, 24 h, 87%; (iv) POCl₃, 0 °C–135 °C, 3 h, 48%; (v) sodium alkoxide, THF, 25 °C, 2 h, 61–90%; (vi) sodium thiolate, THF, 25 °C, 2 h, 91–93%.

of FAD. Interestingly, the naphthalen-2-yl-methyl moiety of **56** likely occupies a different hydrophobic area than **10**, interacting in a bent-shaped conformation with Phe362, Leu363, Leu317 and Pro316. Such peculiarity has also been observed in the crystallography study with the 2-carboxyquinoxaline derivative QN118, where 3-fluoro-4-methoxybenzylamine moiety of QN118 imposed two alternative conformations, swinging between the two hydrophobic pockets [20]. Additionally, the *N*-ethyl appendage of **56** protrudes to the region delineated by Lys134, Gly117, His132 and Tyr314, which might be designated as being responsible for slightly enhanced antitubercular activity and also DprE1 affinity compared to **10**. According to *in silico* prediction, Glu221 and Leu368, whose mutations to Gln and Pro, respectively, caused resistance to compound **10**, neither interact nor lie in the close vicinity of compound **10** in the active site of DprE1 (Figs. 6A and 7). Indeed, the nearest interatomic distance between compound **10** and Leu368 is 7.0 Å (not shown), indicating no ligand-amino acid interaction. This is surprising at first glance and seemingly calls into question the results of the prediction, where an interaction between these residues and compound **10** would be expected. Nonetheless, the same mutations have been described to cause resistance to other DprE1 inhibitors, such as QN118 analogue Ty38c (resistance-causing mutation L368P) [20] or TCA1 (resistance-causing mutation E221Q) [17,19], and these inhibitors also do not bind to the close vicinity of these residues and do not interact with them. Another DprE1 inhibitor, whose activity is hampered by L368P and E221Q mutations, is antibacterial agent **14**,

pyrido-benzimidazole derivative identified by high-throughput screening of the GlaxoSmithKline (GSK) collection [42]. Despite the absence of direct interactions between these inhibitors including compounds **10** and **56** with Glu221 and/or Leu368, we can speculate that their mutations induce conformational changes of the binding pocket and affect the interaction with these inhibitors. Accordingly, we can expect similar binding modes of compounds **10**, Ty38c and TCA1 into the DprE1 binding pocket (Fig. 7).

On the contrary, the inactive regioisomer **11** (Fig. 6C and D) displayed a 180° rotated topology compared with DprE1-active ligands **10** and **56**. Indeed, such orientation cannot result in a productive interaction with the DprE1 enzyme as the ligand **11** is completely distorted, shifted outwards the FAD cofactor, with N9 engaged in hydrogen bond Arg325 residue. The naphthalen-1-yl-methyl moiety is implicated in several hydrophobic interactions, specifically with His132 and Phe366 by heterogenous π - π stackings. Deazapurine derivative **84** (Fig. 6E and F) displayed similar location of the naphthalen-2-yl-methyl moiety as for compound **10**, exerting interactions with Phe320, Gly321, Glu322, and Arg325. The disparity can be observed in the core scaffold, where missing nitrogen N9 of compound **84** cannot display a hydrogen bond interaction with Lys418, thus rendering this compound completely inactive.

Chemoinformatic and QSAR analyses. Chemical structures and bacteriostatic activities of the studied compounds against *Mtb* after 14-days of incubation (*i.e.*, pMIC (14 d) values) were chemoinformatically



Scheme 4. Synthesis of purine-based compounds 79–80 and 9-deazapurine derivative 84. ^{a a} Reagents and conditions: (i) K_2CO_3 , DMF, 24 h, 25 °C; (ii) 1 M NaOH, 100 °C, 24 h, 96%; (iii) thiourea, EtOH, reflux, 24 h, 89%; (iv) 2 M NaOH/dioxane, 100 °C, 2 h, 72%; (v) morpholine, MW, dioxane/water, 180 °C, 150 W, 3 h, 81%.

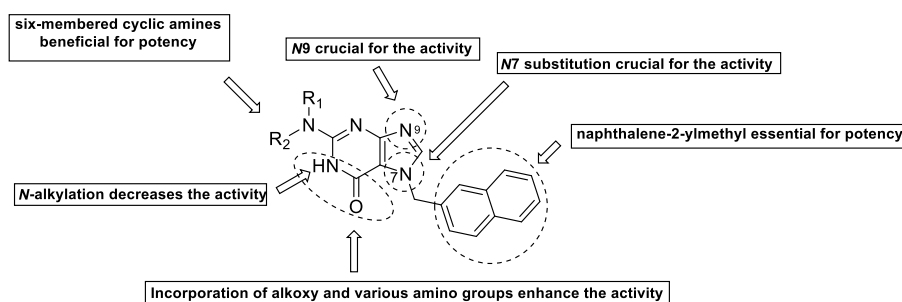


Fig. 4. Highlighted observations from the SAR study in the family of 2,6-disubstituted 7-(naphthalen-2-ylmethyl)-7H-purines as antitubercular agents.

analyzed with AutoQSAR and 3D Field-Based QSAR applications in Schrodinger 2022–2. Furthermore, we analyzed the atomistic fingerprint contributions and contributions of five Gaussian interaction fields determined by 3D QSAR models to the antimycobacterial activities of studied compounds. For a detailed description, see [Supporting information](#). In summary, the QSAR analyses suggested that the antimycobacterial activity of the studied compounds is enhanced by hydrophobic substituents at position 2 and 6 of the purine core. However, the size of substituents at position 6 should be limited to a certain level, otherwise they decrease the activity. The activity is also supported by a higher potency of the substituents at position 6 to provide hydrogen bonds, which corresponds well with the requirement of a lower electron density in this region, as follows from the contour map for the electrostatic interaction field. Nonetheless, all these interaction fields are

necessary to consider simultaneously for rich reliable activity predictions based on the developed 3D QSAR model. Both QSAR models developed in this study by the AutoQSAR and 3D-Field QSAR analyses proved statistical significance, mutual correspondence and are, therefore, suitable for application, for example, in ligand-based virtual screening.

3. Conclusions

In this study, whole-cell phenotypic screening of the in-house compound library identified purine derivative 10 with high *anti*-TB activity against *Mtb* H₃₇Rv strain (MIC₉₉ = 4 μM). The extensive structure-activity relationships study underlined the importance of the naphthalen-2-yl methyl moiety attached at position 7 of the purine core

Table 4

Viability of mammalian cell line determined after 24 h of treatment with newly developed purine-based compounds **4**, **5**, **10**, **30**, **33**, **35**, **54**, **60**, **63–66**, and **71–75**.^a For the sake of clarity, *Mtb* H₃₇Rv MIC₉₉ values are also displayed.

Compound	HepG2 IC ₅₀ ± SD (μM) ^a	<i>Mtb</i> H ₃₇ Rv MIC ₉₉ (μM)	SI ^b
4	>125	16	>7.8
5	>125	16	>7.8
10	>125	4	31.25
30	87.2 ± 10.9	2	43.6
33	>32	2	16
35	>125	16	>7.8
54	58.8 ± 9.6	4	14.7
55	55.9 ± 1.2	8	6.99
56	63.9 ± 4.8	1	63.88
57	40.5 ± 4.7	4	10.1
58	30.8 ± 3.4	4	7.7
59	33.0 ± 4.2	2	16.5
60	18.9 ± 3.1	32	0.59
63	33.8 ± 2.5	2	16.9
64	>125	1	>125
65	40.7 ± 4.4	4	10.18
66	96.4 ± 1.9	4	24.08
71	65.6 ± 5.5	16	4.09
72	64.3 ± 1.4	2	32
73	43.5 ± 9.1	1	43.45
74	42.4 ± 3.5	8	5.3
75	64.2 ± 0.1	4	16.1

^a IC₅₀ determined after 24 h incubation.

^b selectivity index calculated as ratio between HepG2 IC₅₀ and antitubercular MIC₉₉ values.

Table 5

Viability of two mammalian cell lines determined after 72 h of treatment with purine-based compounds **10**, **30**, **33**, **56**, **64**, **72** and **73**.^a

	HepG2 Viability (%) at 50 μM ± SD	IC ₅₀ (μM)	H9c2 Viability (%) at 50 μM ± SD	IC ₅₀ (μM)
10	60.5 ± 6.4	59.01	86.0 ± 0.9	>50
30	42.2 ± 11.8	54.82	79.4 ± 1.6	>50
33	72.9 ± 8.9	>50	97.1 ± 3.5	>50
56	66.9 ± 15.0	>50	88.0 ± 3.2	>50
64	77.0 ± 3.3	>50	91.7 ± 4.8	>50
72	66.4 ± 13.2	>50	92.6 ± 3.4	>50
73	23.5 ± 9.8	33.14	94.8 ± 5.4	>50

^a Data are presented as mean values with SD obtained from at least four independent experiments. IC₅₀ values were calculated using GraphPad Prism 9 software.

Table 6

Aqueous solubility (5% DMSO/water), microsomal stability expressed as microsomal half-life (T_{1/2}) and intrinsic clearance (CL_{int}) and plasma stability (%) for selected purine-based compounds. Diazepam and verapamil were included as reference drugs with low and high intrinsic clearance, respectively.

Compound	Aqueous solubility [μM]	HLM T _{1/2} (min)	Human CL _{int} (μL/min/mg)	Plasma stability (%) ^b
diazepam	n.d.	433.0	3.2 (2.6) ^a	n.d.
verapamil	n.d.	9.53	146.0 (138.7) ^a	n.d.
10	46.9	110.0	12.6	96.6
30	8.4	17.8	77.9	96.7
33	9.3	10.9	127.0	98.2
56	150.4	51.3	27.0	95.5
59	158.9	37.9	36.6	97.5
63	58.9	19.3	72.1	99.2
64	97.7	82.5	16.8	103.3
73	81.3	56.8	24.4	99.6

^a Calculated from published data [39] – shown for comparative purposes.

^b percentage of remaining compound after 120 min incubation.

^c n.d. stands for not determined.

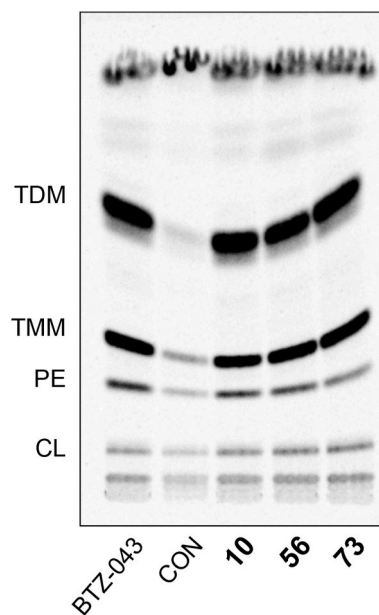


Fig. 5. TLC analysis of [¹⁴C]-acetate labeled lipids from *Mtb* H₃₇Rv grown in the presence of **10**, **56** and **73**. Concentrations of the drugs in media were at 10 × MIC. TDM – trehalose dimycolates, TMM – trehalose monomycolates, PE – phosphatidyl ethanolamine, CL – cardiolipin, CON – control culture (without a drug).

in retaining high *anti*-TB activity. Interestingly, isomer **9** bearing naphthalen-2-yl-methyl moiety at position 9, naphthalen-1-yl-methyl analogue **11** and also 9-deazapurine derivative **84** were inactive. Further structure modifications showed that secondary cyclic amines bound at the 2-position were advantageous for *anti*-TB activity, while primary or acyclic secondary amines reduced the activity. Structural modification at position 6 (the “lactam region”), *i.e.*, the replacement of the oxo group by alkoxy, alkylthio or alkylamino groups proved to be favorable in terms of conserving the activity or giving a mild potency increase. The introduction of ethylamino (**56**), amino (**64**) or ethoxy (**73**) moieties at position 6 proved to be the most beneficial for *anti*-TB activity. These derivatives even outperformed the purin-6-ones compounds in *anti*-TB activity against both the drug-susceptible strain *Mtb* H₃₇Rv (all having MIC₉₉ = 1 μM) and against several clinically isolated MDR-TB/XDR-TB strains. Purine-based compounds **56** and **64** also displayed better aqueous solubility and acceptable microsomal/plasma stabilities, and showed limited toxicity to HepG2 and to noncancerous H9c2 cell lines even after 72 h of incubation (IC₅₀ > 50 μM), which resulted in high selectivity to *Mtb*. Furthermore, pilot experiment showed that compound **56** is active also against intracellularly localized *Mtb* H₃₇Rv.

The mechanism of action of the purine-based compounds developed in this work was determined by whole-genome sequencing of mutants resistant to derivative **10**, revealing non-synonymous mutations L368P and E221Q in DprE1 enzyme. These mutations were previously reported to be responsible for the resistance to other non-covalent DprE1 inhibitors such as Ty38c [20] or TCA1 [17,19]. In line with this observation, the mechanism of action of compounds **10** and its alkylamino and alkoxy analogues **56** and **73**, respectively, was confirmed based on their effect on the cell wall biosynthesis in *Mtb* H₃₇Rv via [¹⁴C]-acetate radiolabeling experiments and their structure-binding relationships with respect to DprE1, predicted *in silico*.

In conclusion, the 2,6-disubstituted 7-(naphthalen-2-ylmethyl)-7H-purines described in this study are new class of DprE1 non-covalent inhibitors with good efficiencies against drug sensitive and drug-resistant strains of *Mtb* and with high selectivity toward *Mtb* with acceptable cytotoxicity profile. The large number of structural

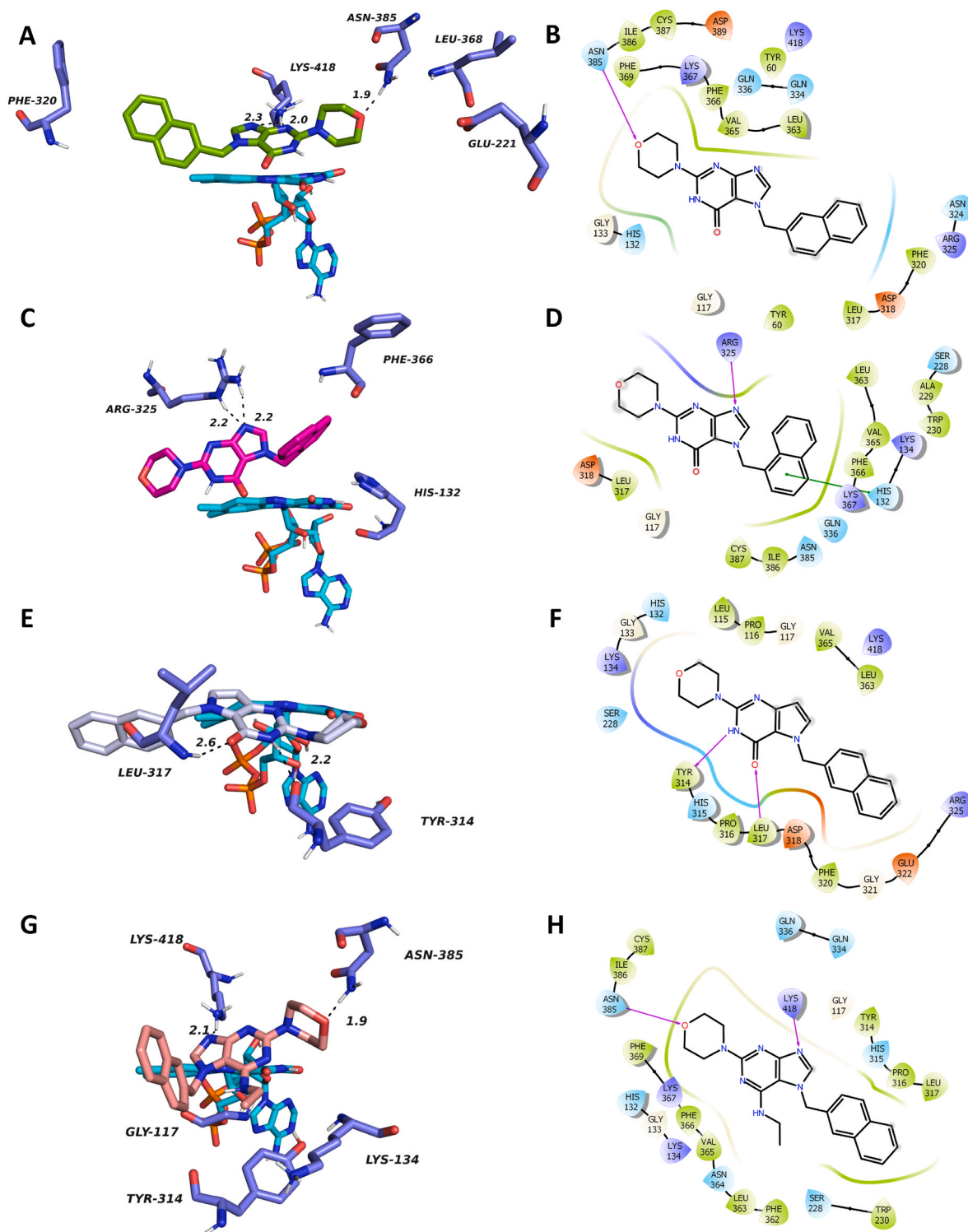


Fig. 6. The top-scored docking poses of **10** (A and B), **11** (C and D), **84** (E and F), and **56** (G and H) in DprE1 (PDB ID: 4P8N). The ligands are displayed in green (A), purple (C), grey (E) and salmon (G) for **10**, **11**, **84**, and **56**, respectively; important amino acid residues responsible for ligand anchoring are shown in dark blue, FAD cofactor is displayed in light blue. Important interactions are rendered by black dashed lines; distances are measured in angstroms (Å). Figures A, C, E, G were created with The PyMOL Molecular Graphics System, Version 2.4.1, Schrödinger, LLC. 2D figures (B, D, F, H) were generated with Maestro 12.3 (Schrödinger Release, Schrödinger, LLC, New York, NY, 2020).

modifications offered by the purine scaffold combined with the scaffold hopping strategy may lead to new highly active non-covalent DprE1 inhibitors in future. The compounds developed herein are the first non-covalent purine-based DprE1 inhibitors described to date, paving the way for further structure optimization of DprE1 inhibitors.

4. Experimental section

General. The newly developed compounds were characterized using ^1H NMR and ^{13}C NMR spectroscopy and HPLC–HRMS experiments. All compounds are >95% pure by HPLC analysis. All chemical reagents

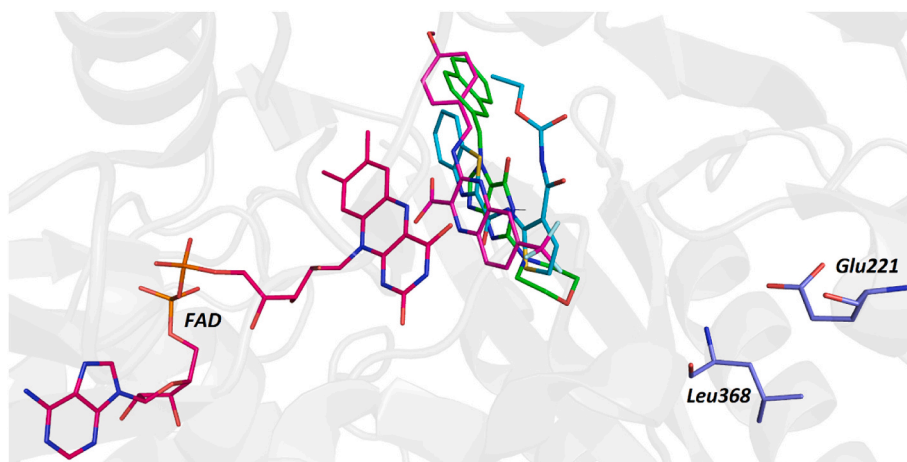


Fig. 7. Overlap between compound **10** (green), Ty38c (purple, PDB ID: 4P8K) and TCA1 (light blue, PDB ID: 4KW5) in DprE1 active site. For the sake of clarity, amino acid residues Leu368 and Glu221 are shown in dark blue sticks, FAD cofactor in red (both taken from 4KW5). Figure was created with The PyMOL Molecular Graphics System, Version 2.4.1, Schrödinger, LLC.

were obtained from Sigma-Aldrich (Schnellendorf, Germany), PENTA s. r. o. (Prague, Czech Republic), FluoroChem (Hadfield, UK) and were used as received. Solvents for chromatographic procedures were supplied in LC-MS grade. An internal standard **67** was synthesized by us and used during the experiment. A CEM Explorer SP 12 S was used for the MW-assisted reactions. The reactions were monitored by thin-layer chromatography (TLC) on silica gel plates (60 F254, Merck, Prague, Czech Republic), and the spots were visualized by UV light (254 nm). Purification of crude products was carried out using a PuriFlash Gen5 column, 5.250 (Interchim, Montluçon, France) (silica gel 100, 60 Å, 230–400-mesh ASTM, Sigma-Aldrich, Prague, Czech Republic). The NMR spectra were all recorded on a Varian S500 spectrometer (500 MHz for ^1H and 126 MHz for ^{13}C) and Jeol JNM-ECZ600R (600 MHz for ^1H and 151 MHz for ^{13}C NMR). Chemical shifts are reported in δ ppm referenced to residual solvent signals (for ^1H NMR and ^{13}C NMR: chloroform-*d* (CDCl_3 ; 7.26 (H) or 77.16 (C) ppm) or dimethylsulfoxide-*d*₆ ($\text{DMSO-}d_6$; 2.52 (H) or 39.7 (C) ppm). Spin multiplicities are given as broad singlet (bs), doublet (d), doublet of doublet (dd), triplet (t), doublet of triplet (dt), quartet (q), or multiplet (m). Coupling constants (*J*) are reported in Hz. Recorded NMR spectra are available in the Supplementary Information. Melting points were measured using an automated melting point recorder M – 565 (Büchi, Flawil, Switzerland). The synthesized compounds were analyzed by an LC-MS system consisting of UHPLC Dionex Ultimate 3000 RS coupled with a Q Exactive Plus orbitrap mass spectrometer to obtain HRMS spectra (Thermo Fisher Scientific, Waltham, Massachusetts, USA). The samples were dissolved in DMSO/methanol 50/50 (v/v). Reverse-phase C18 column Kinetex EVO (2.1 × 50 mm, 1.7 μm, Phenomenex, Torrance, CA, USA) was used as a stationary phase, and purified water with 0.1% formic acid (mobile phase A) and LC-MS grade acetonitrile with 0.1% formic acid (mobile phase B) were used as the mobile phases. Gradient elution was used to determine purities and mass spectra. The method started with 5% B for 0.3 min, then the gradient switched B to 100% in 3 min, remained at 100% B for 0.7 min and then went back to 5% B with equilibration for 3.5 min. The total run time of the method was 7.5 min. The column temperature was kept constant at 27 °C, the flow of the mobile phase was 0.4 mL/min, and the injection volume was 1 μL. Gradient LC analysis with UV detection (diode array) confirmed ≥95% purity for all the compounds. HRMS spectra were collected from the total ion current in the scan range 105–1000 *m/z*, with the resolution set to 140,000.

General Procedure 1: Preparation of compounds 23a-c. A suspension of 2,6-dichloro-9H-purine (1.0 g, 5.29 mmol), K_2CO_3 (0.88 g, 6.35 mmol) in DMF (10 mL) was stirred at RT. After 30 min, the appropriate alkyl bromide (5.82 mmol) was added and the reaction

mixture was kept stirring overnight. Water (100 mL) was added to the reaction mixture, and the suspension was extracted with CH_2Cl_2 (3 × 50 mL). The combined organics were dried over sodium sulfate, filtered and evaporated. Each regioisomer was separated *via* column chromatography with petroleum ether (PE)/ethyl acetate (EtOAc) as eluent. The desired 7-substituted derivatives were always the minor products with lower *R_f* value.

General Procedure 2: Preparation of compounds 10, 25–38. 2-Chloro-7-(naphthalen-2-ylmethyl)-6,7-dihydro-1H-purin-6-one (0.384 mmol) and the appropriate amine (1.15 mmol) were added to a sealed reaction tube with *tert*-butanol (5 mL). The reaction was carried out under microwave irradiation at 110 °C with power 150 W and maximum pressure 300 psi for 3 h. The solvent was evaporated *in vacuo* and the residue was purified by flash chromatography with CH_2Cl_2 /MeOH as eluent.

General procedure 3: Preparation of compounds 41–48, 52 and 53. A solution of compound **23a** (for the synthesis of compounds 41–48, 0.42 mmol), **23b** (for the synthesis of compound **52**, 0.42 mmol) or **23c** (for the synthesis of compound **53**, 0.42 mmol) and 5 equiv. of the appropriate amine (2.1 mmol) was stirred at 45 °C overnight in acetonitrile (15 mL). The reaction was monitored by TLC. After completion of the reaction, the solvent was evaporated to the dryness *in vacuo* and water (10 mL) was added to the reaction residue. The mixture was extracted with CH_2Cl_2 (3 × 10 mL), and the combined organic layers were dried over sodium sulfate, filtered and evaporated *in vacuo*. The product was purified by flash chromatography.

General procedure 4: Preparation of compounds 54–66. Compounds **40–52** (0.384 mmol), morpholine (0.5 g, 5.7 mmol), dioxane (5 mL) and water (1 mL) were charged to a sealed reaction tube. The reaction was carried out under microwave irradiation at 180 °C with power 150 W and maximum pressure 300psi for 3 h. After completion of the reaction, the solvent was evaporated *in vacuo*, and the mixture was purified by flash chromatography (EtOAc/MeOH, 95:5).

2-Morpholino-7-(naphthalen-2-ylmethyl)-1,7-dihydro-6H-purin-6-one (10). Compound **10** was prepared according to General Procedure 2. Morpholine was used as the starting material. The final product was purified by flash chromatography (CH_2Cl_2 /MeOH, 20:1). Yield 60% (white solid); mp 233 °C (compound decomposition). ^1H NMR (500 MHz, $\text{DMSO-}d_6$) δ 11.18 (s, 1H), 8.24 (s, 1H), 7.92–7.83 (m, 3H), 7.79 (s, 1H), 7.54–7.46 (m, 3H), 5.63 (s, 2H), 3.63 (m, 4H), 3.47 (m, 4H) ppm. ^{13}C NMR (126 MHz, $\text{DMSO-}d_6$) δ 159.04, 155.34, 152.67, 143.91, 135.30, 132.84, 132.45, 128.38, 127.81, 127.64, 126.49, 126.26, 126.14, 125.52, 108.61, 65.70, 49.27, 46.02 ppm. HRMS: *m/z* [*M*+*H*]⁺ 362.1601 (calculated for: $[\text{C}_{20}\text{H}_{19}\text{N}_5\text{O}_2]^+$ 362.1612). HPLC

purity: 99.9%.

2,6-Dichloro-7-(naphthalen-2-ylmethyl)-7H-purine (23a). Compound **23a** was prepared according to General Procedure 1.2-(Bromomethyl)naphthalene was used as alkylating agent. The final product was purified by flash chromatography (PE/EtOAc, 1:1). Yield: 23% (white solid); mp 141–143 °C. ^1H NMR (500 MHz, DMSO- d_6) δ 9.11 (s, 1H), 7.94–7.82 (m, 3H), 7.64 (s, 1H), 7.52–7.41 (m, 3H), 5.90 (s, 2H) ppm. ^{13}C NMR (126 MHz, DMSO- d_6) δ 163.63, 151.28, 143.39, 143.39, 134.21, 133.0, 132.56, 128.69, 128.0, 127.73, 126.64, 126.48, 125.32, 124.73, 122.22, 49.92 ppm. HRMS: m/z $[\text{M}+\text{H}]^+$ 329.0349 (calculated for: $[\text{C}_{16}\text{H}_{11}\text{Cl}_2\text{N}_4]^+$ 329.0355). HPLC purity: 98.8%.

2,6-Dichloro-7-[(6-fluoronaphthalen-2-yl)methyl]-7H-purine (23b). Compound **23b** was prepared according to General Procedure 1.2-(Bromomethyl)-6-fluoronaphthalene was prepared according to the literature procedure [43] and was used as starting material. The final product was purified by flash chromatography (PE/EtOAc, 1:1). Yield: 18% (white solid); mp 182–184 °C. ^1H NMR (600 MHz, CDCl_3) δ 8.30 (s, 1H), 7.82 (d, $J = 8.5$ Hz, 1H), 7.77 (dd, $J = 9.0, 5.5$ Hz, 1H), 7.55 (d, $J = 2.0$ Hz, 1H), 7.46 (dd, $J = 9.6, 2.5$ Hz, 1H), 7.34–7.28 (m, 2H), 5.81 (s, 2H) ppm. ^{13}C NMR (151 MHz, CDCl_3) δ 164.07, 161.56 (d, $^1J_{\text{C-F}} = 248.3$ Hz), 153.83, 150.79, 144.32, 134.41 (d, $^3J_{\text{C-F}} = 9.5$ Hz), 131.29 (d, $^4J_{\text{C-F}} = 2.8$ Hz), 130.73 (d, $^3J_{\text{C-F}} = 8.9$ Hz), 130.56, 129.31 (d, $^4J_{\text{C-F}} = 5.5$ Hz), 126.68, 125.57, 122.15, 117.92 (d, $^2J_{\text{C-F}} = 25.4$ Hz), 111.43 (d, $^2J_{\text{C-F}} = 20.5$ Hz), 51.26 ppm. HRMS: m/z $[\text{M}+\text{H}]^+$ 347.0262 (calculated for: $[\text{C}_{16}\text{H}_{10}\text{N}_4\text{Cl}_2\text{F}]^+$ 347.0261). HPLC purity: 99.9%.

2-[(2,6-Dichloro-7H-purin-7-yl)methyl]quinoline (23c). Compound **23c** was prepared according to General Procedure 1.2-(Bromomethyl)quinoline was used as alkylating agent. The crude reaction mixture was purified by flash chromatography (PE/EtOAc, 1:1). Yield: 16% (white solid); mp 199–201 °C. ^1H NMR (500 MHz, CDCl_3) δ 8.58 (s, 1H), 8.24 (d, $J = 6.7$ Hz, 1H), 7.92 (d, $J = 8.3$ Hz, 1H), 7.84 (d, $J = 8.0$ Hz, 1H), 7.72 (t, $J = 7.6$ Hz, 1H), 7.58 (t, $J = 7.3$ Hz, 1H), 7.33 (d, $J = 7.1$ Hz, 1H), 5.97 (s, 2H) ppm. ^{13}C NMR (126 MHz, CDCl_3) δ 164.04, 153.69, 153.47, 152.24, 147.68, 144.08, 138.65, 130.99, 129.29, 128.04, 127.89, 127.81, 122.35, 118.83, 52.35 ppm. HRMS: m/z $[\text{M}+\text{H}]^+$ 330.0303 (calculated for: $[\text{C}_{15}\text{H}_{10}\text{N}_5\text{Cl}_2]^+$ 330.0308). HPLC purity: 95.5%.

2-Chloro-7-(naphthalen-2-ylmethyl)-1,7-dihydro-6H-purin-6-one (24). A suspension of 2,6-dichloro-7-(naphthalen-2-ylmethyl)-7H-purine (0.716 mmol) in 1 M aqueous solution of NaOH (20 mL) was heated at 100 °C. After 24 h the solution was acidified with 2 N HCl (aq) to pH 3–4, resulting in the precipitation of a white solid. This solid was filtered, washed with water (20 mL), and dried *in vacuo*. Yield: 94% (white solid); mp 240 °C (compound decomposition). ^1H NMR (500 MHz, DMSO- d_6) δ 8.20 (s, 1H), 7.91–7.82 (m, 3H), 7.79 (s, 1H), 7.55–7.45 (m, 3H), 5.70 (s, 2H) ppm. ^{13}C NMR (126 MHz, DMSO- d_6) δ 160.56, 158.59, 149.77, 143.32, 135.88, 133.29, 132.88, 128.84, 128.29, 128.09, 126.97, 126.79, 126.77, 126.18, 114.55, 49.56 ppm. HRMS: m/z $[\text{M}+\text{H}]^+$ 311.0687 (calculated for: $[\text{C}_{16}\text{H}_{12}\text{ClN}_4\text{O}]^+$ 311.0694). HPLC purity: 97.5%.

2-(4-Methylpiperazin-1-yl)-7-(naphthalen-2-ylmethyl)-1,7-dihydro-6H-purin-6-one (25). Compound **25** was prepared according to General Procedure 2.1-Methylpiperazine was used as the starting material. The final product was purified by flash chromatography ($\text{CH}_2\text{Cl}_2/\text{MeOH}$, 20:1). Yield 49% (white solid); mp 223 °C (compound decomposition). ^1H NMR (500 MHz, DMSO- d_6) δ 11.13 (s, 1H), 8.22 (s, 1H), 7.91–7.81 (m, 3H), 7.79 (s, 1H), 7.51–7.46 (m, 3H), 5.62 (s, 2H), 3.56–3.42 (m, 4H), 2.35–2.30 (m, 4H), 2.16 (s, 3H) ppm. ^{13}C NMR (126 MHz, DMSO- d_6) δ 160.89, 159.27, 155.51, 152.60, 143.93, 135.41, 132.93, 132.54, 128.46, 127.90, 127.73, 126.56, 126.33, 126.23, 125.62, 108.46, 54.20, 49.34, 45.58 ppm. HRMS: m/z $[\text{M}+\text{H}]^+$ 375.1921 (calculated for: $[\text{C}_{21}\text{H}_{23}\text{N}_6\text{O}]^+$ 375.1928). HPLC purity: 97.7%.

2-(Diethylamino)-7-(naphthalen-2-ylmethyl)-1,7-dihydro-6H-purin-6-one (26). Compound **26** was prepared according to General Procedure 2. *N,N*-Diethylamine was used as the starting material. The

final product was purified by flash chromatography ($\text{CH}_2\text{Cl}_2/\text{MeOH}$, 20:1). Yield 54% (white solid); mp 195 °C (compound decomposition). ^1H NMR (500 MHz, DMSO- d_6) δ 10.61 (s, 1H), 8.15 (s, 1H), 7.88 (d, $J = 8.7$ Hz, 2H), 7.86–7.80 (m, 1H), 7.78 (s, 1H), 7.52–7.44 (m, 3H), 5.61 (s, 2H), 3.44–3.38 (m, 4H), 1.90–1.83 (m, 6H) ppm. ^{13}C NMR (151 MHz, DMSO- d_6) δ 159.90, 155.25, 150.56, 143.58, 135.41, 132.76, 132.35, 128.24, 127.70, 127.55, 126.38, 126.13, 125.96, 125.43, 107.30, 49.10, 46.79, 24.84 ppm. HRMS: m/z $[\text{M}+\text{H}]^+$ 348.1808 (calculated for: $[\text{C}_{20}\text{H}_{22}\text{N}_5\text{O}]^+$ 348.1819). HPLC purity: 99.81%.

7-(Naphthalene-2-ylmethyl)-2-(pyrrolidin-1-yl)-1,7-dihydro-6H-purin-6-one (27). Compound **27** was prepared according to General Procedure 2. Pyrrolidine was used as the starting material. The final product was purified by flash chromatography ($\text{CH}_2\text{Cl}_2/\text{MeOH}$, 20:1). Yield 51% (white solid); mp 225 °C (compound decomposition). ^1H NMR (500 MHz, DMSO- d_6) δ 10.61 (s, 1H), 8.15 (s, 1H), 7.88 (d, $J = 8.7$ Hz, 2H), 7.86–7.80 (m, 1H), 7.78 (s, 1H), 7.52–7.44 (m, 3H), 5.61 (s, 2H), 3.44–3.38 (m, 4H), 1.90–1.83 (m, 4H) ppm. ^{13}C NMR (151 MHz, DMSO- d_6) δ 159.90, 155.25, 150.56, 143.58, 135.41, 132.76, 132.35, 128.24, 127.70, 127.55, 126.38, 126.13, 125.96, 125.43, 107.30, 49.10, 46.79, 24.84 ppm. HRMS: m/z $[\text{M}+\text{H}]^+$ 346.1650 (calculated for: $[\text{C}_{20}\text{H}_{20}\text{N}_5\text{O}]^+$ 346.1662). HPLC purity: 98.8%.

2-(Dimethylamino)-7-(naphthalen-2-ylmethyl)-1,7-dihydro-6H-purin-6-one (29). Compound **29** was prepared according to General Procedure 2. *N,N*-Dimethylamine was used as the starting material. The final product was purified by flash chromatography ($\text{CH}_2\text{Cl}_2/\text{MeOH}$, 20:1). Yield 46% (white solid); mp 189 °C (compound decomposition). ^1H NMR (500 MHz, DMSO- d_6) δ 10.62 (s, 1H), 7.87 (t, $J = 8.0$ Hz, 2H), 7.84–7.80 (m, 1H), 7.71 (s, 1H), 7.52–7.47 (m, 2H), 7.43 (dd, $J = 5.9, 2.3$ Hz, 2H), 5.68 (s, 2H), 3.00 (s, 6H) ppm. ^{13}C NMR (126 MHz, DMSO- d_6) δ 155.35, 151.43, 147.45, 136.92, 132.97, 132.40, 131.61, 128.23, 127.80, 127.69, 126.43, 126.07, 125.75, 125.65, 101.17, 50.94, 38.18 ppm. HRMS: m/z $[\text{M}+\text{H}]^+$ 320.1502 (calculated for: $[\text{C}_{18}\text{H}_{18}\text{N}_5\text{O}]^+$ 320.1506). HPLC purity: 99.9%.

7-(Naphthalen-2-ylmethyl)-2-(piperidin-1-yl)-1,7-dihydro-6H-purin-6-one (30). Compound **30** was prepared according to General Procedure 2. Piperidine was used as the starting material. The final product was purified by flash chromatography ($\text{CH}_2\text{Cl}_2/\text{MeOH}$, 9:1). Yield 54% (white solid); mp 224 °C (compound decomposition). ^1H NMR (500 MHz, DMSO- d_6) δ 10.98 (s, 1H), 8.22 (s, 1H), 7.93–7.80 (m, 4H), 7.55–7.48 (m, 3H), 5.62 (s, 2H), 3.54–3.47 (m, 4H), 1.62–1.55 (m, 2H), 1.55–1.48 (m, 4H). ^{13}C NMR (126 MHz, DMSO- d_6) δ 159.86, 155.84, 152.71, 144.14, 135.73, 133.22, 132.83, 128.74, 128.19, 128.02, 126.85, 126.62, 126.57, 125.95, 108.38, 49.61, 46.93, 25.41, 24.41 ppm. HRMS: m/z $[\text{M}+\text{H}]^+$ 360.1813 (calculated for: $[\text{C}_{21}\text{H}_{22}\text{N}_5\text{O}]^+$ 360.1819). HPLC purity: 98.6%.

2-(Cyclopropylamino)-7-(naphthalen-2-ylmethyl)-1,7-dihydro-6H-purin-6-one (31). Compound **31** was prepared according to General Procedure 2. Cyclopropylamine was used as the starting material. The final product was purified by flash chromatography ($\text{CH}_2\text{Cl}_2/\text{MeOH}$, 20:1). Yield 57% (white solid); mp 196 °C (compound decomposition). ^1H NMR (600 MHz, DMSO- d_6) δ 10.54 (s, 1H), 8.20 (s, 1H), 7.92–7.89 (m, 2H), 7.88–7.85 (m, 1H), 7.79 (s, 1H), 7.54–7.51 (m, 2H), 7.49 (dd, $J = 8.5, 1.8$ Hz, 1H), 6.50 (d, $J = 1.7$ Hz, 1H), 5.62 (s, 2H), 2.69–2.63 (m, 1H), 0.74–0.69 (m, 2H), 0.48–0.43 (m, 2H) ppm. ^{13}C NMR (151 MHz, DMSO- d_6) δ 159.76, 154.50, 152.75, 143.36, 135.29, 132.77, 132.36, 128.27, 127.73, 127.55, 126.39, 126.15, 125.97, 125.42, 108.23, 49.17, 23.32, 6.73 ppm. HRMS: m/z $[\text{M}+\text{H}]^+$ 332.1499 (calculated for: $[\text{C}_{19}\text{H}_{18}\text{N}_5\text{O}]^+$ 332.1506). HPLC purity: 98.01%.

2-(Cyclobutylamino)-7-(naphthalen-2-ylmethyl)-1,7-dihydro-6H-purin-6-one (32). Compound **32** was prepared according to General Procedure 2. Cyclobutylamine was used as the starting material. The final product was purified by flash chromatography ($\text{CH}_2\text{Cl}_2/\text{MeOH}$, 20:1). Yield 62% (white solid); mp 194 °C (compound decomposition). ^1H NMR (600 MHz, DMSO- d_6) δ 10.48 (s, 1H), 8.18 (s, 1H), 7.91–7.88 (m, 2H), 7.88–7.84 (m, 1H), 7.77 (s, 1H), 7.53–7.49 (m, 2H), 7.48 (dd, $J = 8.5, 1.8$ Hz, 1H), 6.35 (d, $J = 7.4$ Hz, 1H), 5.61 (s, 2H), 4.33–4.23 (m,

1H), 2.32–2.23 (m, 2H), 1.90–1.80 (m, 2H), 1.72–1.60 (m, 2H) ppm. ¹³C NMR (151 MHz, DMSO-*d*₆) δ 160.25, 155.03, 151.36, 143.83, 135.83, 133.31, 132.90, 128.80, 128.28, 128.09, 126.92, 126.68, 126.45, 125.93, 108.59, 49.70, 46.02, 31.15, 15.18 ppm. HRMS: *m/z* [M+H]⁺ 346.1657 (calculated for: [C₂₀H₂₀N₅O]⁺ 346.1662). HPLC purity: 99.1%.

7-(Naphthalen-2-ylmethyl)-2-thiomorpholino-1,7-dihydro-6H-purin-6-one (33). Compound 33 was prepared according to General Procedure 2. Thiomorpholine was used as the starting material. The final product was purified by flash chromatography (CH₂Cl₂/MeOH, 9:1). Yield 56% (white solid); mp 230 °C (compound decomposition). ¹H NMR (500 MHz, DMSO-*d*₆) δ 11.15 (s, 1H), 8.23 (s, 1H), 7.91–7.83 (m, 3H), 7.81 (s, 1H), 7.52–7.47 (m, 3H), 5.61 (s, 2H), 3.86–3.78 (m, 4H), 2.65–2.56 (m, 4H). ¹³C NMR (126 MHz, DMSO-*d*₆) δ 159.13, 155.36, 151.63, 143.75, 135.19, 132.75, 132.37, 128.27, 127.72, 127.55, 126.39, 126.17, 126.14, 125.50, 108.17, 48.96, 48.23, 25.58 ppm. HRMS: *m/z* [M+H]⁺ 378.1378 (calculated for: [C₂₀H₂₀N₅OS]⁺ 378.1383). HPLC purity: 96.0%.

2-[(2-Methoxyethyl) (methyl)amino]-7-(naphthalen-2-ylmethyl)-1,7-dihydro-6H-purin-6-one (34). Compound 34 was prepared according to General Procedure 2.2-Methoxyethyl (methyl)amine was used as the starting material. The final product was purified by flash chromatography (CH₂Cl₂/MeOH, 20:1). Yield 54% (white solid); mp 212 °C (compound decomposition). ¹H NMR (600 MHz, DMSO-*d*₆) δ 10.68 (s, 1H), 8.21 (d, *J* = 6.3 Hz, 1H), 7.93–7.88 (m, 2H), 7.88–7.85 (m, 1H), 7.82 (s, 1H), 7.54–7.49 (m, 3H), 5.62 (s, 2H), 3.67 (t, *J* = 5.4 Hz, 2H), 3.51 (t, *J* = 5.4 Hz, 2H), 3.26 (s, 3H), 3.05 (s, 3H) ppm. ¹³C NMR (151 MHz, DMSO-*d*₆) δ 160.18, 155.71, 152.59, 144.24, 135.84, 133.30, 132.91, 128.81, 128.26, 128.10, 126.93, 126.70, 126.62, 126.02, 107.96, 70.52, 58.75, 49.71, 37.33, 31.83 ppm. HRMS: *m/z* [M+H]⁺ 364.1768 (calculated for: [C₂₀H₂₂N₅O₂]⁺ 364.1768). HPLC purity: 95.0%.

2-[Cyclopropyl(methyl)amino]-7-(naphthalen-2-ylmethyl)-1,7-dihydro-6H-purin-6-one (35). Compound 35 was prepared according to General Procedure 2. Cyclopropyl (methyl)amine was used as the starting material. The final product was purified by flash chromatography (CH₂Cl₂/MeOH, 20:1). Yield 59% (white solid); mp 196 °C (compound decomposition). ¹H NMR (600 MHz, DMSO-*d*₆) δ 10.42 (s, 1H), 8.23 (s, 1H), 7.92–7.89 (m, 2H), 7.88–7.85 (m, 1H), 7.82 (s, 1H), 7.55–7.48 (m, 3H), 5.64 (s, 2H), 3.02 (s, 3H), 2.79–2.71 (m, 1H), 0.91 (m, 2H), 0.70–0.64 (m, 2H) ppm. ¹³C NMR (151 MHz, DMSO-*d*₆) δ 159.76, 154.50, 152.75, 143.36, 135.29, 132.77, 132.36, 128.27, 127.73, 127.55, 126.39, 126.15, 125.97, 125.42, 108.23, 49.17, 31.29, 23.32, 6.73 ppm. HRMS: *m/z* [M+H]⁺ 346.1664 (calculated for: [C₂₀H₂₀N₅O]⁺ 346.1662). HPLC purity: 98.9%.

2-[(2-Methoxyethyl)amino]-7-(naphthalen-2-ylmethyl)-1,7-dihydro-6H-purin-6-one (36). Compound 36 was prepared according to General Procedure 2.2-Methoxyethylamine was used as the starting material. The final product was purified by flash chromatography (CH₂Cl₂/MeOH, 20:1). Yield 52% (white solid); mp 218 °C (compound decomposition). ¹H NMR (600 MHz, DMSO-*d*₆) δ 10.61 (s, 1H), 8.18 (s, 1H), 7.92–7.89 (m, 2H), 7.88–7.86 (m, 1H), 7.78 (s, 1H), 7.54–7.50 (m, 2H), 7.49 (dd, *J* = 8.5, 1.7 Hz, 1H), 6.19 (t, *J* = 5.3 Hz, 1H), 5.61 (s, 2H), 3.49–3.46 (m, 2H), 3.46–3.42 (m, 2H), 3.29 (s, 3H) ppm. ¹³C NMR (151 MHz, DMSO-*d*₆) δ 160.19, 155.00, 152.40, 143.80, 135.81, 133.31, 132.90, 128.81, 128.28, 128.09, 126.93, 126.69, 126.50, 125.95, 108.54, 70.91, 58.48, 49.70, 40.58 ppm. HRMS: *m/z* [M+H]⁺ 350.1605 (calculated for: [C₁₉H₂₀N₅O₂]⁺ 350.1612). HPLC purity: 99.9%.

2-[(2-Hydroxyethyl)amino]-7-(naphthalen-2-ylmethyl)-1,7-dihydro-6H-purin-6-one (37). Compound 37 was prepared according to General Procedure 2.2-Hydroxyethylamine was used as the starting material. The final product was purified by flash chromatography (CH₂Cl₂/MeOH, 20:1). Yield 39% (white solid); mp 218 °C (compound decomposition). ¹H NMR (600 MHz, DMSO-*d*₆) δ 10.66 (s, 1H), 8.17 (s, 1H), 7.92–7.89 (m, 2H), 7.89–7.86 (m, 1H), 7.78 (s, 1H), 7.54–7.50 (m, 2H), 7.48 (dd, *J* = 8.4, 1.6 Hz, 1H), 6.19 (t, *J* = 5.4 Hz, 1H), 5.61 (s, 2H),

4.84 (t, *J* = 5.1 Hz, 1H), 3.54 (q, *J* = 5.4 Hz, 2H), 3.33–3.31 (m, 2H) ppm. ¹³C NMR (151 MHz, DMSO-*d*₆) δ 159.71, 154.51, 152.05, 143.24, 135.29, 132.77, 132.35, 128.27, 127.74, 127.55, 126.39, 126.14, 125.93, 125.41, 107.93, 59.50, 49.14, 42.97 ppm. HRMS: *m/z* [M+H]⁺ 336.1456 (calculated for: [C₁₈H₁₈N₅O₂]⁺ 336.1455). HPLC purity: 98.4%.

7-(Naphthalen-2-ylmethyl)-2-(2-oxa-6-azaspiro [3.3] heptan-6-yl)-1,7-dihydro-6H-purin-6-one (38). Compound 38 was prepared according to General Procedure 2.2-Oxa-6-azaspiro [3.3]heptane was used as the starting material. The final product was purified by flash chromatography (CH₂Cl₂/MeOH, 20:1). Yield 42% (white solid); mp 215 °C (compound decomposition). ¹H NMR (600 MHz, DMSO-*d*₆) δ 11.28 (s, 1H), 8.21 (s, 1H), 7.92–7.87 (m, 2H), 7.87–7.83 (m, 1H), 7.79 (s, 1H), 7.53–7.50 (m, 2H), 7.48 (dd, *J* = 8.5, 1.7 Hz, 1H), 5.64 (s, 2H), 4.68 (s, 4H), 4.19 (s, 4H) ppm. ¹³C NMR (151 MHz, DMSO-*d*₆) δ 159.26, 155.18, 153.50, 143.57, 135.29, 132.75, 132.36, 128.27, 127.70, 127.56, 126.41, 126.16, 125.99, 125.40, 108.30, 79.74, 60.06, 49.12, 37.91 ppm. HRMS: *m/z* [M+H]⁺ 374.1612 (calculated for: [C₂₁H₂₀N₅O₂]⁺ 374.1612). HPLC purity: 96.5%.

2-Chloro-1-methyl-7-(naphthalene-2-ylmethyl)-1,7-dihydro-6H-purin-6-one (39). To a stirred solution of 24 (0.16 g, 0.5 mmol) in dry DMF (4 mL), NaH was added (60% dispersion in mineral oil, 0.025 g). After 10 min of mixing at RT, iodomethane was added dropwise (0.075 g, 0.53 mmol). The reaction mixture was stirred 1 h at RT followed by the addition of water (20 mL). The resulting suspension was extracted with CH₂Cl₂ (3 × 15 mL), and the combined organic layers were dried over sodium sulfate, filtered and evaporated *in vacuo*. The crude product was purified by flash chromatography (PE/EtOAc, 5:95). Yield 62% (white solid); 175–176 °C; ¹H NMR (600 MHz, CDCl₃) δ 7.91 (s, 1H), 7.84–7.78 (m, 3H), 7.72 (s, 1H), 7.51–7.46 (m, 2H), 7.38 (dd, *J* = 8.4, 1.8 Hz, 1H), 5.71 (s, 2H), 3.72 (s, 3H) ppm; ¹³C NMR (151 MHz, CDCl₃) δ 155.76, 155.16, 145.38, 144.27, 133.60, 133.46, 133.17, 129.46, 128.31, 128.11, 127.35, 127.01, 126.97, 125.47, 114.01, 50.92, 33.45 ppm; HRMS: *m/z* [M+H]⁺ 325.0855 (calculated for: [C₁₇H₁₃N₄OCl]⁺ 325.0851); HPLC purity: 97.5%.

1-Methyl-2-morpholino-7-(naphthalene-2-ylmethyl)-1,7-dihydro-6H-purin-6-one (40). Compound 39 (0.087 g, 0.27 mmol) and morpholine (0.1 g, 1.15 mmol) were charged to a sealed tube with *tert*-butanol (5 mL). The reaction was carried out under microwave irradiation at 110 °C with power 150 W and maximum pressure 300 psi for 3 h. The solvent was evaporated *in vacuo*, and the reaction mixture was purified by flash chromatography (PE/EtOAc, 5:95) as eluent. Yield 54% (white solid); mp 189–191 °C; ¹H NMR (500 MHz, CDCl₃) δ 7.84 (s, 1H), 7.82–7.76 (m, 3H), 7.72 (s, 1H), 7.49–7.44 (m, 2H), 7.40 (dd, *J* = 8.5, 1.8 Hz, 1H), 5.69 (s, 2H), 3.89–3.80 (m, 4H), 3.57 (s, 3H), 3.24–3.16 (m, 4H); ¹³C NMR (126 MHz, CDCl₃) δ 156.54, 156.50, 156.44, 143.31, 133.51, 133.34, 133.12, 129.01, 128.04, 127.82, 126.98, 126.62, 126.53, 125.40, 111.74, 66.43, 50.51, 50.35, 32.41; HRMS: *m/z* [M+H]⁺ 376.1765 (calculated for: [C₂₁H₂₂N₅O₂]⁺ 376.1768); HPLC purity: 99.9%.

2-Chloro-N-methyl-7-(naphthalen-2-ylmethyl)-7H-purin-6-amine (41). Compound 41 was prepared according to General Procedure 3. N-Methylamine was used as the starting material. The product was purified by flash chromatography (CHCl₃/MeOH, 9:1). Yield 98% (white solid); mp 168–170 °C; ¹H NMR (600 MHz, CDCl₃) δ 7.94 (s, 1H), 7.88 (d, *J* = 8.5 Hz, 1H), 7.87–7.83 (m, 1H), 7.78–7.75 (m, 1H), 7.56–7.51 (m, 3H), 7.21 (dd, *J* = 8.5, 1.4 Hz, 1H), 5.61 (s, 2H), 5.00 (q, *J* = 4.8 Hz, 1H), 2.78 (d, *J* = 4.8 Hz, 3H) ppm; ¹³C NMR (151 MHz, CDCl₃) δ 161.71, 154.96, 152.18, 145.91, 133.61, 132.33, 130.41, 128.24, 127.63, 127.51, 125.82, 125.78, 123.71, 123.65, 111.28, 51.51, 31.24 ppm; HRMS: *m/z* [M+H]⁺ 324.1001 (calculated: [C₁₇H₁₅ClN₅]⁺ 324.1010); HPLC purity: 99.0%.

2-Chloro-N,N-dimethyl-7-(naphthalen-2-ylmethyl)-7H-purin-6-amine (42). Compound 42 was prepared according to General Procedure 3. N,N-Dimethylamine was used as the starting material. The product was purified by flash chromatography (CH₂Cl₂/MeOH, 20:1).

Yield 78% (yellow oil); ^1H NMR (600 MHz, CDCl_3) δ 7.96 (s, 1H), 7.79–7.75 (m, 2H), 7.73–7.70 (m, 1H), 7.50 (s, 1H), 7.48–7.44 (m, 2H), 7.12 (dd, $J = 8.5, 1.7$ Hz, 1H), 5.61 (s, 2H), 3.03 (s, 6H) ppm; ^{13}C NMR (151 MHz, CDCl_3) δ 163.36, 156.31, 153.39, 148.03, 133.38, 133.19, 132.88, 129.58, 128.06, 127.96, 127.09, 126.95, 126.13, 124.28, 113.89, 51.83, 41.63 ppm; HRMS: m/z $[\text{M}+\text{H}]^+$ 338.1175 (calculated for: $[\text{C}_{18}\text{H}_{17}\text{ClN}_5]^+$ 338.1167); HPLC purity: 98.0%.

2-Chloro-*N*-ethyl-7-(naphthalen-2-ylmethyl)-7H-purin-6-amine (43). Compound 43 was prepared according to General Procedure 3. *N*-Ethylamine was used as the starting material. The product was purified by flash chromatography ($\text{CH}_2\text{Cl}_2/\text{MeOH}$, 20:1). Yield 92% (white solid); mp 173–174 °C; ^1H NMR (600 MHz, CDCl_3) δ 8.01 (s, 1H), 7.91 (d, $J = 8.5$ Hz, 1H), 7.88–7.84 (m, 1H), 7.81–7.77 (m, 1H), 7.63 (s, 1H), 7.58–7.53 (m, 2H), 7.22 (dd, $J = 8.5, 1.9$ Hz, 1H), 5.63 (s, 2H), 4.66 (t, $J = 5.0$ Hz, 1H), 3.23–3.17 (m, 2H), 0.67 (t, $J = 7.2$ Hz, 3H) ppm; ^{13}C NMR (151 MHz, CDCl_3) δ 161.88, 154.93, 151.37, 146.03, 133.62, 133.55, 132.50, 130.53, 128.21, 128.10, 127.72, 127.56, 125.98, 123.64, 110.98, 51.65, 36.23, 14.06 ppm; HRMS: m/z $[\text{M}+\text{H}]^+$ 338.1166 (calculated for: $[\text{C}_{18}\text{H}_{17}\text{ClN}_5]^+$ 338.1167); HPLC purity: 99.9%.

2-Chloro-*N*-propyl-7-(naphthalen-2-ylmethyl)-7H-purin-6-amine (44). Compound 44 was prepared according to General Procedure 3. *N*-Propylamine was used as the starting material. The product was purified by flash chromatography (EtOAc/MeOH , 95:5). Yield 99% (beige solid); mp 172–174 °C; ^1H NMR (600 MHz, CDCl_3) δ 8.09 (s, 1H), 7.91 (d, $J = 8.5$ Hz, 1H), 7.88–7.84 (m, 1H), 7.79–7.76 (m, 1H), 7.61 (s, 1H), 7.57–7.53 (m, 2H), 7.22 (dd, $J = 8.5, 1.8$ Hz, 1H), 5.65 (s, 2H), 4.72 (t, $J = 5.3$ Hz, 1H), 3.20–3.15 (m, 2H), 1.11–1.02 (m, 2H), 0.45 (t, $J = 7.3$ Hz, 3H) ppm; ^{13}C NMR (151 MHz, CDCl_3) δ 161.57, 154.98, 151.51, 145.90, 133.59, 133.51, 132.26, 130.53, 128.11, 127.98, 127.65, 127.50, 125.70, 123.35, 110.90, 51.60, 42.95, 22.06, 11.00 ppm; HRMS: m/z $[\text{M}+\text{H}]^+$ 352.1319 (calculated for: $\text{C}_{19}\text{H}_{19}\text{N}_5\text{Cl}$ [352.1323] $^+$); HPLC purity: 96.4%.

2-Chloro-*N*-butyl-7-(naphthalen-2-ylmethyl)-7H-purin-6-amine (45). Compound 45 was prepared according to General Procedure 3. *N*-Butylamine was used as the starting material. The product was purified by flash chromatography (EtOAc/MeOH , 95:5). Yield 98% (beige solid); mp 192–194 °C; ^1H NMR (600 MHz, CDCl_3) δ 8.14 (s, 1H), 7.91 (d, $J = 8.4$ Hz, 1H), 7.88–7.84 (m, 1H), 7.80–7.76 (m, 1H), 7.62 (s, 1H), 7.57–7.52 (m, 2H), 7.21 (dd, $J = 8.4, 1.9$ Hz, 1H), 5.66 (s, 2H), 4.71 (t, $J = 5.2$ Hz, 1H), 3.22–3.18 (m, 2H), 0.97–0.93 (m, 2H), 0.78–0.71 (m, 2H), 0.51 (t, $J = 7.4$ Hz, 3H) ppm; ^{13}C NMR (151 MHz, CDCl_3) δ 161.40, 155.02, 151.47, 145.88, 133.60, 133.53, 132.27, 130.52, 128.12, 128.02, 127.66, 127.50, 125.67, 123.32, 110.86, 51.61, 40.92, 30.90, 19.68, 13.54 ppm; HRMS: m/z $[\text{M}+\text{H}]^+$ 366.1480 (calculated for: $\text{C}_{20}\text{H}_{21}\text{N}_5\text{Cl}$ [366.1480] $^+$); HPLC purity: 95.1%.

2-Chloro-*N*-cyclobutyl-7-(naphthalen-2-ylmethyl)-7H-purin-6-amine (46). Compound 46 was prepared according to General Procedure 3. *N*-Cyclobutylamine was used as the starting material. The product was purified by flash chromatography (EtOAc/MeOH , 95:5). Yield 49% (white solid); mp 193–195 °C; ^1H NMR (600 MHz, CDCl_3) δ 8.07 (s, 1H), 7.95 (d, $J = 8.6$ Hz, 1H), 7.90–7.87 (m, 1H), 7.83–7.80 (m, 1H), 7.69 (d, $J = 1.9$ Hz, 1H), 7.61–7.54 (m, 2H), 7.23 (dd, $J = 8.7, 1.9$ Hz, 1H), 5.64 (s, 2H), 4.79 (d, $J = 7.4$ Hz, 1H), 4.35–4.29 (m, 1H), 2.10–1.99 (m, 2H), 1.45–1.41 (m, 1H), 1.29–1.22 (m, 1H), 1.09–0.98 (m, 2H) ppm; ^{13}C NMR (151 MHz, CDCl_3) δ 161.99, 154.94, 150.32, 146.04, 133.60, 133.47, 132.45, 130.64, 128.15, 127.94, 127.79, 127.61, 126.10, 123.58, 110.77, 51.73, 45.76, 30.90, 14.86 ppm; HRMS: m/z $[\text{M}+\text{H}]^+$ 364.1320 (calculated for: $\text{C}_{20}\text{H}_{19}\text{N}_5\text{Cl}$ [364.1323] $^+$); HPLC purity: 95.7%.

2-Chloro-*N*-cyclohexyl-7-(naphthalen-2-ylmethyl)-7H-purin-6-amine (47). Compound 47 was prepared according to General Procedure 3. *N*-Cyclohexylamine was used as the starting material following. The product was purified by flash chromatography (EtOAc/MeOH , 95:5). Yield 49% (yellow solid); mp 197–199 °C; ^1H NMR (600 MHz, CDCl_3) δ 8.04 (s, 1H), 7.89 (d, $J = 8.5$ Hz, 1H), 7.87–7.82 (m, 1H), 7.79–7.74 (m, 1H), 7.61 (s, 1H), 7.57–7.52 (m, 2H), 7.17 (dd, $J = 8.5,$

1.9 Hz, 1H), 5.62 (d, $J = 1.1$ Hz, 2H), 4.55 (d, $J = 7.7$ Hz, 1H), 3.87–3.67 (m, 1H), 1.56–1.42 (m, 2H), 1.38–1.31 (m, 1H), 1.29–1.24 (m, 2H), 1.16–1.04 (m, 2H), 0.77–0.66 (m, 1H), 0.50–0.41 (m, 2H) ppm; ^{13}C NMR (151 MHz, CDCl_3) δ 162.02, 155.02, 150.84, 146.11, 133.65, 133.58, 132.63, 130.58, 128.19, 128.07, 127.72, 127.56, 125.93, 123.54, 110.96, 51.70, 49.19, 32.34, 25.52, 24.38 ppm. HRMS: m/z $[\text{M}+\text{H}]^+$ 392.1632 (calculated for: $\text{C}_{22}\text{H}_{23}\text{N}_5\text{Cl}$ [392.1636] $^+$); HPLC purity: 95.7%.

N^1 -[2-Chloro-7-(naphthalene-2-ylmethyl)-7H-purin-6-yl]- N^2 , N^2 -dimethylethane-1,2-diamine (48). Compound 48 was prepared according to General Procedure 3. N^1,N^1 -Dimethylethane-1,2-diamine was used as the starting material. The product was purified by flash chromatography ($\text{EtOAc}/\text{MeOH}/\text{TEA}$, 95:5:0.1). Yield 84% (white solid); mp 80–90 °C; ^1H NMR (600 MHz, CDCl_3) δ 8.41 (s, 1H), 7.81 (d, $J = 8.7$ Hz, 2H), 7.77–7.72 (m, 1H), 7.59–7.56 (m, 1H), 7.53–7.45 (m, 2H), 7.26 (dd, $J = 8.5, 1.9$ Hz, 1H), 6.89 (s, 1H), 5.92 (s, 2H), 3.65 (d, $J = 5.4$ Hz, 2H), 3.00 (s, 2H), 2.54 (s, 6H) ppm; ^{13}C NMR (151 MHz, CDCl_3) δ 161.31, 154.47, 150.89, 146.57, 133.34, 133.20, 132.65, 129.29, 128.08, 127.82, 126.83, 126.76, 125.55, 123.93, 110.47, 57.52, 50.95, 44.55, 37.13 ppm; HRMS: m/z $[\text{M}+\text{H}]^+$ 381.1584 (calculated for: $\text{C}_{20}\text{H}_{22}\text{N}_6\text{Cl}$ [381.1589] $^+$); HPLC purity: 96.1%.

2-Chloro-7-(naphthalene-2-ylmethyl)-*N*-(pyridine-4-ylmethyl)-7H-purin-6-amine (49). Solution of 23a (0.11 g, 0.36 mmol), 4-picolyamine (0.039 g, 0.36 mmol) and DIPEA (75 mg, 58 mmol) was stirred at 45 °C in acetonitrile (15 mL) for 24 h. After completion was finished (monitored by TLC), the solvent was evaporated *in vacuo* and water (10 mL) was added to the residue. The mixture was extracted with CH_2Cl_2 (3 \times 10 mL), and the combined organics were dried over sodium sulfate, filtered and evaporated *in vacuo*. The product was purified by flash chromatography (EtOAc/MeOH , 95:5). Yield 27% (brown oil); ^1H NMR (500 MHz, CDCl_3) δ 8.07 (s, 1H), 8.06–8.03 (m, 2H), 7.82 (dd, $J = 17.0, 8.3$ Hz, 2H), 7.66 (d, $J = 7.9$ Hz, 1H), 7.60–7.52 (m, 2H), 7.51 (s, 1H), 7.13 (dd, $J = 8.5, 1.9$ Hz, 1H), 6.57–6.39 (m, 2H), 5.70 (s, 2H), 5.34 (t, $J = 5.7$ Hz, 1H), 4.45 (d, $J = 5.7$ Hz, 2H) ppm; ^{13}C NMR (126 MHz, CDCl_3) δ 162.41, 154.79, 150.97, 149.57, 146.83, 146.69, 133.63, 133.57, 132.44, 130.62, 128.29, 128.15, 127.94, 127.81, 125.69, 123.41, 122.39, 111.06, 51.63, 43.92 ppm; HRMS: m/z $[\text{M}+\text{H}]^+$ 401.1265 (calculated for: $\text{C}_{22}\text{H}_{18}\text{N}_6\text{Cl}$ [401.1276] $^+$); HPLC purity: 99.9%.

***N*-Benzyl-2-chloro-7-(naphthalene-2-ylmethyl)-7H-purin-6-amine (50).** Solution of 23a (0.19 g, 0.607 mmol), benzylamine (0.065 mg, 0.61 mmol) and DIPEA (75 mg, 58 mmol) was stirred at 45 °C in acetonitrile (15 mL) for 24 h. The crude product was filtered off, washed Et_2O (3 \times 15 mL) and dried *in vacuo*. Yield 45% (white solid); mp 210–212 °C; ^1H NMR (500 MHz, CDCl_3) δ 8.05 (s, 1H), 7.83 (d, $J = 8.0$ Hz, 1H), 7.77 (d, $J = 8.5$ Hz, 1H), 7.63–7.58 (m, 1H), 7.58–7.51 (m, 2H), 7.42 (s, 1H), 7.10 (td, $J = 7.3, 1.1$ Hz, 1H), 7.07 (dd, $J = 8.5, 1.9$ Hz, 1H), 6.93 (t, $J = 7.8$ Hz, 2H), 6.69–6.63 (m, 2H), 5.58 (s, 2H), 4.90 (t, $J = 5.0$ Hz, 1H), 4.38 (d, $J = 5.0$ Hz, 2H); ^{13}C NMR (151 MHz, CDCl_3) δ 162.37, 155.13, 151.17, 146.34, 137.05, 133.72, 133.63, 132.23, 130.66, 128.83, 128.39, 128.30, 127.95, 127.92, 127.69, 127.58, 125.65, 123.26, 111.12, 51.62, 45.70 ppm; HRMS: m/z $[\text{M}+\text{H}]^+$ 400.1324 (calculated for: $\text{C}_{23}\text{H}_{19}\text{N}_5\text{Cl}$ [400.1323] $^+$); HPLC purity: 99.9%.

2-Chloro-7-(naphthalene-2-ylmethyl)-7H-purin-6-amine (51). To a solution of 23a (0.13 g, 0.42 mmol) in acetonitrile (20 mL), 25% aqueous ammonia solution (15 mL) was added and the solution was stirred at RT for two days. An additional portion of 25% aqueous ammonia solution (15 mL) was added. After 5 days (7 days total reaction time), the solvent was evaporated *in vacuo* and the product was purified by flash chromatography (EtOAc/EtOH , 95:5). Yield 36% (white solid); mp 173–175 °C; ^1H NMR (600 MHz, $\text{DMSO}-d_6$) δ 8.48 (s, 1H), 7.87–7.83 (m, 2H), 7.81–7.78 (m, 1H), 7.59 (s, 1H), 7.48–7.44 (m, 2H), 7.31 (br, 2H), 7.25 (dd, $J = 8.5, 1.8$ Hz, 1H), 5.81 (s, 2H) ppm; ^{13}C NMR (151 MHz, $\text{DMSO}-d_6$) δ 162.17, 153.36, 152.92, 147.94, 135.22, 133.29, 132.92, 129.08, 128.30, 128.13, 127.09, 126.87, 125.74, 125.19, 110.50, 49.80 ppm. HRMS: m/z $[\text{M}+\text{H}]^+$ 310.0851 (calculated for: $[\text{C}_{16}\text{H}_{13}\text{ClN}_5]^+$ 310.0854); HPLC purity: 99.9%.

2-Chloro-N-ethyl-7-[(6-fluoronaphthalen-2-yl)methyl]-7H-purin-6-amine (52). Compound 52 was prepared according to General Procedure 3. *N*-Ethylamine was used as the starting material. The product was purified by flash chromatography (EtOAc/MeOH, 95:5). Yield 82% (white solid); mp 176–178 °C; $^1\text{H NMR}$ (600 MHz, CDCl_3) δ 7.98 (s, 1H), 7.84 (d, $J = 8.5$ Hz, 1H), 7.78 (dd, $J = 9.1, 5.4$ Hz, 1H), 7.61 (d, $J = 2.0$ Hz, 1H), 7.46 (dd, $J = 9.5, 2.7$ Hz, 1H), 7.31 (td, $J = 8.7, 2.5$ Hz, 1H), 7.26–7.24 (m, 1H), 5.62 (s, 2H), 4.61 (t, $J = 5.0$ Hz, 1H), 3.24–3.17 (m, 2H), 0.67 (t, $J = 7.3$ Hz, 3H) ppm; $^{13}\text{C NMR}$ (151 MHz, CDCl_3) δ 161.66 (d, $^1J_{\text{C-F}} = 248.6$ Hz), 161.61, 154.65, 151.16, 145.86, 134.22 (d, $^3J_{\text{C-F}} = 10.0$ Hz), 131.78 (d, $^4J_{\text{C-F}} = 3.8$ Hz), 130.47 (d, $^3J_{\text{C-F}} = 9.8$ Hz), 130.34, 129.51 (d, $^4J_{\text{C-F}} = 6.5$ Hz), 126.03, 124.82, 117.90 (d, $^2J_{\text{C-F}} = 25.8$ Hz), 111.22 (d, $^2J_{\text{C-F}} = 21.0$ Hz), 110.74, 51.27, 36.05, 13.95 ppm; HRMS: m/z $[\text{M}+\text{H}]^+$ 356.1070 (calculated for: $\text{C}_{18}\text{H}_{16}\text{N}_5\text{ClF}$ [356.1073] $^+$); HPLC purity: 97.3%.

2-Chloro-N-ethyl-7-(quinolin-2-ylmethyl)-7H-purin-6-amine (53). Compound 53 was prepared according to General Procedure 3. *N*-Ethylamine was used as the starting material. The product was purified by flash chromatography (EtOAc/MeOH, 95:5). Yield 89% (white solid); mp 182–183 °C; $^1\text{H NMR}$ (600 MHz, CDCl_3) δ 8.43–8.40 (m, 1H), 8.33 (d, $J = 8.3$ Hz, 1H), 8.08 (d, $J = 8.6$ Hz, 1H), 7.91 (d, $J = 8.2$ Hz, 1H), 7.88–7.83 (m, 1H), 7.67 (t, $J = 7.5$ Hz, 1H), 7.62 (d, $J = 8.4$ Hz, 1H), 5.73 (s, 1H), 3.70 (q, $J = 7.3$ Hz, 2H), 2.76 (s, 1H), 1.38 (t, $J = 7.3$ Hz, 2H) ppm. $^{13}\text{C NMR}$ (151 MHz, CDCl_3) δ 160.28, 155.18, 154.60, 151.97, 146.87, 144.12, 139.55, 131.21, 128.25, 128.21, 128.12, 128.03, 120.65, 111.22, 53.46, 36.37, 14.74 ppm; HRMS: m/z $[\text{M}+\text{H}]^+$ 339.1114 (calculated for: $\text{C}_{17}\text{H}_{16}\text{N}_6\text{Cl}$ [339.1119] $^+$); HPLC purity: 99.7%.

***N*-Methyl-2-morpholino-7-(naphthalen-2-ylmethyl)-7H-purin-6-amine (54).** Compound 54 was prepared according to General Procedure 4. Compound 41 was used as the starting material. Yield 51% (white solid); mp 165–167 °C; $^1\text{H NMR}$ (600 MHz, CDCl_3) δ 7.87 (d, $J = 8.5$ Hz, 1H), 7.86–7.83 (m, 1H), 7.81 (s, 1H), 7.76–7.72 (m, 1H), 7.55–7.49 (m, 3H), 7.22 (dd, $J = 8.5, 1.6$ Hz, 1H), 5.52 (s, 2H), 4.48 (q, $J = 4.4$ Hz, 1H), 3.81–3.77 (m, 4H), 3.75–3.71 (m, 4H), 2.72 (d, $J = 4.4$ Hz, 3H) ppm; $^{13}\text{C NMR}$ (151 MHz, CDCl_3) δ 162.52, 159.58, 151.35, 144.12, 144.10, 133.43, 133.30, 132.99, 129.88, 127.95, 127.20, 127.02, 125.22, 125.19, 123.44, 106.42, 67.12, 51.00, 45.17 ppm; HRMS: m/z $[\text{M}+\text{H}]^+$ 375.1921 (calculated for: $[\text{C}_{21}\text{H}_{23}\text{N}_6\text{O}]^+$ 375.1928); HPLC purity: 99.5%.

***N,N*-Dimethyl-2-morpholino-7-(naphthalen-2-ylmethyl)-7H-purin-6-amine (55).** Compound 55 was prepared according to General Procedure 4. Compound 42 was used as the starting material. Yield 58% (yellow oil); $^1\text{H NMR}$ (500 MHz, CDCl_3) δ 7.86–7.84 (m, 1H), 7.84–7.78 (m, 2H), 7.77–7.74 (m, 1H), 7.54 (s, 1H), 7.52–7.48 (m, 2H), 7.19 (dd, $J = 8.5, 1.8$ Hz, 1H), 5.56 (s, 2H), 3.84–3.81 (m, 4H), 3.80–3.76 (m, 4H), 2.98 (s, 6H) ppm; $^{13}\text{C NMR}$ (126 MHz, CDCl_3) δ 164.27, 158.93, 156.43, 146.35, 133.64, 133.26, 133.02, 129.14, 127.89, 127.78, 126.80, 126.56, 125.93, 124.45, 109.52, 67.04, 51.03, 45.09, 41.39 ppm; HRMS: m/z $[\text{M}+\text{H}]^+$ 389.2076 (calculated for: $[\text{C}_{22}\text{H}_{25}\text{N}_6\text{O}]^+$ 389.2084); HPLC purity: 99.1%.

***N*-Ethyl-2-morpholino-7-(naphthalen-2-ylmethyl)-7H-purin-6-amine (56).** Compound 56 was prepared according to General Procedure 4. Compound 43 was used as the starting material. Yield 74% (orange solid); mp 174–176 °C; $^1\text{H NMR}$ (500 MHz, CDCl_3) δ 7.91–7.87 (m, 1H), 7.87–7.84 (m, 2H), 7.75 (dd, $J = 5.4, 4.1$ Hz, 1H), 7.58 (s, 1H), 7.56–7.51 (m, 2H), 7.23 (dd, $J = 8.5, 1.8$ Hz, 1H), 5.51 (s, 2H), 4.20 (t, $J = 4.9$ Hz, 1H), 3.78–3.75 (m, 4H), 3.75–3.70 (m, 4H), 3.19–3.11 (m, 2H), 0.69 (t, $J = 7.2$ Hz, 3H) ppm; $^{13}\text{C NMR}$ (126 MHz, CDCl_3) δ 162.82, 159.60, 150.52, 144.06, 133.63, 133.58, 133.35, 130.27, 128.21, 128.13, 127.56, 127.34, 125.69, 123.72, 106.07, 67.01, 51.06, 45.02, 35.41, 14.07 ppm. HRMS: m/z $[\text{M}+\text{H}]^+$ 389.2079 (calculated for: $[\text{C}_{22}\text{H}_{25}\text{N}_6\text{O}]^+$ 389.2084); HPLC purity: 99.8%.

2-Morpholino-7-(naphthalen-2-ylmethyl)-*N*-propyl-7H-purin-6-amine (57). Compound 57 was prepared according to General Procedure 4. Compound 44 was used as the starting material. Yield 72%

(brown oil); $^1\text{H NMR}$ (500 MHz, CDCl_3) δ 7.86 (d, $J = 8.6$ Hz, 1H), 7.82 (d, $J = 5.1$ Hz, 2H), 7.74–7.70 (m, 1H), 7.55–7.53 (m, 1H), 7.52–7.48 (m, 2H), 7.20 (dd, $J = 8.4, 1.9$ Hz, 1H), 5.50 (s, 2H), 4.35 (t, $J = 5.3$ Hz, 1H), 3.76–3.73 (m, 4H), 3.72–3.70 (m, 4H), 3.16–3.05 (m, 2H), 1.12–1.06 (m, $J = 7.3$ Hz, 2H), 0.44 (t, $J = 7.4$ Hz, 3H) ppm; $^{13}\text{C NMR}$ (126 MHz, CDCl_3) δ 162.96, 159.86, 151.00, 144.40, 133.63, 133.54, 133.32, 130.18, 128.13, 128.06, 127.45, 127.24, 125.52, 123.63, 106.38, 67.31, 51.33, 45.36, 42.64, 22.38, 11.29 ppm; HRMS: m/z $[\text{M}+\text{H}]^+$ 403.2237 (calculated for: $\text{C}_{23}\text{H}_{26}\text{N}_6\text{O}$ [403.2241] $^+$); HPLC purity: 95.9%.

***N*-Butyl-2-morpholino-7-(naphthalen-2-ylmethyl)-7H-purin-6-amine (58).** Compound 58 was prepared according to General Procedure 4. Compound 45 was used as the starting material. Yield 47% (brown oil); $^1\text{H NMR}$ (500 MHz, CDCl_3) δ 7.86 (d, $J = 8.5$ Hz, 1H), 7.83 (d, $J = 5.1$ Hz, 2H), 7.75–7.70 (m, 1H), 7.55–7.53 (m, 1H), 7.53–7.48 (m, 2H), 7.19 (dd, $J = 8.5, 1.9$ Hz, 1H), 5.50 (s, 2H), 4.34 (t, $J = 5.3$ Hz, 1H), 3.75–3.69 (m, 8H), 3.14 (td, $J = 6.7, 5.1$ Hz, 2H), 1.05–0.97 (m, 2H), 0.76–0.68 (m, 2H), 0.50 (t, $J = 7.3$ Hz, 3H) ppm; $^{13}\text{C NMR}$ (126 MHz, CDCl_3) δ 162.82, 159.81, 150.94, 144.36, 133.60, 133.51, 133.29, 130.12, 128.10, 128.05, 127.42, 127.20, 125.45, 123.57, 106.33, 67.26, 51.27, 45.32, 40.43, 31.19, 19.84, 13.71 ppm; [HRMS: m/z $[\text{M}+\text{H}]^+$ = 417.2385 (calculated for: $\text{C}_{24}\text{H}_{29}\text{N}_6\text{O}$ [417.2397] $^+$); HPLC purity: 96.5%.

***N*-Cyclobutyl-2-morpholino-7-(naphthalen-2-ylmethyl)-7H-purin-6-amine (59).** Compound 59 was prepared according to General Procedure 4. Compound 46 was used as the starting material. Yield 44% (brown oil); $^1\text{H NMR}$ (600 MHz, CDCl_3) δ 7.91 (d, $J = 8.5$ Hz, 1H), 7.87 (d, $J = 6.2$ Hz, 2H), 7.78 (dd, $J = 6.1, 3.4$ Hz, 1H), 7.64 (d, $J = 1.9$ Hz, 1H), 7.55 (dt, $J = 6.3, 3.4$ Hz, 2H), 7.24 (dd, $J = 8.5, 1.8$ Hz, 1H), 5.52 (s, 2H), 4.41 (d, $J = 7.1$ Hz, 1H), 4.27–4.18 (m, 1H), 3.76–3.71 (m, 8H), 2.05–1.99 (m, 2H), 1.49–1.42 (m, 1H), 1.32–1.23 (m, 1H), 1.13–1.05 (m, 2H) ppm; $^{13}\text{C NMR}$ (151 MHz, CDCl_3) δ 163.33, 159.91, 150.00, 144.61, 133.68, 133.46, 130.42, 128.26, 128.11, 127.68, 127.46, 126.02, 123.89, 106.35, 67.38, 51.59, 46.08, 45.40, 31.16, 15.26 ppm. HRMS: m/z $[\text{M}+\text{H}]^+$ 415.2234 (calculated for: $\text{C}_{24}\text{H}_{28}\text{N}_6\text{O}$ [415.2241] $^+$); HPLC purity: 97.4%.

***N*-Cyclohexyl-2-morpholino-7-(naphthalen-2-ylmethyl)-7H-purin-6-amine (60).** Compound 60 was prepared according to General Procedure 4. Compound 47 was used as the starting material. Yield 43% (brown solid); mp 246–248 °C; $^1\text{H NMR}$ (600 MHz, CDCl_3) δ 7.87 (d, $J = 8.5$ Hz, 1H), 7.84 (d, $J = 9.6$ Hz, 2H), 7.76–7.71 (m, 1H), 7.58–7.56 (m, 1H), 7.54–7.50 (m, 2H), 7.19 (dd, $J = 8.5, 1.9$ Hz, 1H), 5.50 (d, $J = 1.1$ Hz, 2H), 4.20 (d, $J = 7.2$ Hz, 1H), 3.72 (s, 8H), 3.70–3.65 (m, 1H), 1.53–1.46 (m, 2H), 1.40–1.32 (m, 1H), 1.32–1.25 (m, 2H), 1.14–1.04 (m, 2H), 0.84–0.75 (m, 1H), 0.59–0.53 (m, 2H) ppm; $^{13}\text{C NMR}$ (151 MHz, CDCl_3) δ 163.26, 160.03, 150.33, 144.47, 133.69, 133.64, 133.42, 130.31, 128.20, 128.12, 127.56, 127.34, 125.77, 123.70, 106.41, 67.40, 51.50, 49.07, 45.44, 32.54, 25.82, 24.57 ppm; HRMS: m/z $[\text{M}+\text{H}]^+$ 443.2550 (calculated for: $[\text{C}_{26}\text{H}_{31}\text{N}_6\text{O}]^+$ 443.2554); HPLC purity: 98.1%.

***N*¹,*N*¹-Dimethyl-*N*²-[2-morpholino-7-(naphthalen-2-ylmethyl)-7H-purin-6-yl] ethane-1,2-diamine (61).** Compound 61 was prepared according to General Procedure 4. Compound 48 was used as the starting material. Yield 39% (brown solid); mp 166–168 °C; $^1\text{H NMR}$ (600 MHz, CDCl_3) δ 7.84–7.81 (m, 3H), 7.72–7.69 (m, 1H), 7.51–7.47 (m, 2H), 7.46 (d, $J = 1.9$ Hz, 1H), 7.18 (dd, $J = 8.5, 1.9$ Hz, 1H), 5.53 (s, 1H), 5.26 (s, 2H), 3.80–3.77 (m, 4H), 3.76–3.73 (m, 4H), 3.27 (td, $J = 5.9, 4.4$ Hz, 2H), 2.16 (t, $J = 5.9$ Hz, 2H), 1.83 (s, 6H) ppm; $^{13}\text{C NMR}$ (151 MHz, CDCl_3) δ 163.04, 160.07, 151.06, 144.37, 133.72, 133.52, 133.37, 129.56, 128.26, 128.09, 127.14, 126.98, 125.15, 123.70, 106.55, 67.42, 57.36, 51.18, 45.46, 44.91, 38.13 ppm; HRMS: m/z $[\text{M}+\text{H}]^+$ 432.2507 (calculated for: $\text{C}_{24}\text{H}_{30}\text{N}_7\text{O}$ [432.2506] $^+$); HPLC purity: 96.1%.

2-Morpholino-7-(naphthalen-2-ylmethyl)-*N*-(pyridine-4-ylmethyl)-7H-purin-6-amine (62). Compound 62 was prepared according to General Procedure 4. Compound 49 was used as the starting

material. Yield 45% (brown oil); mp 161–164 °C; ^1H NMR (600 MHz, CDCl_3) δ 8.09–8.06 (m, 2H), 7.92 (s, 1H), 7.87–7.85 (m, 1H), 7.85–7.83 (m, 1H), 7.70–7.67 (m, 1H), 7.60–7.53 (m, 2H), 7.50 (d, $J = 1.7$ Hz, 1H), 7.19 (dd, $J = 8.3, 1.9$ Hz, 1H), 6.48 (d, $J = 6.1$ Hz, 2H), 5.58 (s, 2H), 4.76 (t, $J = 5.8$ Hz, 1H), 4.39 (d, $J = 5.6$ Hz, 2H), 3.71–3.67 (m, 8H) ppm; ^{13}C NMR (151 MHz, CDCl_3) δ 163.70, 159.76, 150.30, 149.91, 147.70, 145.14, 133.70, 133.63, 133.28, 130.42, 128.29, 128.15, 127.81, 127.61, 125.47, 123.50, 121.99, 106.32, 67.25, 51.44, 45.34, 43.75 ppm; HRMS: m/z $[\text{M}+\text{H}]^+$ 452.2197 (calculated for: $\text{C}_{26}\text{H}_{26}\text{N}_7\text{O}$ [452.2193] $^+$); HPLC purity: 98.8%.

N-Benzyl-2-morpholino-7-(naphthalen-2-ylmethyl)-7H-purin-6-amine (63). Compound 63 was prepared according to General Procedure 4. Compound 50 was used as the starting material. Yield 45% (white solid); mp 196–198 °C; ^1H NMR (500 MHz, CDCl_3) δ 7.86 (s, 1H), 7.84 (dd, $J = 7.9, 1.4$ Hz, 1H), 7.78 (d, $J = 8.5$ Hz, 1H), 7.63 (dd, $J = 7.8, 1.6$ Hz, 1H), 7.58–7.49 (m, 2H), 7.43 (d, $J = 1.8$ Hz, 1H), 7.14–7.05 (m, 2H), 6.92 (t, $J = 7.7$ Hz, 2H), 6.67–6.62 (m, 2H), 5.50 (s, 2H), 4.64 (t, $J = 5.3$ Hz, 1H), 4.36 (d, $J = 5.2$ Hz, 2H), 3.79–3.76 (m, 4H), 3.74–3.70 (m, 4H) ppm; ^{13}C NMR (126 MHz, CDCl_3) δ 163.43, 159.90, 150.57, 144.71, 138.38, 133.66, 133.58, 133.16, 130.25, 128.62, 128.33, 128.21, 127.55, 127.46, 127.43, 127.26, 125.45, 123.49, 106.38, 67.35, 51.35, 45.41, 45.14 ppm. HRMS: m/z $[\text{M}+\text{H}]^+$ 451.2239 (calculated for: $\text{C}_{27}\text{H}_{27}\text{N}_6\text{O}$ [451.2241] $^+$); HPLC purity: 99.9%.

2-Morpholino-7-(naphthalene-2-ylmethyl)-7H-purin-6-amine (64). Compound 64 was prepared according to General Procedure 4. Compound 51 was used as the starting material. Yield 42% (white solid); mp 252–254 °C; ^1H NMR (600 MHz, CDCl_3) δ 8.07 (s, 1H), 8.00 (d, $J = 8.4$ Hz, 1H), 7.98–7.96 (m, 1H), 7.89–7.86 (m, 1H), 7.67 (s, 1H), 7.66–7.62 (m, 2H), 7.36 (dd, $J = 8.5, 1.9$ Hz, 1H), 5.69 (s, 2H), 4.82 (s, 2H), 3.90–3.87 (m, 4H), 3.86–3.83 (m, 4H); ^{13}C NMR (151 MHz, CDCl_3) δ 164.04, 150.81, 145.99, 133.71, 133.65, 133.18, 130.33, 128.27, 128.26, 127.58, 127.40, 125.48, 123.64, 106.38, 67.29, 51.31, 45.45 ppm; HRMS: m/z $[\text{M}+\text{H}]^+$ 361.1764 (calculated for: $\text{C}_{20}\text{H}_{20}\text{N}_6\text{O}$ [361.1771] $^+$); HPLC purity: 99.9%.

N-Ethyl-7-[(6-fluoronaphthalen-2-yl)methyl]-2-morpholino-7H-purin-6-amine (65). Compound 65 was prepared according to General Procedure 4. Compound 52 was used as the starting material. Yield 53% (white solid); mp 208–210 °C; ^1H NMR (600 MHz, CDCl_3) δ 7.85 (s, 1H), 7.82 (d, $J = 8.5$ Hz, 1H), 7.74 (dd, $J = 9.0, 5.5$ Hz, 1H), 7.57–7.54 (m, 1H), 7.45 (dd, $J = 9.5, 2.6$ Hz, 1H), 7.29 (td, $J = 8.7, 2.6$ Hz, 1H), 7.26 (d, $J = 9.1$ Hz, 1H), 5.52 (s, 2H), 4.33 (t, $J = 5.2$ Hz, 1H), 3.77–3.74 (m, 4H), 3.74–3.70 (m, 4H), 3.25–3.16 (m, 2H), 0.71 (t, $J = 7.2$ Hz, 3H); ^{13}C NMR (151 MHz, CDCl_3) δ 162.81, 161.48 (d, $^1J_{\text{C-F}} = 248.5$ Hz), 159.78, 150.87, 144.40, 134.36 (d, $^3J_{\text{C-F}} = 9.9$ Hz), 132.72, 130.59 (d, $^3J_{\text{C-F}} = 8.6$ Hz), 129.49 (d, $^4J_{\text{C-F}} = 5.6$ Hz), 125.13, 124.88, 117.98 (d, $^2J_{\text{C-F}} = 25.9$ Hz), 111.42 (d, $^2J_{\text{C-F}} = 24.1$ Hz), 106.36, 67.32, 51.24, 45.38, 35.80, 14.47 ppm; HRMS: m/z $[\text{M}+\text{H}]^+$ 407.1989 (calculated for: $\text{C}_{22}\text{H}_{24}\text{N}_6\text{OF}$ [407.1990] $^+$); HPLC purity: 98.86%.

N-Ethyl-2-morpholino-7-(quinolin-2-ylmethyl)-7H-purin-6-amine (66). Compound 66 was prepared according to General Procedure 4. Compound 53 was used as the starting material. Yield 34% (brown solid); mp 212–214 °C; ^1H NMR (600 MHz, CDCl_3) δ 8.22 (d, $J = 8.4$ Hz, 1H), 8.09–8.02 (m, 1H), 7.95 (s, 1H), 7.85 (dd, $J = 8.2, 1.3$ Hz, 1H), 7.83–7.80 (m, 1H), 7.62 (t, $J = 7.5$ Hz, 1H), 7.43 (d, $J = 8.4$ Hz, 1H), 7.37 (t, $J = 5.2$ Hz, 1H), 5.56 (s, 2H), 3.77–3.75 (m, 4H), 3.74–3.72 (m, 4H), 3.59–3.50 (m, 2H), 1.27 (t, $J = 7.2$ Hz, 3H) ppm; ^{13}C NMR (151 MHz, CDCl_3) δ 162.45, 161.19, 159.84, 155.94, 151.37, 147.36, 143.02, 139.09, 131.01, 128.87, 128.31, 128.10, 127.97, 120.55, 67.38, 53.88, 45.47, 36.08, 15.11 ppm; HRMS: m/z $[\text{M}+\text{H}]^+$ 390.2039 (calculated for: $\text{C}_{21}\text{H}_{24}\text{N}_7\text{O}$ [390.2037] $^+$); HPLC purity: 98.8%.

2-Chloro-6-methoxy-7-(naphthalen-2-ylmethyl)-7H-purine (67). Sodium methoxide in methanol (28% solution, 0.48 g) was added dropwise to a solution of compound 23a (0.78 g, 2.38 mmol) in THF (13 mL) at 0 °C. The reaction mixture was then stirred at RT for 2 h before being quenched with water (2 mL), and the resulting precipitate was collected by filtration, washed with Et_2O (5 mL) and dried *in vacuo* to

give compound 67. Yield 74% (white solid); mp 186–188 °C; ^1H NMR (600 MHz, CDCl_3) δ 8.09 (s, 1H), 7.86–7.83 (m, 2H), 7.81–7.76 (m, 1H), 7.62 (d, $J = 1.7$ Hz, 1H), 7.56–7.49 (m, 2H), 7.31 (dd, $J = 8.5, 1.8$ Hz, 1H), 5.66 (s, 2H), 4.14 (s, 3H) ppm; ^{13}C NMR (151 MHz, CDCl_3) δ 163.28, 157.71, 153.07, 146.67, 133.32, 133.22, 132.56, 129.33, 127.98, 127.91, 126.98, 126.89, 126.74, 124.78, 112.24, 55.08, 51.47 ppm. HRMS: m/z $[\text{M}+\text{H}]^+$ 325.0851 (calculated for: $\text{C}_{17}\text{H}_{14}\text{N}_4\text{OCl}$ [325.0851] $^+$); HPLC purity: 99.9%.

2-Chloro-6-ethoxy-7-(naphthalen-2-ylmethyl)-7H-purine (68). Sodium ethoxide in ethanol (21% solution, 0.6 g) was added dropwise to a solution of compound 23a (0.78 g, 2.38 mmol) in THF (13 mL) at 0 °C. The reaction mixture was then stirred at RT for 2 h before being quenched with water (2 mL), and the resulting precipitate was collected by filtration, washed with Et_2O (8 mL) and dried *in vacuo* to give compound 68. Yield 68% (white solid); mp 194–197 °C; ^1H NMR (600 MHz, CDCl_3) δ 8.10 (s, 1H), 7.85–7.81 (m, 2H), 7.78–7.75 (m, 1H), 7.61 (s, 1H), 7.53–7.47 (m, 2H), 7.28 (dd, $J = 8.5, 1.7$ Hz, 1H), 5.64 (s, 2H), 4.56 (q, $J = 7.1$ Hz, 2H), 1.38 (t, $J = 7.1$ Hz, 3H) ppm. ^{13}C NMR (151 MHz, CDCl_3) δ 176.85, 163.75, 157.80, 153.51, 146.98, 133.66, 133.59, 133.08, 129.66, 128.29, 127.36, 127.23, 127.06, 125.05, 112.52, 64.59, 51.87, 14.77 ppm; HRMS: m/z $[\text{M}+\text{H}]^+$ 339.1010 (calculated for: $\text{C}_{18}\text{H}_{16}\text{N}_4\text{OCl}$ [339.1007] $^+$); HPLC purity: 96.9%.

4,4'-[7-(Naphthalene-2-ylmethyl)-7H-purin-2,6-diyl] dimorpholine (69). Compound 23a (0.15 g, 0.45 mmol) and morpholine (0.5 g, 5.7 mmol), in a mixture of dioxane (5 mL) and water (1 mL) were charged to a sealed reaction tube. The reaction was carried out under microwave irradiation at 180 °C with power 150 W and maximum pressure 300 psi for 5 h. After the reaction proceeded, the solvent was evaporated *in vacuo*, and the residue was purified by flash chromatography (EtOAc/MeOH , 95:5). Yield 76% (yellow oil); ^1H NMR (600 MHz, CDCl_3) δ 7.89 (s, 1H), 7.83–7.79 (m, 2H), 7.75–7.71 (m, 1H), 7.51 (s, 1H), 7.51–7.48 (m, 2H), 7.19 (dd, $J = 8.5, 1.8$ Hz, 1H), 5.52 (s, 2H), 3.82–3.80 (m, 4H), 3.80–3.75 (m, 8H), 3.32–3.29 (m, 4H) ppm; ^{13}C NMR (126 MHz, CDCl_3) δ 164.55, 159.10, 155.82, 146.72, 133.47, 133.30, 133.04, 129.30, 127.89, 127.86, 126.93, 126.71, 125.71, 124.13, 109.84, 67.04, 66.49, 50.52, 50.46, 45.14 ppm; HRMS: m/z $[\text{M}+\text{H}]^+$ 431.21823 (calculated for: $\text{C}_{24}\text{H}_{27}\text{N}_6\text{O}_2$ [431.2190] $^+$); HPLC purity: 99.2%.

7-(Naphthalene-2-ylmethyl)-3,7-dihydro-1H-2,6-dithione (70). Thiourea (0.15 g, 2.1 mmol) was added to a solution of compound 23a (0.12 g, 0.36 mmol) in EtOH (13 mL) and the mixture was heated to reflux for 2 h before being cooled to RT. The resulting precipitate was collected by filtration, washed with EtOH (10 mL) and dried *in vacuo*. Yield 82% (yellow solid); 298 °C (compound decomposition); ^1H NMR (600 MHz, $\text{DMSO}-d_6$) δ 13.97 (s, 1H), 13.20 (s, 1H), 8.48 (s, 1H), 7.93–7.85 (m, 3H), 7.65 (s, 1H), 7.52–7.49 (m, 2H), 7.46–7.41 (m, 1H), 6.06 (s, 2H) ppm; ^{13}C NMR (151 MHz, $\text{DMSO}-d_6$) δ 174.20, 171.23, 147.38, 145.26, 134.94, 132.78, 132.29, 128.23, 127.77, 127.52, 126.35, 126.13, 125.43, 125.03, 120.51, 48.74 ppm; HRMS: m/z $[\text{M}+\text{H}]^+$ 325.0578 (calculated for: $\text{C}_{16}\text{H}_{13}\text{N}_4\text{S}_2$ [325.0576] $^+$); HPLC purity: 99.9%.

4-[6-Chloro-7-(naphthalen-2-ylmethyl)-7H-purin-2-yl] morpholine (71). Into a 10 mL round-bottom flask was placed compound 10 (0.04 g; 0.11 mmol). The reaction mixture was cooled to 0 °C and POCl_3 (2 mL) was added portion-wise. After addition, the flask was removed from the ice bath and heated to 135 °C. After 2 h, the reaction mixture was cooled down in an ice bath and the aqueous ammonia was added to the flask until the excess of POCl_3 was neutralized. The mixture was then extracted with CH_2Cl_2 (3×10 mL), and the combined organic layers were dried over sodium sulfate, filtered and evaporated *in vacuo*. The crude product was purified by flash chromatography (PE/EtOAc , 1:1). Yield 48% (white solid); mp 152–154 °C. ^1H NMR (600 MHz, CDCl_3) δ 8.01 (s, 1H), 7.86–7.81 (m, 2H), 7.77–7.71 (m, 1H), 7.54–7.47 (m, 3H), 7.27 (dd, $J = 8.5, 1.8$ Hz, 1H), 5.67 (s, 2H), 3.84 (m, 4H), 3.76 (m, 4H) ppm. ^{13}C NMR (151 MHz, CDCl_3) δ 164.80, 159.33, 148.80, 143.78, 133.60, 133.41, 133.07, 129.54, 128.20, 128.12, 127.15, 127.00,

126.26, 124.60, 115.97, 67.15, 50.94, 45.33 ppm. HRMS: m/z $[M+H]^+$ 380.1267 (calculated for: $[C_{20}H_{19}N_5OCl]^+$ 380.1273). HPLC purity: 99.61%.

4-[6-Methoxy-7-(naphthalen-2-ylmethyl)-7H-purin-2-yl] morpholine (72). 4-(6-Chloro-7-(naphthalen-2-ylmethyl)-7H-purin-2-yl) morpholine (0.03 g; 0.078 mmol) was dissolved dry THF (8 mL). Sodium methoxide in MeOH (25% solution; 0.4 mL) was added dropwise. The reaction mixture was stirred at RT for 2 h and then quenched with water (0.5 mL). The solvent was evaporated to dryness and the crude reaction mixture was purified by flash chromatography ($CH_2Cl_2/MeOH$, 20:1). Yield 90% (white solid); mp 137–138 °C. 1H NMR (500 MHz, $CDCl_3$) δ 7.85 (s, 1H), 7.84–7.79 (m, 2H), 7.78–7.73 (m, 1H), 7.57 (s, 1H), 7.51–7.46 (m, 2H), 7.31–7.28 (m, 1H), 5.54 (s, 2H), 3.99 (s, 3H), 3.84–3.80 (m, 4H), 3.79–3.74 (m, 4H) ppm. ^{13}C NMR (126 MHz, $CDCl_3$) δ 164.49, 159.31, 157.59, 144.98, 133.92, 133.57, 133.30, 129.17, 128.17, 128.07, 126.94, 126.77, 126.52, 125.10, 107.05, 67.28, 53.66, 51.30, 45.47 ppm. HRMS: m/z $[M+H]^+$ 376.1761 (calculated for: $[C_{21}H_{22}N_5O]^+$ 376.1768). HPLC purity: 96.32%.

4-[6-Ethoxy-7-(naphthalen-2-ylmethyl)-7H-purin-2-yl] morpholine (73). 4-(6-Chloro-7-(naphthalen-2-ylmethyl)-7H-purin-2-yl) morpholine **72** (0.06 g; 0.16 mmol) was dissolved in 8 mL of dry THF. Sodium ethoxide in EtOH (21% solution; 1.0 mL) was added dropwise. The reaction mixture was stirred at RT for 2 h and then quenched with water (0.5 mL). The solvent was evaporated to dryness and the crude reaction mixture was purified by flash chromatography ($CH_2Cl_2/MeOH$, 20:1). Yield 61% (white solid); mp 162–163 °C. 1H NMR (500 MHz, $CDCl_3$) δ 7.88 (s, 1H), 7.84–7.78 (m, 2H), 7.77–7.72 (m, 1H), 7.58 (s, 1H), 7.51–7.45 (m, 2H), 7.29 (dd, $J = 8.5, 1.7$ Hz, 1H), 5.54 (s, 2H), 4.43 (q, $J = 7.1$ Hz, 2H), 3.81–3.78 (m, 4H), 3.77–3.73 (m, 4H), 1.32 (t, $J = 7.1$ Hz, 3H) ppm. ^{13}C NMR (126 MHz, $CDCl_3$) δ 164.45, 159.30, 157.21, 144.88, 133.97, 133.48, 133.23, 129.07, 128.07, 128.03, 126.89, 126.69, 126.50, 125.02, 106.87, 67.23, 62.13, 51.32, 45.39, 14.71 ppm. HRMS: m/z $[M+H]^+$ 390.1916 (calculated for: $[C_{22}H_{24}N_5O_2]^+$ 390.1925). HPLC purity: 95.9%.

4-[6-(Methylthio)-7-(naphthalen-2-ylmethyl)-7H-purin-2-yl] morpholine (74). 4-(6-Chloro-7-(naphthalen-2-ylmethyl)-7H-purin-2-yl) morpholine **72** (0.07 g; 0.18 mmol) was dissolved in 10 mL of dry THF. An aqueous solution of sodium thiomethoxide (25% solution; 1.0 mL) was added dropwise and the reaction mixture was stirred at 40 °C for 3 h. Water (15 mL) was added to reaction mixture and reaction mixture was extracted with CH_2Cl_2 (3×10 mL); the combined organic layers were dried over sodium sulfate, filtered and evaporated *in vacuo* with no need for further purification. Yield 93% (white solid); mp 178–180 °C. 1H NMR (500 MHz, $CDCl_3$) δ 7.87 (s, 1H), 7.86–7.80 (m, 2H), 7.75–7.70 (m, 1H), 7.51–7.46 (m, 2H), 7.45 (s, 1H), 7.28 (dd, $J = 8.5, 1.7$ Hz, 1H), 5.66 (s, 2H), 3.89–3.83 (m, 4H), 3.82–3.76 (m, 4H), 2.56 (s, 3H) ppm. ^{13}C NMR (126 MHz, $CDCl_3$) δ 161.51, 159.17, 154.14, 146.60, 133.61, 133.58, 133.32, 129.33, 128.22, 128.09, 127.00, 126.83, 125.97, 124.60, 117.47, 67.28, 51.31, 45.36, 12.50 ppm. HRMS: m/z $[M+H]^+$ 392.1530 (calculated for: $[C_{21}H_{22}N_5OS]^+$ 392.1540). HPLC purity: 98.8%.

4-[6-(Ethylthio)-7-(naphthalen-2-ylmethyl)-7H-purin-2-yl] morpholine (75). 4-(6-Chloro-7-(naphthalen-2-ylmethyl)-7H-purin-2-yl) morpholine **72** (0.06 g; 0.16 mmol) and sodium thioethoxide (0.034 g; 0.32 mmol) were dissolved in a mixture of THF (8 mL) and water (2 mL). After 3 h of stirring at 40 °C, the solvent was evaporated *in vacuo*, followed by the addition of 15 mL water. The crude mixture was extracted with CH_2Cl_2 (3×10 mL), and the combined organics were dried over sodium sulfate, filtered, evaporated *in vacuo*, and purified by flash chromatography ($EtOAc/MeOH$, 95:5). Yield 91% (white solid); mp 172–174 °C. 1H NMR (500 MHz, $CDCl_3$) δ 7.87–7.81 (m, 3H), 7.76–7.71 (m, 1H), 7.51–7.46 (m, 3H), 7.28 (dd, $J = 8.5, 1.8$ Hz, 1H), 5.66 (s, 2H), 3.84 (m, 4H), 3.79 (m, 4H), 3.23 (q, $J = 7.3$ Hz, 2H), 1.34 (t, $J = 7.3$ Hz, 3H) ppm. ^{13}C NMR (126 MHz, $CDCl_3$) δ 161.60, 159.17, 153.82, 146.64, 133.59, 133.33, 129.32, 128.22, 128.09, 126.99, 126.82, 126.13, 125.88, 124.73, 117.43, 67.28, 51.30, 45.36, 24.20,

14.87 ppm. HRMS: m/z $[M+H]^+$ 406.1690 (calculated for: $[C_{22}H_{24}N_5OS]^+$ 406.1696). HPLC purity: 99.5%.

6-Chloro-7-(naphthalene-2-ylmethyl)-7H-purine (78). A suspension of 6-chloro-9H-purine (1.0 g, 6.49 mmol) and K_2CO_3 (1.0 g, 7.37 mmol) in DMF (10 mL) was stirred at RT. After 30 min, 2-(bromomethyl) naphthalene (1.58 g, 7.14 mmol) was added and the reaction mixture was kept stirring overnight. Water (100 mL) was added to the reaction mixture, and the suspension was extracted with CH_2Cl_2 (3×50 mL). The combined organics were dried over sodium sulfate, filtered and evaporated. The single analogues were separated *via* column chromatography with $PE/EtOAc$ as eluent. The 7-substituted derivative was the minor product with lower R_f . Yield 16%; mp 168–170 °C. 1H NMR (500 MHz, $CDCl_3$) δ 8.91 (s, 1H), 8.30 (s, 1H), 7.89–7.84 (m, 2H), 7.79–7.75 (m, 1H), 7.57 (s, 1H), 7.55–7.50 (m, 2H), 7.31 (dd, $J = 8.5, 1.9$ Hz, 1H), 5.85 (s, 2H). ^{13}C NMR (126 MHz, $CDCl_3$) δ 162.43, 153.02, 149.55, 143.60, 133.55, 133.49, 132.32, 129.82, 128.21, 128.17, 127.34, 127.25, 126.64, 124.58, 122.95, 51.24. HRMS: m/z $[M+H]^+$ 295.0744 (calculated for: $[C_{16}H_{12}ClN_4]^+$ 295.0745). HPLC purity: 97.5%.

7-(Naphthalene-2-ylmethyl)-1,7-dihydro-6H-purin-6-one (79). A suspension of 6-chloro-7-(naphthalene-2-ylmethyl)-7H-purine (0.32 mmol) in 1 M aqueous solution of NaOH (10 mL) was heated at 100 °C. After 24 h the solution was acidified with 2 N aqueous HCl to pH 3–4, resulting in the precipitation of a white solid. This solid was filtered, washed with water (20 mL) and dried *in vacuo*. Yield 96% (white solid); mp 215 °C (compound decomposition). 1H NMR (500 MHz, $DMSO-d_6$) δ 12.33 (s, 1H), 8.48 (s, 1H), 8.00 (s, 1H), 7.95–7.85 (m, 3H), 7.83 (s, 1H), 7.57–7.49 (m, 3H), 5.76 (s, 2H). ^{13}C NMR (126 MHz, $DMSO-d_6$) δ 157.24, 154.41, 144.71, 144.04, 134.93, 132.76, 132.40, 128.39, 127.78, 127.56, 126.44, 126.25, 126.19, 125.44, 114.79, 49.44. HRMS: m/z $[M+H]^+$ 277.1081 (calculated for: $[C_{16}H_{13}N_4O]^+$ 277.1084). HPLC purity: 98.9%.

7-(Naphthalene-2-ylmethyl)-1,7-dihydro-6H-purin-6-thione (80). Thiourea (0.075 g, 1.0 mmol) was added to a solution of compound **78** (0.1 g, 0.36 mmol) in EtOH (10 mL) and the reaction was stirred at reflux for 2 h. After the reaction mixture cooled down, the resulting precipitate was collected by filtration, washed with EtOH (10 mL) and dried *in vacuo*. Yield 91% (yellow solid); mp 294 °C (compound decomposition); 1H NMR (500 MHz, $DMSO-d_6$) δ 13.77 (s, 1H), 8.72 (s, 1H), 8.23 (d, $J = 3.1$ Hz, 1H), 7.95–7.82 (m, 3H), 7.72 (d, $J = 1.8$ Hz, 1H), 7.55–7.44 (m, 3H), 6.26 (s, 2H) ppm; ^{13}C NMR (126 MHz, $DMSO-d_6$) δ 170.00, 153.08, 148.48, 145.10, 135.39, 132.77, 132.29, 128.28, 127.74, 127.54, 126.37, 126.15, 125.75, 125.25, 125.15, 48.96 ppm; HRMS: m/z $[M+H]^+$ 293.0855 (calculated for: $C_{16}H_{13}N_4S$ [293.0855] $^+$); HPLC purity: 95.6%.

2,4-Dichloro-5-[(naphthalen-2-yl)methyl]-5H-pyrrolo[3,2-d]pyrimidine (82). A suspension of 2,4-dichloro-5H-pyrrolo [3,2-d]pyrimidine (1.0 g, 5.31 mmol) and K_2CO_3 (0.88 g, 6.35 mmol) in DMF (10 mL) was stirred at RT. After 30 min, 2-(bromomethyl)naphthalene (1.28 g, 5.82 mmol) was added, and the reaction mixture was kept stirring at RT overnight. Water (3×100 mL) was added to the reaction mixture, and the resulting suspension was extracted with CH_2Cl_2 (3×50 mL). The combined organics were dried over sodium sulfate, filtered and evaporated. The regioisomers were separated *via* flash chromatography ($PE/EtOAc$, 1:1). Yield: 86% (yellow solid); mp 109–111 °C. 1H NMR (500 MHz, $CDCl_3$) δ 7.89–7.82 (m, 2H), 7.78–7.73 (m, 1H), 7.59 (d, $J = 3.2$ Hz, 1H), 7.52–7.49 (m, 2H), 7.44 (s, 1H), 7.23 (dd, $J = 8.5, 1.9$ Hz, 1H), 6.74 (d, $J = 3.2, 0.6$ Hz, 1H), 5.84 (s, 2H) ppm. ^{13}C NMR (126 MHz, $CDCl_3$) δ 154.39, 150.54, 143.01, 138.79, 133.62, 133.22, 132.95, 129.14, 127.80, 127.73, 126.73, 126.55, 125.60, 124.09, 123.08, 102.96, 52.43 ppm. HRMS: m/z $[M+H]^+$ 328.0402 (calculated for: $[C_{16}H_{12}Cl_2N_4]^+$ 328.0403). HPLC purity: 99.0%.

2-Chloro-5-[(naphthalen-2-yl)methyl]-3H,4H,5H-pyrrolo[3,2-d]pyrimidin-4-one (83). 2,4-Dichloro-5-[(naphthalen-2-yl)methyl]-5H-pyrrolo [3,2-d]pyrimidine (0.76 mmol) was dissolved in dioxane (5 mL). The solution was added to 2 N aqueous solution of NaOH (5 mL) and the mixture was heated to 100 °C. After 2 h, the solution was cooled

to room temperature and acidified with 2 N aqueous HCl to pH 3–4, resulting in the precipitation of a white solid. This solid was filtered, washed with water (20 mL) and dried *in vacuo*. Yield 72% (white solid); mp 234–236 °C. ¹H NMR (500 MHz, DMSO-*d*₆) δ 12.89 (s, 1H), 7.90–7.79 (m, 3H), 7.70 (s, 1H), 7.64 (d, *J* = 2.9 Hz, 1H), 7.51–7.45 (m, 2H), 7.42–7.39 (m, 1H), 6.39 (d, *J* = 2.9 Hz, 1H), 5.75 (s, 2H) ppm. ¹³C NMR (126 MHz, DMSO-*d*₆) δ 154.72, 144.67, 139.16, 136.14, 132.97, 132.49, 132.42, 128.45, 127.90, 127.73, 126.55, 126.27, 125.94, 125.56, 115.53, 103.01, 51.15 ppm. HRMS: *m/z* [M+H]⁺ 310.0740 (calculated for: [C₁₇H₁₃ClN₃O]⁺ 310.0742). HPLC purity: 98.2%.

2-(Morpholin-4-yl)-5-[(naphthalen-2-yl)methyl]-3H,4H,5H-pyrrolo[3,2-*d*]pyrimidin-4-one (84). Compound **83** (0.13 g, 0.40 mmol) and morpholine (0.5 g, 5.7 mmol) in a mixture of dioxane (5 mL) and water (1 mL) were charged to a sealed reaction tube. The reaction was carried out under microwave irradiation at 180 °C with power 150 W and maximum pressure 300 psi for 3 h. After the reaction proceeded, the solvent was evaporated *in vacuo*, and the residue was purified by flash chromatography (EtOAc/PE, 3:1). Yield 81% (white solid); mp 246–248 °C. ¹H NMR (500 MHz, DMSO-*d*₆) δ 10.98 (s, 1H), 7.88–7.79 (m, 3H), 7.69 (s, 1H), 7.47 (dd, *J* = 6.1, 2.2 Hz, 2H), 7.44 (d, *J* = 2.9 Hz, 1H), 7.40 (dd, *J* = 8.5, 1.5 Hz, 1H), 6.12 (d, *J* = 2.8 Hz, 1H), 5.67 (s, 2H), 3.66–3.60 (m, 4H), 3.41–3.36 (m, 4H) ppm. ¹³C NMR (126 MHz, DMSO-*d*₆) δ 155.31, 151.26, 146.52, 136.78, 132.96, 132.41, 131.66, 128.26, 127.81, 127.69, 126.45, 126.11, 125.76, 125.62, 112.41, 101.65, 65.85, 50.95, 46.54 ppm. HRMS: *m/z* [M+H]⁺ 361.1661 (calculated for: [C₂₁H₂₁N₄O₂]⁺ 361.1659); HPLC purity: 99.9%.

Determination of antimycobacterial activity. The *in vitro* antimycobacterial activity of the prepared compounds was evaluated as described previously [41,44]. Briefly, *Mycobacterium tuberculosis* CNCTC My 331/88 (H₃₇Rv), *M. kansasii* CNCTC My 235/80 and *M. avium* CNCTC My 330/88 from the Czech National Collection of Type Cultures (CNCTC) were used for the determination of activity against standard drug-susceptible strains. Clinically isolated strains *M. tuberculosis* 234/2005, *M. tuberculosis* 9449/2007, *M. tuberculosis* 8666/2010, *M. tuberculosis* Praha 1, *M. tuberculosis* Praha 4 and *M. tuberculosis* Praha 131 were used for the determination of activity against MDR/XDR strains. The activities of the compounds were determined *via* the micromethod for the determination of the minimum inhibitory concentration in Sula's semisynthetic medium (SEVAC, Prague). Investigated purine derivatives were dissolved in dimethyl sulfoxide and added to the medium at concentrations of 1000, 500, 250, 125, 62, 32, 16, 8, 4, 2, 1 and 0.5 μmol/L. MICs, defined as the lowest concentration of a compound at which mycobacterial growth inhibition occurred (the concentration that inhibited >99% of the mycobacterial population), were determined after incubation at 37 °C for 7/14/21 days for *M. kansasii* and after 14/21 days for the *M. tuberculosis* and *M. avium* strains. INH was used as a standard anti-TB drug.

Determination of efficacy against intracellular *Mtb* H₃₇Rv. First, IC₅₀ of compound **56** to MonoMac6 cells was determined using MTT (3-(4,5-dimethylthiazol-2-yl)-2,5-diphenyltetrazolium bromide) assay. RPMI-1640 medium supplemented with 10% FBS, 2 mM L-glutamine and 160 μg/mL gentamicin (CM) was used for maintaining MonoMac6 cells. One day before the experiment, cells were seeded during the exponential growth phase on 96-well cell culture plates (6.5 × 10³ cells/100 μL/well) in CM. Cells were treated for 48 h with the compounds dissolved in incomplete medium (ICM) with 1% (v/v) DMSO in the concentration range 2.56 × 10⁻³ – 250 μM. As control ICM and ICM containing 1% (v/v) DMSO were used. After incubation, cells were washed with ICM three times, and in the last step, ICM was added. After the washing steps 45 μL sterile-filtered MTT was added (2 mg/mL) to the cells. After 3.5 h incubation, plates were centrifuged (2000 rpm, 5 min), supernatant was removed, and formazan crystals were dissolved in DMSO. Absorbance was determined with an ELISA plate reader (Lab-systems iEMS reader, Helsinki, Finland) at λ = 540 and 620 nm. The 50% inhibitory concentration (IC₅₀) values were determined from the dose-response curves. The curves were calculated with Microcal

OriginPro (version: 2018) software.

To assess the intracellular inhibition activity of compound **56**, infected MonoMac6 monocytes (2 × 10⁵ cells/1 mL medium/well) were used. MonoMac 6 cells were cultured with RPMI-1640 medium containing 10% FBS. Adherent cells were infected with *Mtb* H₃₇Rv at a multiplicity of infection (MOI) of 10 for 4 h. Extracellular bacteria were removed, and the culture was washed three times with RPMI-1640 ICM. The infected monolayer was incubated for 1 day before the treatment. Infected cells were then treated with compound **56** at 25 μM final concentration. After 3 days the treatment was repeated with freshly prepared solution of compounds for an additional 3 days. Untreated cells were considered as negative control. After washing steps – in order to remove the compounds – infected cells were lysed with 2.5% sodium dodecyl sulfate solution. The CFU of *Mtb* was enumerated on Löwenstein-Jensen solid media after 4 weeks of incubation.

Determination of antibacterial activity. The antibacterial susceptibility testing was performed on 8 bacterial strains, four Gram-positive (*Staphylococcus aureus* C1947, methicillin-resistant *Staphylococcus aureus*/MRSA/C1923, *Staphylococcus epidermidis* C1936, vancomycin-resistant *Enterococcus faecium*) and four Gram-negative (*Escherichia coli* A1235, *Klebsiella pneumoniae* C1950, ESBLs producing *Klebsiella pneumoniae* C1914, multidrug-resistant *Pseudomonas aeruginosa* A1245) strains. All bacterial strains used in this study were obtained as clinical isolates from patients (University Hospital, Hradec Králové, Czech Republic) and stored at –70 °C in Cryobank. Before testing, all strains were cultivated on Mueller-Hinton agar (HiMedia, Cadarsky-Envitek, Prague, Czech Republic) and second subculture was used for susceptibility testing.

The antibacterial susceptibility was determined by the microdilution broth method using the previously published optimized protocol [45]. Mueller-Hinton broth (HiMedia, Cadarsky-Envitek, Prague, Czech Republic) adjusted to pH 7.4 (±0.2) was used as the test medium. DMSO served as a diluent for all compounds and its final concentration did not exceed 1% in the test medium. The wells of the microdilution tray contained 200 μL of the Mueller-Hinton broth with two-fold serial dilutions of the tested compounds and were inoculated with 10 μL of the bacterial suspension (1.5 × 10⁸ viable colony forming units/CFU/per 1 mL). The MIC values, defined as 95% inhibition of bacterial growth, were determined after 24 h and 48 h of incubation at 36 °C ± 1 °C. The MBC values were determined as the concentration of compound causing a decrease in the number of bacterial colonies by ≥ 99.9%, after subculturing of a 10 μL aliquot of each well without a visible growth.

Cytotoxicity assay. HepG2 – 24 h incubation: The cytotoxicity profile of tested compounds was evaluated using human origin cell lines HepG2. The cells were cultivated in Dulbecco's modified Eagle's medium (DMEM, Biosera, Nuaille, France) supplemented with 10% fetal bovine serum (FBS, Biosera), 1% penicillin (10,000 U/mL) – streptomycin (10,000 μg/mL) antibiotic solution (Merck, Germany) at 37 °C in CO₂ incubator (Binder CO₂ Incubator CB160, Tuttlingen, Germany) and routinely passaged by trypsinization at 75–85% confluence.

The MTT (3-(4,5-dimethylthiazol-2-yl)-2,5-diphenyl-tetrazolium bromide (Merck) reduction assay was used for measurement of compounds cytotoxicity. Cell viability was detected after 24-h incubation with the tested substances. For the assay, HepG2 cells were seeded into 96-well plates in 100 μL volume and density of 15 × 10³ cells per well. Cells were allowed to attach overnight before the treatment. The stock solutions of tested compounds were prepared in DMSO, which were further serially diluted in the appropriate culture medium and added to the cells in 96-well culture plate. The final concentration of DMSO did not exceed 1% (v/v).

After 24 h incubation, the medium containing serially diluted substances was aspirated from each well and replaced by 100 μL of fresh medium containing MTT (0.5 mg/mL). Plates were subsequently incubated at 37 °C in a CO₂ incubator for 1 h. Thereafter, medium was aspirated and purple crystals of MTT formazan were dissolved in 100 μL DMSO under shaking. The optical density of each well was measured

using Spark® multimode microplate reader (Tecan Group Ltd., Männedorf, Switzerland) at 570 nm.

The cytotoxicity of tested compounds was expressed as value IC_{50} , which was calculated using 4-parametric nonlinear regression with statistic software GraphPad Prism (version 9.3.0 for Windows, GraphPad Software Inc., USA). Data were obtained from three independent experiments performed in triplicates. The IC_{50} value was expressed as mean \pm SD.

HepG2 and H9c2 – 72 h incubation: HepG2 (human hepatocellular carcinoma) and H9c2 (embryonic rat heart myoblast) cell lines were cultivated in DMEM supplemented with FBS (Lonza) and 1% penicillin/streptomycin (Lonza) at 37 °C in a humidified atmosphere of 5% CO_2 in air. For the toxicity/antiproliferation experiments, the cells were seeded on 96-well plates at a density of 10,000 cells per well. After 24 h, the cells were treated with the tested compounds at the specified final concentration for 72 h. Treatment with vehicle alone (DMSO 0.1% final concentration) or Triton X-100 (1% final concentration; Sigma, Germany) was used for negative and positive controls, respectively. Viability after 72 h was determined using an assay based on the ability of active mitochondria to change yellow MTT to purple formazan. Briefly, 3 mg/mL of MTT solution in phosphate buffered saline was added to the culture medium and after 2 h of incubation at 37 °C, cells were lysed with lysis buffer (isopropanol, 0.1 M HCl, 5% Triton X-100) for 30 min at room temperature. After dissolution, the concentration of product was measured spectrophotometrically with a Tecan Infinite 200 M plate reader at 570 nm, subtracting the background obtained at 690 nm. The viability of the experimental groups was expressed as percentages of the negative controls (100%). IC_{50} values were calculated using GraphPad Prism 9 software.

Aqueous solubility determination. The water solubility of tested compounds was determined in the ultrapure distilled water containing 5% of DMSO. Briefly, calculated amounts of compounds **10**, **30**, **33**, **56**, **59**, **63**, **64**, and **73** were first dissolved in DMSO (50 μ L) and then diluted by ultrapure distilled water (950 μ L) to reach 50 μ M concentrations. Then, 200 μ L of these solutions were analyzed for the UV/VIS absorption spectrum by the multimode microplate reader (TECAN Spark®, Tecan Group Ltd., Switzerland) and the wavelength of maximum absorbance was used for further testing of the corresponding compounds. Subsequently, six consecutive concentrations were prepared for each compound by serial dilution of 50 μ M standard solution and the absorbance of these solutions (200 μ L) was measured by microplate reader. The data were used to calculate the calibration curve by the linear regression method. Finally, the over-saturated solutions of the tested compounds were prepared and incubated in ultrasound water bath at 37 °C for 10 min. Then the solutions were centrifuged at 8000 RPM for 10 min and the UV/VIS absorption of the supernatant was measured by microplate reader. The obtained absorption value was used to calculate the maximum water solubility of the tested compounds. In case the absorption value of the supernatant was higher than the calibration curve range, the supernatant was diluted with 5% DMSO/water solution to match the calibration curve.

Microsomal stability determination. The tested compounds **10**, **30**, **33**, **56**, **59**, **63**, **64** and **73** were incubated with Human Liver Microsomes according to the Cyprotex assay protocol [46]. Briefly, compounds were dissolved in DMSO to produce stock sample solutions. 5 μ L of stock solution was mixed with 12.5 μ L of pooled Human Liver Microsomes (concentration 0.5 mg/mL, H2620, LOT no. 1210347, SekiSui, XenoTech, Canada) and 458 μ L of 0.1 M potassium phosphate buffer solution (pH = 7.4, adjusted by addition of NaOH) and preincubated for 5 min (300 RPM, 25 °C). The final concentration of DMSO in the incubation mixture did not exceed 1% (v/v) and the concentration of tested compounds was set at 3 μ M. The biotransformation reaction was started by addition of 25 μ L of RapidStart NADPH Regenerating System (K5000, LOT. 1910008, SekiSui, XenoTech, Canada) and then incubated for 5 different time points (0, 5, 15, 30, 45 min). The reaction was terminated by addition of 500 μ L of cooled acetonitrile (–20 °C) with 1 μ M internal

standard [IS; **67**] and centrifuged for 5 min (14,000 RPM, 20 °C). Subsequently, 400 μ L of supernatant was transferred to the vial and analyzed by LC-MS. Three types of blank samples were prepared in the same way, with a one-step exception. In the biological blank sample was added 5 μ L of DMSO instead of 5 μ L stock solution, in the chemical blanks was added 50 μ L of water instead of HLM, and in the case of control blank sample was added 25 μ L of water instead of 25 μ L of RapidStart System. LC-MS system and the chromatographic conditions for the measurement of the samples are mentioned above in the section General chemistry method. The peak areas of the compounds (Acmp) and internal standards (AIS) were detected in extracted ion chromatograms from the mass spectrometer data in positive mode. The Acmp/AIS was calculated a logarithmized. From a plot of \ln Acmp/AIS against time of incubation, the gradient (k value) was established. The $T_{1/2}$ value, and CL_{int} were calculated according to the Cyprotex protocol and compared with known fast and slow metabolically degraded standards of verapamil and diazepam (Table 6) [46].

In vitro stability testing in human plasma. Compounds **10**, **30**, **33**, **56**, **59**, **63**, **64**, and **73** were incubated with Human Pooled Plasma (Batch S00G71, Biowest, France). Briefly, compounds were dissolved in DMSO to produce stock sample solutions. 10 μ L of stock solution was added to 990 μ L of human plasma to initiate the reaction. The final concentration of DMSO in the incubation mixture did not exceed 1% (v/v) and the concentration of tested compounds was set at 1 μ M. Each compound was incubated for 0, 15, 30, 60 and 120 min at 37 °C. The reactions were stopped by transferring 100 μ L of incubate to 100 μ L of acetonitrile containing internal standard (IS; **67**) at the appropriate time points and centrifuged at 12,000 rpm for 5 min at 4 °C to precipitate the protein. After that, 150 μ L of supernatant was transferred to the vial and analyzed by LC-MS under the same conditions as in the section General chemistry method. The areas of the compounds (Acmp) and internal standards (AIS) were detected in extracted ion chromatograms from the mass spectrometer data in positive mode. From the ratio between peak area ratios (compound peak area/internal standard peak area) obtained at incubation times 0 and 120 min, the percentage of remaining compound was calculated.

Selection of compound 10 resistant isolates. The strain H₃₇Rv was grown to log phase in Middlebrook 7H9 media supplemented with 10% OADC, 0.2% glycerol and 0.05% Tween 80. The bacterial culture was then centrifuged (3000 \times g, 6 min), and concentrated to an OD₆₀₀ = 50, and 50 μ L plated onto solid media (Middlebrook 7H11, supplemented with 10% OADC and 0.2% glycerol) containing 128, 64, 32, 16, 8, and 0 μ M of **10**. Following incubation for 4–6 weeks, resistant colonies appeared. From the plate containing 128 μ M **10**, 3 colonies were selected and grown in liquid media without **10**, and resistance of the grown culture to **10** was confirmed by microplate dilution assays. Genomic DNA was extracted and sequencing by Illumina technology, with subsequent variant analysis performed as described previously [47].

Metabolic labeling. *Mtb* H₃₇Rv were grown shaking at 37 °C in 7H9 medium containing 10% OADC, 0.2% glycerol and 0.05% Tween 80 until OD₆₀₀ 0.28. The cultures were aliquoted (95 μ L) into Eppendorf tubes containing DMSO (control) or the drugs dissolved in DMSO (final concentration of the drugs was 10 \times MIC in the above medium, DMSO 2%) and 5 μ L of sterile water containing 0,1 μ Ci of [¹⁴C]-acetate (specific activity: 110 mCi/mmol, American Radiolabeled Chemicals, Inc.). After 24 h of static incubation at 37 °C the whole cultures were transferred into 1.5 mL of $CHCl_3:CH_3OH$ (2:1), and treated for 2 h at 65 °C. The samples were then subjected to biphasic Folch wash. The organic phase was dried, dissolved in 30 μ L of $CHCl_3:CH_3OH$ (2:1) and 5 μ L of each sample was loaded on Silica Gel TLC plate (Merck) followed by separation in $CHCl_3:CH_3OH:H_2O$ (40:8:1). The radiolabeled lipids were visualized by Amersham Typhoon 5 phosphorimager (GE Healthcare).

In silico study. Molecular docking was used for binding pose calculations. The 3D structure ligands were built by OpenBabel, v. 2.3.2 [48] and optimized by Avogadro, v. 1.2.0 using the force fields GAFF

[49]. They were converted into pdbqt-format by OpenBabel, v. 2.3.2. The DprE1 structure was gained from the RCSB database (PDB ID: 4P8N, resolution 1.79 Å) and prepared for docking by the function DockPrep of the software Chimera, v. 1.14 [50] and by MGLTools, v. 1.5.4 [51]. The docking calculation was made by Vina, v. 1.1.2 as semi-flexible with flexible ligand and rigid receptor [52].

The docking pose of all the ligands were improved by MD simulation. The receptor structure was prepared using the software Chimera. The best-scored docking poses were taken as the starting point for MD. The force-field parameters for ligands were assessed by Antechamber [53], v. 20.0 using General Amber force-field 2 [54]. MD simulation was carried out by Gromacs, v. 2018.1 [55]. The complex receptor-ligand was solvated in the periodic water box using the TIP3P model. The system was neutralized by adding Na⁺ and Cl⁻ ions to a concentration of 10 nM. The system energy was minimized and equilibrated in a 100-ps isothermal-isochoric NVT and then a 100-ps isothermal-isobaric NPT phase. Then, a 10-ns MD simulation was run at a temperature of 300 K. The molecular docking and MD results were 3D visualized by the PyMOL Molecular Graphics System, Version 2.4.1, Schrödinger, LLC.

Computational chemistry studies. For the QSAR analyses, only compounds with defined MIC activities against *Mycobacterium tuberculosis* after 14 days of incubation were selected. The compound MIC activities defined only by the lower limit (e.g., >500 µM) were omitted from the analyses. The involved molecules ($n = 33$) were first modeled in Schrodinger 2022–2, geometrically optimized and polarized for pH = 7.4 in LigPrep utility. First QSAR analyses were performed in the AutoQSAR application of Schrodinger 2022–2 using the negative decadic logarithm of MIC values (i.e., pMIC (14 d)) as the dependent variable. The numerical QSAR analyses in AutoQSAR employed random distribution of the compounds into the training and test sets, in a ratio 3:1. Automatic statistical analyses tested four regression methods: MLR, PLS, KPLS, and PCR. As molecular descriptors of the compounds, binary fingerprints of radial, linear, dendritic, and molprint 2D types were calculated and used. In addition, several hundreds of numerical molecular descriptors such as topological and physical-chemical descriptors were automatically generated and tested in the QSAR analyses. In total, 200 various regression models were developed and evaluated by the following statistical criteria for the training and test sets: R^2 , SD , Q^2 , $RMSE$, Q^2 -MW. The optimal QSAR model was selected for the interpretation of the structure-antimycobacterial activity relationships.

The 3D Field-Based QSAR analyses were performed also in Schrodinger 2022–2. The first step was flexible molecular alignment of conformer libraries, with up to 1000 conformer for each compound, using a thorough search and a superimposing algorithm based on the largest common Bemis-Murcko scaffold. As the alignment template, 56 was used for superimposition of all studied compounds ($n = 33$). After the molecular alignment, each molecule was quantum-chemically modeled in Jaguar 11.6 (Schrodinger 2022–2) by single point energy calculation with a DFT method B3LYP-D3/6-31G** to obtain atomic electrostatic potential charges (ESP).

The prepared molecules were analyzed by the 3D Field-Based QSAR utility in Schrodinger 2022–2 employing random distribution of the compounds into the training and test sets, in a ratio 3:1. Five Gaussian interaction fields (i.e., steric, electrostatic, hydrophobic, H-bond accepting, H-bond donating) were generated in a grid box with spacing of 1 Å and boundaries 3 Å beyond the volume of the training set compounds. Within the 3D QSAR analyses, interactions closer than 2 Å to any atoms were ignored and steric and electrostatic interactions greater than 30 kcal/mol in absolute value were truncated. Each interaction field variable with standard deviation lower than 0.01 and absolute Student's t -value lower than 1.5 were removed. The 3D QSAR models were developed by PLS regression technique with number of latent variables ranging from 1 to 7 and evaluated by several statistical criteria for the training (i.e. coefficient of determination R^2 , standard residual deviation SD , cross-validated coefficient of determination R^2 -CV by leave-one-out technique, scrambled coefficient of determination R^2 -Sc

with randomly permuted pMIC activities, Fisher-Snedecor F -test, and probability p of the chi-square related F -test randomness) and test sets (i.e. coefficient of determination Q^2 , root-mean-square error $RMSE$, Pearson's correlation coefficient $Pe-R$). The optimal 3D QSAR model with 7 latent variables was graphically represented by contour isosurfaces of the PLS β -coefficients multiplied by their cross-validated standard deviations upon projection onto the Euclidian space of the superimposed molecules and interpreted.

Declaration of competing interest

The authors declare that they have no known competing financial interests or personal relationships that could have appeared to influence the work reported in this paper.

Data availability

Data will be made available on request.

Acknowledgments

This study was supported by the project by Ministry of Health of the Czech Republic (grant Nr. NU21-05-00446), by MH CZ - DRO (UHHK, 00179906), by the project National Institute of Virology and Bacteriology (Programme EXCELES, ID Project No. LX22NPO5103) – Funded by the European Union – Next Generation EU, by the Charles University (project GA UK Nr. 392822 and project SVV 260 547), and by the Ministry of Education, Youth and Sports of the Czech Republic through the e-INFRA CZ (ID: 90140). RD and VS thank the University of Chemistry and Technology for providing hardware and software support. KM acknowledges support by the Slovak Research and Development Agency (grant no. APVV-20-0230) and by the Operation Program of Integrated Infrastructure for the project, Advancing University Capacity and Competence in Research, Development and Innovation, ITMS2014+: 313021X329, co-financed by the European Regional Development Fund. SB acknowledges support by the National Research, Development and Innovation Office, Hungary (grant number: OTKA NKFIH K-142904). LL thanks the financial support of the Doctoral School of Biology, Immunology Program, Institute of Biology, Eötvös Loránd University.

Appendix A. Supplementary data

Supplementary data to this article can be found online at <https://doi.org/10.1016/j.ejmech.2023.115611>.

References

- [1] World Health Organization, Tuberculosis Fact Sheet, Reviewed 27 October 2022. <http://www.who.int/mediacentre/factsheets/fs104/en/>. (accessed February 20, 2023).
- [2] World Health Organization, Global Tuberculosis Report, 2022. <https://www.who.int/teams/global-tuberculosis-programme/tb-reports>. (Accessed 16 February 2023).
- [3] WHO announces updated definitions of extensively drug-resistant tuberculosis. <https://www.who.int/news/item/27-01-2021-who-announces-updated-definitions-of-extensively-drug-resistant-tuberculosis>, (accessed March 16, 2023).
- [4] WHO consolidated guidelines on tuberculosis: module 4: treatment: drug-resistant tuberculosis treatment. <https://www.who.int/publications/i/item/9789240007048>. (accessed February 16, 2023).
- [5] P. Nahid, S.R. Mase, G.B. Migliori, G. Sotgiu, G.H. Bothamley, J.L. Brozek, A. Cattamanchi, J.P. Cegielski, L. Chen, C.L. Daley, T.L. Dalton, R. Duarte, F. Fregonese, J.C. Robert Horsburgh, F.A. Khan, F. Kheir, Z. Lan, A. Lardizabal, M. Lauzardo, J.M. Mangan, S.M. Marks, L. McKenna, D. Menzies, C.D. Mitnick, D. M. Nilsen, F. Parvez, C.A. Peloquin, A. Rafferty, H.S. Schaaf, N.S. Shah, J.R. Starke, J.W. Wilson, J.M. Wortham, T. Chorba, B. Seaworth, Treatment of drug-resistant tuberculosis. An official ATS/CDC/ERS/IDSA clinical practice guideline, *J. Respir. Crit. Care Med.* 200 (2019) e93–e142.
- [6] S. Kadura, N. King, M. Nakhoul, H. Zhu, G. Theron, C.U. Köser, M. Farhat, Systematic review of mutations associated with resistance to the new and repurposed *Mycobacterium tuberculosis* drugs bedaquiline, clofazimine, linezolid, delamanid and pretomanid, *J. Antimicrob. Chemother.* 75 (2020) 2031–2043.

- [7] V. Makarov, G. Manina, K. Mikusova, U. Mollmann, O. Ryabova, B. Saint-Joanis, N. Dhar, M.R. Pasca, S. Buroni, A.P. Lucarelli, A. Milano, E. De Rossi, M. Belanova, A. Bobovska, P. Dianiskova, J. Kordulakova, C. Sala, E. Fullam, P. Schneider, J. D. McKinney, P. Brodin, T. Christophe, S. Waddell, P. Butcher, J. Albrethsen, I. Rosenkrands, R. Brosch, V. Nandi, S. Bharath, S. Gaonkar, R.K. Shandil, V. Balasubramanian, T. Balganes, S. Tyagi, J. Grosset, G. Riccardi, S.T. Cole, Benzothiazinones kill Mycobacterium tuberculosis by blocking arabinan synthesis, *Science* 324 (2009) 801–804.
- [8] V. Makarov, B. Lechartier, M. Zhang, J. Neres, A.M. van der Sar, S.A. Raadsen, R. C. Hartkoorn, O.B. Ryabova, A. Vocat, L.A. Decosterd, N. Widmer, T. Buclin, W. Bitter, K. Andries, F. Pojer, P.J. Dyson, S.T. Cole, Towards a new combination therapy for tuberculosis with Next generation benzothiazinones, *EMBO Mol. Med.* 6 (2014) 372–383.
- [9] P.S. Shirude, R. Shandil, C. Sadler, M. Naik, V. Hosagrahara, S. Hameed, V. Shinde, C. Bathula, V. Humnabadkar, N. Kumar, J. Reddy, V. Panduga, S. Sharma, A. Ambady, N. Hegde, J. Whiteaker, R.E. McLaughlin, H. Gardner, P. Madhavapeddi, V. Ramachandran, P. Kaur, A. Narayan, S. Gupta, D. Awasthy, C. Narayan, J. Mahadevaswamy, K.G. Vishwas, V. Ahuja, A. Srivastava, K. R. Shikawa, S. Bharath, R. Kale, M. Ramaiah, N.R. Choudhury, V. K. Sambandamurthy, S. Solapure, P.S. Iyer, S. Narayanan, M. Chatterji, Azaindoles: noncovalent DprE1 inhibitors from scaffold morphing efforts, kill Mycobacterium tuberculosis and are efficacious in vivo, *J. Med. Chem.* 56 (2013) 9701–9708.
- [10] N. Hariguchi, X. Chen, Y. Hayashi, Y. Kawano, M. Fujiwara, M. Matsuba, H. Shimizu, Y. Ohba, I. Nakamura, R. Kitamoto, T. Shinohara, Y. Uematsu, S. Ishikawa, M. Itotani, Y. Haraguchi, I. Takemura, M. Matsumoto, OPC-167832, a novel carbostyryl derivative with potent antituberculosis activity as a DprE1 inhibitor, *Antimicrob. Agents Chemother.* 64 (2020), e02020-02019.
- [11] K. Mikusova, H.R. Huang, T. Yagi, M. Holsters, D. Vereecke, W. D'Haese, M. S. Scherman, P.J. Brennan, M.R. McNeil, D.C. Crick, Decaprenylphosphoryl arabinofuranose, the donor of the D-arabinofuranosyl residues of mycobacterial arabinan, is formed via a two-step epimerization of decaprenylphosphoryl ribose, *J. Bacteriol.* 187 (2005) 8020–8025.
- [12] B.A. Wolucka, M.R. McNeil, E. de Hoffmann, T. Chojnacki, P.J. Brennan, Recognition of the lipid intermediate for arabinogalactan/arabinomannan biosynthesis and its relation to the mode of action of ethambutol on mycobacteria, *J. Biol. Chem.* 269 (1994) 23328–23335.
- [13] R.V. Chikhale, M.A. Barmade, P.R. Murumkar, M.R. Yadav, Overview of the development of DprE1 inhibitors for combating the menace of tuberculosis, *J. Med. Chem.* 61 (2018) 8563–8593.
- [14] C. Trefzer, H. Skovierova, S. Buroni, A. Bobovska, S. Nenci, E. Molteni, F. Pojer, M. R. Pasca, V. Makarov, S.T. Cole, G. Riccardi, K. Mikusova, K. Johnson, Benzothiazinones are suicide inhibitors of mycobacterial decaprenylphosphoryl-beta-D-ribofuranose 2'-oxidase DprE1, *J. Am. Chem. Soc.* 134 (2012) 912–915.
- [15] J. Piton, C.S.Y. Foo, S.T. Cole, Structural studies of Mycobacterium tuberculosis DprE1 interacting with its inhibitors, *Drug Discov. Today Off.* 22 (2017) 526–533.
- [16] R. Liu, X. Lyu, S.M. Batt, M.-H. Hsu, M.B. Harbut, C. Vilchère, B. Cheng, K. Ajayi, B. Yang, Y. Yang, H. Guo, C. Lin, F. Gan, C. Wang, S.G. Franzblau, W.R. Jacobs Jr., G.S. Besra, E.F. Johnson, M. Petrassi, A.K. Chatterjee, K. Fütterer, F. Wang, Determinants of the inhibition of DprE1 and CYP2C9 by antitubercular thiophenes, *Angew. Chem. Int. Ed.* 56 (2017) 13011–13015.
- [17] O. Balabon, E. Pitta, M.K. Rogacki, E. Meiler, R. Casanueva, L. Guijarro, S. Huss, E. M. Lopez-Roman, A. Santos-Villarejo, K. Augustyns, L. Ballell, D.B. Aguirre, R. H. Bates, F. Cunningham, M. Cacho, P. Van der Veken, Optimization of hydantoin as potent antimycobacterial decaprenylphosphoryl-β-d-ribose oxidase (DprE1) inhibitors, *J. Med. Chem.* 63 (2020) 5367–5386.
- [18] M. Panda, S. Ramachandran, V. Ramachandran, P.S. Shirude, V. Humnabadkar, K. Nagalapur, S. Sharma, P. Kaur, S. Gupta, A. Narayan, J. Mahadevaswamy, A. Ambady, N. Hegde, S.S. Rudrapatna, V.P. Hosagrahara, V.K. Sambandamurthy, A. Raichurkar, Discovery of pyrazolopyridones as a novel class of noncovalent DprE1 inhibitor with potent anti-mycobacterial activity, *J. Med. Chem.* 57 (2014) 4761–4771.
- [19] S.M. Batt, M. Cacho Izquierdo, J. Castro Pichel, C.J. Stubbs, L. Vela-Glez Del Peral, E. Pérez-Herrán, N. Dhar, B. Mounzon, M. Rees, J.P. Hutchinson, R.J. Young, J. D. McKinney, D. Barros Aguirre, L. Ballell, G.S. Besra, A. Argyrou, Whole cell target engagement identifies novel inhibitors of Mycobacterium tuberculosis decaprenylphosphoryl-β-D-ribose oxidase, *ACS Infect. Dis.* 1 (2015) 615–626.
- [20] J. Neres, R.C. Hartkoorn, L.R. Chiarelli, R. Gadupudi, M.R. Pasca, G. Mori, A. Venturelli, S. Savina, V. Makarov, G.S. Kolly, E. Molteni, C. Binda, N. Dhar, S. Ferrari, P. Brodin, V. Delorme, V. Landry, A.L. de Jesus Lopes Ribeiro, D. Farina, P. Saxena, F. Pojer, A. Carta, R. Luciani, A. Porta, G. Zanoni, E. De Rossi, M. P. Costi, G. Riccardi, S.T. Cole, 2-Carboxyquinoxalines kill Mycobacterium tuberculosis through noncovalent inhibition of DprE1, *ACS Chem. Biol.* 10 (2015) 705–714.
- [21] M. Andrs, M. Pospisilova, M. Seifrtova, R. Havelek, A. Tichy, K. Vejrychova, M. Polednickova, L. Gorecki, D. Jun, J. Korabecny, M. Rezacova, Purin-6-one and pyrrolo[2,3-d]pyrimidin-4-one derivatives as potentiating agents of doxorubicin cytotoxicity, *Future Med. Chem.* 10 (2018) 2029–2038.
- [22] S.P. Vincent, C. Mioskowski, L. Lebean, Regioselective N1-alkylation of guanosine derivatives protected at N2 by an N,N-dialkyl amidine group, *Nucleos Nucleot.* 18 (1999) 2127–2139.
- [23] Y.S. Abe, S. Sasaki, The adduct formation between the thioguanine-polyamine ligands and DNA with the AP site under UVA irradiated and non-irradiated conditions, *Bioorg. Med. Chem.* 27 (2019), 115160.
- [24] J. Janockova, J. Korabecny, J. Plisikova, K. Babkova, E. Konkolova, D. Kucerova, J. Vargova, J. Koval, R. Jendzelovsky, P. Fedorocko, J. Kasparkova, V. Brabec, J. Rosocha, O. Soukup, S. Hamulakova, K. Reuca, M. Kozurkova, In vitro investigating of anticancer activity of new 7-MEOTA-tacrine heterodimers, *J. Enzym. Inhib. Med. Chem.* 34 (2019) 877–897.
- [25] N.S. Gargis, M.A. Michael, D.F. Smee, H.A. Alghamandan, R.K. Robins, H. B. Cottam, Direct C-glycosylation of guanine analogs: the synthesis and antiviral activity of certain 7- and 9-deazaguanine C-nucleosides, *J. Med. Chem.* 33 (1990) 2750–2755.
- [26] M. Brændvang, L.-L. Gundersen, Synthesis, biological activity, and SAR of antimycobacterial 2- and 8-substituted 6-(2-furyl)-9-(p-methoxybenzyl)purines, *Bioorg. Med. Chem.* 15 (2007) 7144–7165.
- [27] A.K. Bakkestuen, L.-L. Gundersen, B.T. Utenova, Synthesis, biological activity, and SAR of antimycobacterial 9-aryl-, 9-arylsulfonyl-, and 9-Benzyl-6-(2-furyl)purines, *J. Med. Chem.* 48 (2005) 2710–2723.
- [28] A.K. Pathak, V. Pathak, L.E. Seitz, W.J. Suling, R.C. Reynolds, 6-Oxo and 6-thio purine analogs as antimycobacterial agents, *Bioorg. Med. Chem.* 21 (2013) 1685–1695.
- [29] A.K. Pathak, V. Pathak, L.E. Seitz, W.J. Suling, R.C. Reynolds, Antimycobacterial agents. 1. Thio analogues of purine, *J. Med. Chem.* 47 (2004) 273–276.
- [30] D. Rai, M. Johar, N.C. Srivastav, T. Manning, B. Agrawal, D.Y. Kunimoto, R. Kumar, Inhibition of Mycobacterium tuberculosis, Mycobacterium bovis, and Mycobacterium avium by novel dideoxy nucleosides, *J. Med. Chem.* 50 (2007) 4766–4774.
- [31] J.A. Ferreras, J.-S. Ryu, F. Di Lello, D.S. Tan, L.E.N. Quadri, Small-molecule inhibition of siderophore biosynthesis in Mycobacterium tuberculosis and Yersinia pestis, *Nat. Chem. Biol.* 1 (2005) 29–32.
- [32] C. Qiao, A. Gupte, H.I. Boshoff, D.J. Wilson, E.M. Bennett, R.V. Somu, C.E. Barry, C. C. Aldrich, 5'-O-[(N-Acyl)sulfamoyl]adenosines as antitubercular agents that inhibit MbtA: an adenylation enzyme required for siderophore biosynthesis of the mycobactins, *J. Med. Chem.* 50 (2007) 6080–6094.
- [33] K. Horváti, K. Fodor, B. Pályi, J. Henczkó, G. Balka, G. Gyulai, É. Kiss, B. Biri-Kovács, Z. Senoner, S. Bőse, Novel assay platform to evaluate intracellular killing of Mycobacterium tuberculosis: in vitro and in vivo validation, *Front. Immunol.* 12 (2021).
- [34] L. Borbála Horváth, M. Krátký, V. Pfléger, E. Méhes, G. Gyulai, G. Kohut, Á. Babiczky, B. Biri-Kovács, Z. Baranyai, J. Vinšová, S. Bőse, Host cell targeting of novel antimycobacterial 4-aminosalicylic acid derivatives with tuftsin carrier peptides, *Eur. J. Pharm. Biopharm.* 174 (2022) 111–130.
- [35] D.C. Ayala, D. Morin, A.R. Buckpitt, Simultaneous quantification of multiple urinary naphthalene metabolites by liquid chromatography tandem mass spectrometry, *PLoS One* 10 (2015), e0121937.
- [36] E. Elmsors, S. Attalla, E. Fikry, A. Kocoon, R. Turner, D. Christie, A. Warren, L. Nwidi, W. Carter, Adverse effects of anti-tuberculosis drugs on HepG2 cell bioenergetics, *Hum. Exp. Toxicol.* 36 (2017) 616–625.
- [37] T. Andersson, J. Miners, M. Veronese, D. Birckett, Diazepam metabolism by human liver microsomes is mediated by both S-mephenytoin hydroxylase and CYP3A isoforms, *Br. J. Clin. Pharmacol.* 38 (1994) 131–137.
- [38] J. Nicolai, T. De Bruyn, P.P. Van Veldhoven, J. Keemink, P. Augustijns, P. Annaert, Verapamil hepatic clearance in four preclinical rat models: towards activity-based scaling, *Biopharm. Drug Dispos.* 36 (2015) 462–480.
- [39] R.S. Obach, Prediction of human clearance of twenty-nine drugs from hepatic microsomal intrinsic clearance data: an examination of in vitro half-life approach and nonspecific binding to microsomes, *Drug Metab. Dispos.* 27 (1999) 1350–1359.
- [40] D. Fan, B. Wang, G. Stelitano, K. Savková, R. Shi, S. Huszár, Q. Han, K. Mikušová, L.R. Chiarelli, Y. Lu, C. Qiao, Structural and activity relationships of 6-sulfonyl-8-nitrobenzothiazinones as antitubercular agents, *J. Med. Chem.* 64 (2021) 14526–14539.
- [41] G. Karabanovich, J. Dušek, K. Savková, O. Pavliš, I. Pávková, J. Korábečný, T. Kučera, H. Kočová Vlčková, S. Huszár, Z. Konyariková, K. Konečná, O. Jand'ourek, J. Stolaríková, J. Korduláková, K. Vávrová, P. Pávek, V. Klimešová, A. Hrabálek, K. Mikušová, J. Roh, Development of 3,5-dinitrophenyl-containing 1,2,4-triazoles and their trifluoromethyl analogues as highly efficient antitubercular agents inhibiting decaprenylphosphoryl-β-d-ribofuranose 2'-oxidase, *J. Med. Chem.* 62 (2019) 8115–8139.
- [42] T. Warrier, K. Kapilashrami, A. Argyrou, T.R. Ioerger, D. Little, K.C. Murphy, M. Nandakumar, S. Park, B. Gold, J. Mi, T. Zhang, E. Meiler, M. Rees, S. Somersan-Karakaya, E. Porras-De Francisco, M. Martinez-Hoyos, K. Burns-Huang, J. Roberts, Y. Ling, K.Y. Rhee, A. Mendoza-Losana, M. Luo, C.F. Nathan, N-methylation of a bactericidal compound as a resistance mechanism in Mycobacterium tuberculosis, *Proc. Natl. Acad. Sci. USA* 113 (2016) E4523–E4530.
- [43] E.A. Dixon, A. Fischer, F.P. Robinson, Preparation of a series of substituted fluoromethylnaphthalenes, *Can. J. Chem.* 59 (1981) 2629–2641.
- [44] G. Karabanovich, J. Zemanova, T. Smutny, R. Szekeley, M. Sarkani, I. Centarova, A. Vocat, I. Pavkova, P. Conka, J. Nemecek, J. Stolarikova, M. Vejsova, K. Vavrova, V. Klimesova, A. Hrabalek, P. Pavek, S.T. Cole, K. Mikusova, J. Roh, Development of 3,5-Dinitrobenzylsulfanyl-1,3,4-oxadiazoles and thiaziazoles as selective antitubercular agents active against replicating and nonreplicating Mycobacterium tuberculosis, *J. Med. Chem.* 59 (2016) 2362–2380.
- [45] D. Malina, R. Dolezal, J. Marek, S. Salajkova, O. Soukup, M. Vejsova, J. Korabecny, J. Honegr, M. Penhaker, K. Musilek, K. Kuca, 6-Hydroxyquinolinium salts differing in the length of alkyl side-chain: synthesis and antimicrobial activity, *Bioorg. Med. Chem. Lett.* 24 (2014) 5238–5241.
- [46] Microsomal stability assay. <https://www.cyprotex.com/admepk/in-vitro-metaboli-sm/microsomal-stability>, (accessed June 8, 2022).
- [47] S. Dam, S. Tangara, C. Hamela, T. Hattabi, L. Faïon, P. Carre, R. Antoine, A. Herledan, F. Leroux, C. Piveteau, M. Eveque, M. Flipo, B. Deprez, L. Kremer, N. Willand, B. Villemagne, R.C. Hartkoorn, Tricyclic SpiroLactams kill

- mycobacteria in vitro and in vivo by inhibiting type II NADH dehydrogenases, *J. Med. Chem.* 65 (2022) 16651–16664.
- [48] N.M. O'Boyle, M. Banck, C.A. James, C. Morley, T. Vandermeersch, G. R. Hutchison, Open babel: an open chemical toolbox, *J. Cheminf.* 3 (2011) 33.
- [49] M.D. Hanwell, D.E. Curtis, D.C. Lonie, T. Vandermeersch, E. Zurek, G.R. Hutchison, Avogadro: an advanced semantic chemical editor, visualization, and analysis platform, *J. Cheminf.* 4 (2012) 17.
- [50] E.F. Pettersen, T.D. Goddard, C.C. Huang, G.S. Couch, D.M. Greenblatt, E.C. Meng, T.E. Ferrin, UCSF Chimera - a visualization system for exploratory research and analysis, *J. Comput. Chem.* 25 (2004) 1605–1612.
- [51] G.M. Morris, R. Huey, W. Lindstrom, M.F. Sanner, R.K. Belew, D.S. Goodsell, A. J. Olson, AutoDock4 and AutoDockTools4: automated docking with selective receptor flexibility, *J. Comput. Chem.* 30 (2009) 2785–2791.
- [52] O. Trott, A.J. Olson, AutoDock Vina: Improving the speed and accuracy of docking with a new scoring function, efficient optimization, and multithreading, *J. Comput. Chem.* 31 (2010) 455–461.
- [53] J. Wang, W. Wang, P.A. Kollman, D.A. Case, Automatic atom type and bond type perception in molecular mechanical calculations, *J. Mol. Graph.* 25 (2006) 247–260.
- [54] J. Wang, R.M. Wolf, J.W. Caldwell, P.A. Kollman, D.A. Case, Development and testing of a general amber force field, *J. Comput. Chem.* 25 (2004) 1157–1174.
- [55] M.J. Abraham, T. Murtola, R. Schulz, S. Páll, J.C. Smith, B. Hess, E. Lindahl, GROMACS: high performance molecular simulations through multi-level parallelism from laptops to supercomputers, *SoftwareX* 1–2 (2015) 19–25.